

UNIVERSITY OF CALGARY

Enantioselective Synthesis and Biological Evaluation of Brassinolide Mimetics

By

Michael A. Bey

A THESIS

SUBMITTED TO THE FACULTY OF GRADUATE STUDIES

IN PARTIAL FULFILLMENT OF THE REQUIREMENTS FOR THE

DEGREE OF MASTER OF SCIENCE

DEPARTMENT OF CHEMISTRY

CALGARY, ALBERTA

DECEMBER, 2003

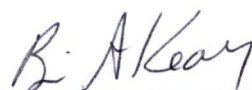
© Michael A. Bey

UNIVERSITY OF CALGARY
FACULTY OF GRADUATE STUDIES

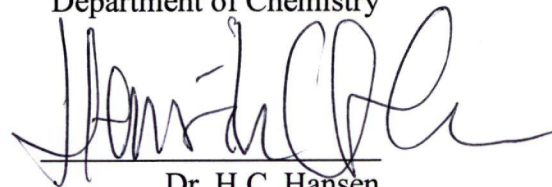
The undersigned certify that they have read, and recommend to the Faculty of Graduate Studies for acceptance, a thesis entitled "Enantioselective Synthesis and Biological Evaluation of Brassinolide Mimetics" submitted by Michael A. Bey in partial fulfillment of the requirements for the degree of Master of Science.



Supervisor, Dr. T.G. Back
Department of Chemistry



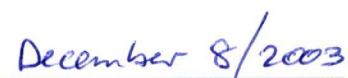
Dr. B.A. Keay
Department of Chemistry



Dr. H.C. Hansen
Department of Chemistry



Dr. R.P. Pharis
Department of Biological
Sciences



Date

Abstract

Brassinolide is a steroidal plant growth regulator that displays remarkable biological activity at very low concentrations. Due to the low natural abundance of brassinolide and the high cost associated with preparing it by chemical synthesis on a large scale, there is considerable value in developing simple and inexpensive molecules that possess the extraordinary biological activity of brassinolide. Previously, several novel nonsteroidal mimetics of brassinolide were prepared as mixtures of stereoisomers. This thesis describes the preparation and biological evaluation of the individual stereoisomers of one such nonsteroidal brassinolide mimetic.

Mimetics (+)-(6*R*,7*S*,6'*S*,7'*R*)-1-(4,6,7-trihydroxy-5,6,7,8-tetrahydronaphthyl)-2-(6,7-dihydroxy-5',6',7',8'-tetrahydronaphthyl)ethyne and its (-)-enantiomer were prepared, along with the (6*S*,7*R*,6'*S*,7'*R*)- and (6*R*,7*S*,6'*R*,7'*S*)-stereoisomers, by coupling chiral subunits that had been resolved via esters formed with *O*-acetylmandelic acid.

In order to evaluate biological activity, the mimetics were subjected to the rice leaf lamina inclination bioassay. It was found that three of the mimetics retained significant biological activity, but only when coapplied with indole-3-acetic acid. Interestingly, it was found that two of the mimetics, when coapplied with brassinolide and indole-3-acetic acid, had either an agonistic or antagonistic effect on the brassinolide response, depending on the dose. These findings imply recognition between the putative receptor and the mimetic. However, as molecular modeling has shown, the mimetics are not a perfect match to brassinolide.

Acknowledgements

I am thankful to my supervisor, Dr. Thomas G. Back for his encouragement and insight over the course of my research project.

I also thank Dr. Richard Pharis for his assistance in providing the biological data. I am thankful to Dr. Brian Keay for helpful discussions during my graduate studies. I am also thankful to Ms. Bonnie King for assistance with academic matters related to the graduate program. I also acknowledge Ms. Dorothy Fox, Ms. Roxanna Smith, Ms. Qiao Wu, and Dr. Raghav Yamdagni for their technical assistance.

I sincerely thank my family for their invaluable support and encouragement during my studies. I also wish to express my sincerest gratitude to Marian Zlomislic for her encouragement and friendship.

I also thank my fellow lab members and friends, Dr. Sultan Chowdhury, Amanda Coolidge, Sean Dalrymple, Mike Hamilton, Matt Hopkins, Vania Lim, Dr. Ziad Moussa, Danica Rankic, Stephanie Sibley, Jovina Sorbetti, Mitch Weston, Jeremy Wulff, and Robby Zhai.

Finally, I acknowledge financial assistance from the University of Calgary.

Table of Contents

Approval Page	ii
Abstract	iii
Acknowledgements	iv
Table of Contents	v
List of Tables	xi
List of Figures	xii
List of Abbreviations	xiv

Chapter One Nonsteroidal Mimetics of Brassinolide

1.1	Plant Growth Regulators	1
1.2	Brassinolide: History and Structural Elucidation	4
1.3	Biosynthesis of Brassinolide	6
1.3.1	Biosynthesis of Brassinolide via Early C6 Oxidation	8
1.3.2	Biosynthesis of Brassinolide via Late C6 Oxidation	10
1.3.3	Inhibitors of Brassinolide Biosynthesis	13
1.4	Metabolism of Brassinosteroids	14
1.4.1	Metabolism of 24-Epicastasterone (25) and 24-Epibrassinolide (26) in Tomato Cell Cultures (<i>Lycopersicon esculentum</i>)	15

1.4.2	Metabolism of 24-Epicastasterone (25) and 24-Epibrassinolide (26) in Serradella Cell Cultures (<i>Ornithopus sativus</i>)	17
1.5	Bioassays for Brassinosteroids	19
1.5.1	Wheat Leaf-Unrolling Bioassay	20
1.5.2	Bean Second Internode Bioassay	20
1.5.3	Rice Leaf Lamina Inclination Bioassay	21
1.5.4	Extension to Field Applications	22
1.6	Structure-Activity Relationships of Brassinosteroids	23
1.6.1	Structure Activity Relationships in the Brassinosteroid Side Chain	24
1.6.2	Structure Activity Relationships in the Brassinosteroid Nucleus	28
1.7	Synthesis of Brassinolide	32
1.7.1	Back's Synthesis of Brassinolide	33
1.8	Design of Nonsteroidal Analogues	37
1.9	Objectives	40

**Chapter Two Synthesis and Biological Evaluation of Nonsteroidal
Brassinolide Mimetics**

2.1	Introduction	42
2.2	Asymmetric Strategy	44

2.3	Sharpless Asymmetric Dihydroxylation	46
2.4	Conversion to Diastereomers	49
2.4.1	Resolution of Racemic <i>cis</i> -Diol 98 with <i>O</i> -Acetylmandelic Acid	50
2.4.2	Resolution of Racemic <i>cis</i> -Diol 99 with <i>O</i> -Acetylmandelic Acid	55
2.5	Synthesis of Enantiopure Subunits 90 and 91	60
2.5.1	Synthesis of Subunits (-)- 90 and (+)- 90	61
2.5.2	Synthesis of Subunits (-)- 91 and (+)- 91	62
2.6	Synthesis of Mimetics	63
2.7	Molecular Modeling	65
2.8	Biological Evaluation	69
2.9	Conclusions	75

Chapter Three Experimental Section

3.1	General Comments	77
3.2	(+/-)- <i>cis</i> -6,7-Dihydroxy-5,6,7,8-tetrahydro-1-naphthyl acetate (99)	79
3.3	(-)-(6 <i>R</i> ,7 <i>S</i>)-6,7-Bis-[(<i>R</i>)- <i>O</i> -acetylmandeloxyl]-5,6,7,8-tetrahydro-1-acetoxy-naphthalene [(-)- 102]	80
3.4	(+)-(6 <i>S</i> ,7 <i>R</i>)-6,7-Bis-[(<i>S</i>)- <i>O</i> -acetylmandeloxyl]-5,6,7,8-tetrahydro-1-acetoxy-naphthalene [(+)- 102]	82

3.5	(+)-(6 <i>S</i> ,7 <i>R</i>)-1-Iodo-5,6,7,8-tetrahydro-6,7-bis-[(<i>S</i>)- <i>O</i> -acetylmandeloxy] naphthalene [(+)- 101]	83
3.6	(-)-(6 <i>R</i> ,7 <i>S</i>)-1-Iodo-5,6,7,8-tetrahydro-6,7-bis-[(<i>S</i>)- <i>O</i> -acetylmandeloxy] naphthalene [(-)- 101]	85
3.7	(-)-(6 <i>R</i> ,7 <i>S</i>)-5,6,7,8-Tetrahydro-1,6,7-naphthalenetriol [(-)- 103]	86
3.8	(+)-(6 <i>S</i> ,7 <i>R</i>)-5,6,7,8-Tetrahydro-1,6,7-naphthalenetriol [(+)- 103]	87
3.9	(-)-(6 <i>R</i> ,7 <i>S</i>)-6,7-(Isopropylidenedioxy)-5,6,7,8-tetrahydro-1-naphthol [(-)- 104]	88
3.10	(+)-(6 <i>S</i> ,7 <i>R</i>)-6,7-(Isopropylidenedioxy)-5,6,7,8-tetrahydro-1-naphthol [(+)- 104]	89
3.11	(+)-(6 <i>R</i> ,7 <i>S</i>)-4-Iodo-6,7-(isopropylidenedioxy)-5,6,7,8-tetrahydro-1-naphthol [(+)- 105]	90
3.12	(-)-(6 <i>S</i> ,7 <i>R</i>)-4-Iodo-6,7-(isopropylidenedioxy)-5,6,7,8-tetrahydro-1-naphthol [(-)- 105]	91
3.13	(+)-(6 <i>R</i> ,7 <i>S</i>)-1- <i>t</i> -Butyldimethylsilyloxy-4-iodo-6,7-(isopropylidenedioxy)-5,6,7,8-tetrahydro-1-naphthol [(+)- 91]	92
3.14	(-)-(6 <i>S</i> ,7 <i>R</i>)-1- <i>t</i> -Butyldimethylsilyloxy-4-iodo-6,7-(isopropylidenedioxy)-5,6,7,8-tetrahydro-1-naphthol [(-)- 91]	93
3.15	(+)-(6 <i>S</i> ,7 <i>R</i>)-1-Iodo-5,6,7,8-tetrahydro-6,7-naphthalenediol [(+)- 98]	94
3.16	(-)-(6 <i>R</i> ,7 <i>S</i>)-1-Iodo-5,6,7,8-tetrahydro-6,7-naphthalenediol [(-)- 98]	95
3.17	(+)-(6 <i>S</i> ,7 <i>R</i>)-1-Ethynyl-5,6,7,8-tetrahydro-6,7-naphthalenediol [(+)- 90]	96

3.18	(-)-(6 <i>R</i> ,7 <i>S</i>)-1-Ethynyl-5,6,7,8-tetrahydro-6,7-naphthalenediol [(-)- 90]	97
3.19	(+)-(6 <i>R</i> ,7 <i>S</i> ,6' <i>S</i> ,7' <i>R</i>)-1-[6,7-(Isopropylidenedioxy)-4- <i>t</i> - butyldimethylsilyloxy-5,6,7,8-tetrahydronaphthyl]-2-[6',7'- dihydroxy-5',6',7',8'-tetrahydronaphthyl]ethyne [(+)- 106]	98
3.20	(-)-(6 <i>S</i> ,7 <i>R</i> ,6' <i>R</i> ,7' <i>S</i>)-1-[6,7-(Isopropylidenedioxy)-4- <i>t</i> - butyldimethylsilyloxy-5,6,7,8-tetrahydronaphthyl]-2-[6',7'- dihydroxy-5',6',7',8'-tetrahydronaphthyl]ethyne [(-)- 106]	100
3.21	(-)-(6 <i>S</i> ,7 <i>R</i> ,6' <i>S</i> ,7' <i>R</i>)-1-[6,7-(Isopropylidenedioxy)-4- <i>t</i> - butyldimethylsilyloxy-5,6,7,8-tetrahydronaphthyl]-2-[6',7'- dihydroxy-5',6',7',8'-tetrahydronaphthyl]ethyne [(-)- 107]	101
3.22	(+)-(6 <i>R</i> ,7 <i>S</i> ,6' <i>R</i> ,7' <i>S</i>)-1-[6,7-(Isopropylidenedioxy)-4- <i>t</i> - butyldimethylsilyloxy-5,6,7,8-tetrahydronaphthyl]-2-[6',7'- dihydroxy-5',6',7',8'-tetrahydronaphthyl]ethyne [(+)- 107]	102
3.23	(+)-(6 <i>R</i> ,7 <i>S</i> ,6' <i>S</i> ,7' <i>R</i>)-1-[1-(4,6,7-Trihydroxy-5,6,7,8- tetrahydronaphthyl)]-2-[1'-(6',7'-dihydroxy-5',6',7',8'- tetrahydronaphthyl)]ethyne [(+)- 88]	103
3.24	(-)-(6 <i>S</i> ,7 <i>R</i> ,6' <i>R</i> ,7' <i>S</i>)-1-[1-(4,6,7-Trihydroxy-5,6,7,8- tetrahydronaphthyl)]-2-[1'-(6',7'-dihydroxy-5',6',7',8'- tetrahydronaphthyl)]ethyne [(-)- 88]	105
3.25	(-)-(6 <i>S</i> ,7 <i>R</i> ,6' <i>S</i> ,7' <i>R</i>)-1-[1-(4,6,7-Trihydroxy-5,6,7,8- tetrahydronaphthyl)]-2-[1'-(6',7'-dihydroxy-5',6',7',8'- tetrahydronaphthyl)]ethyne [(-)- 89]	106

3.26	(+)-(6 <i>R</i> ,7 <i>S</i> ,6' <i>R</i> ,7' <i>S</i>)-1-[1-(4,6,7-Trihydroxy-5,6,7,8-tetrahydronaphthyl)]-2-[1'-(6',7'-dihydroxy-5',6',7',8'-tetrahydronaphthyl)]ethyne [(+)- 89]	107
3.27	Molecular Modeling	108
References		110
Appendix I	X-Ray Crystal Report of (-)-101	117
Appendix II	X-Ray Crystal Report of (-)-102	129

List of Tables

2.1	Selected Dihedral Angles and Interatomic Distances of Brassinolide	66
2.2	Selected Measurements of Mimetics in Conformations that Most Closely Resemble Brassinolide	68

List of Figures

1.1	Traditional Classes of Plant Hormones	2
1.2	Nontraditional Classes of Plant Hormones	3
1.3	Structure of Brassinolide	4
1.4	Examples of Naturally Occurring Brassinosteroids	5
1.5	Inhibitors of Brassinolide Biosynthesis	13
1.6	The First Analogues of Brassinolide	24
1.7	Side Chain Analogues of Brassinolide	27
1.8	B-Ring Brassinosteroid Analogues	29
1.9	A/B Ring Analogues of Brassinolide	31
1.10	A Brassinolide Mimetic With Close Superimposition of Functionality	37
1.11	Nonsteroidal Mimetics of Brassinolide	39
2.1	Mimetics (+)- 88 , (-)- 88 , (+)- 89 , and (-)- 89	43
2.2	Required Chiral Subunits 90 and 91	44
2.3	Cinchona Alkaloid Ligands in the AD-mix Reagents	46
2.4	ORTEP Diagram of (-)- 101	53
2.5	ORTEP Diagram of (-)- 102	58
2.6	Summary of Vicinal Diol Subunits as Individual Enantiomers	60
2.7	Nonsteroidal Brassinolide Mimetics	65
2.8	Rice Leaf Lamina Bending Assay of 79	71
2.9	Rice Leaf Lamina Bending Assay of (+)- 89	71
2.10	Rice Leaf Lamina Bending Assay of (-)- 89	72

2.11	Rice Leaf Lamina Bending Assay of (+)- 88	72
2.12	Rice Leaf Lamina Bending Assay of (+)- 89	73
2.13	Rice Leaf Lamina Bending Assay of (+)- 89	73
2.14	Rice Leaf Lamina Bending Assay of (+)- 89	74

List of Abbreviations

Å	angstrom
Ac	acetyl
$[\alpha]_D$	specific rotation
AD-mix- α	asymmetric dihydroxylation mix alpha
AD-mix- β	asymmetric dihydroxylation mix beta
Ar	aryl
br	broad
Bu	butyl
ca.	approximately
°C	degrees Celsius
^{13}C NMR	carbon-13 nuclear magnetic resonance
CHP	cumene hydroperoxide
cm	centimeters
cm^{-1}	reciprocal centimeters
d	doublet
δ	chemical shift
DCC	dicyclohexylcarbodiimide
DET	diethyl tartrate
DMAP	<i>N,N</i> -dimethyl-4-aminopyridine
DMF	<i>N,N</i> -dimethylformamide
E	energy

ee	enantiomeric excess
Et	ethyl
g	grams
GCMS	gas chromatography-mass spectrometry
h	hours
^1H NMR	proton nuclear magnetic resonance
Hz	Hertz
i	iso
IAA	indole-3-acetic acid
IR	infrared
J	coupling constant
kg	kilograms
kJ	kilojoules
L	linker
(l)	liquid
lit.	literature
M	molar
m	multiplet
M^+	molecular ion
Me	methyl
mg	milligrams
MHz	megahertz
mL	milliliters

μL	microliters
mmol	millimole
mol	mole
mp	melting point
M.Sc.	Master of Science
<i>m/z</i>	mass to charge ratio
<i>n</i>	normal (straight chain)
ng	nanograms
NMO	<i>N</i> -methylnmorpholine- <i>N</i> -oxide
ORTEP	Oak Ridge Thermal Ellipsoid Plot
ox.	oxidation
<i>p</i>	para
p.	page
Ph	phenyl
PhH	benzene
PP	pyrophosphate
pp.	pages
ppm	parts per million
Pr	propyl
pyr	pyridine
R	general alkyl substituent
s	singlet
Tf	trifluoromethanesulfonyl

t	triplet
<i>t</i> -	tertiary
TBAF	tetra- <i>n</i> -butylammonium fluoride
TBDMS	<i>t</i> -butyldimethylsilyl
TFA	trifluoroacetic acid
THF	tetrahydrofuran
TLC	thin layer chromatography
TMSA	trimethylsilylacetylene
Ts	<i>p</i> -toluenesulfonyl

Chapter One

Nonsteroidal Mimetics of Brassinolide

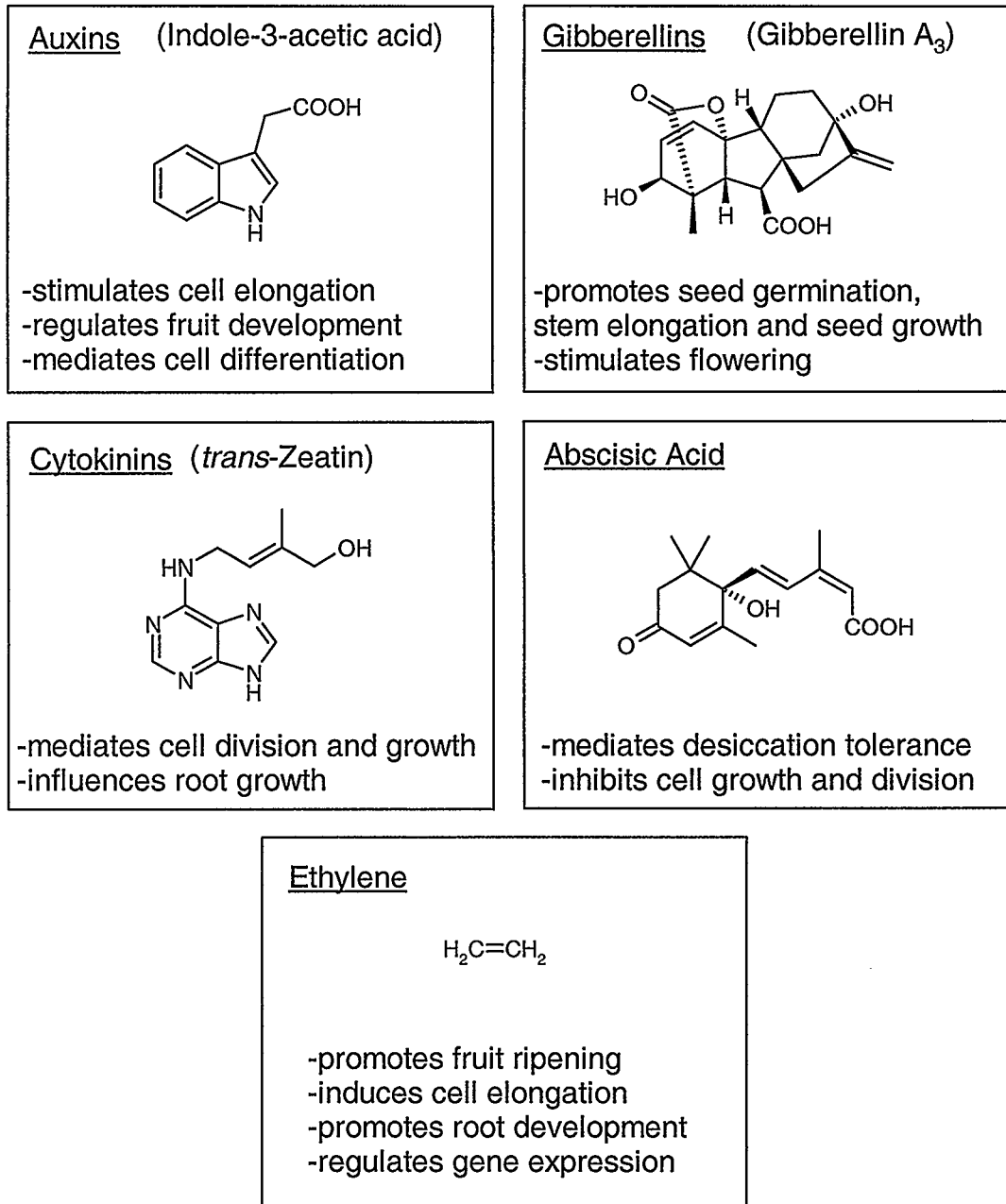
1.1 Plant Growth Regulators

Steroid hormones are signaling molecules important for normal growth, development, and differentiation of multicellular organisms.¹ By definition, a hormone is a compound that is produced in one region of the organism and is then transported to other regions, where it binds to a specific receptor and triggers responses in target cells.² While plant hormones meet most of the criteria to be considered hormones, their action is not always distant from their site of synthesis.³ Hence, it has been pointed out that the terms plant growth substance³ and plant growth regulator⁴ may be more suitable for molecules important for normal growth, development, and differentiation of plant cells. Recently, a general definition was put forward by Davies,⁵ which stated that plant hormones are naturally occurring compounds in plants with an ability to affect physiological processes at concentrations far below those where either nutrients or vitamins would affect them. The term phytohormone is also commonly used to describe such plant hormones.

Plant hormones are produced in very low concentrations and even a minute amount can have a profound effect on the growth and development of plants by affecting division, elongation, and differentiation of plant cells.² Until quite recently, plant development was thought to be regulated by only five types of plant hormones⁶: auxins,

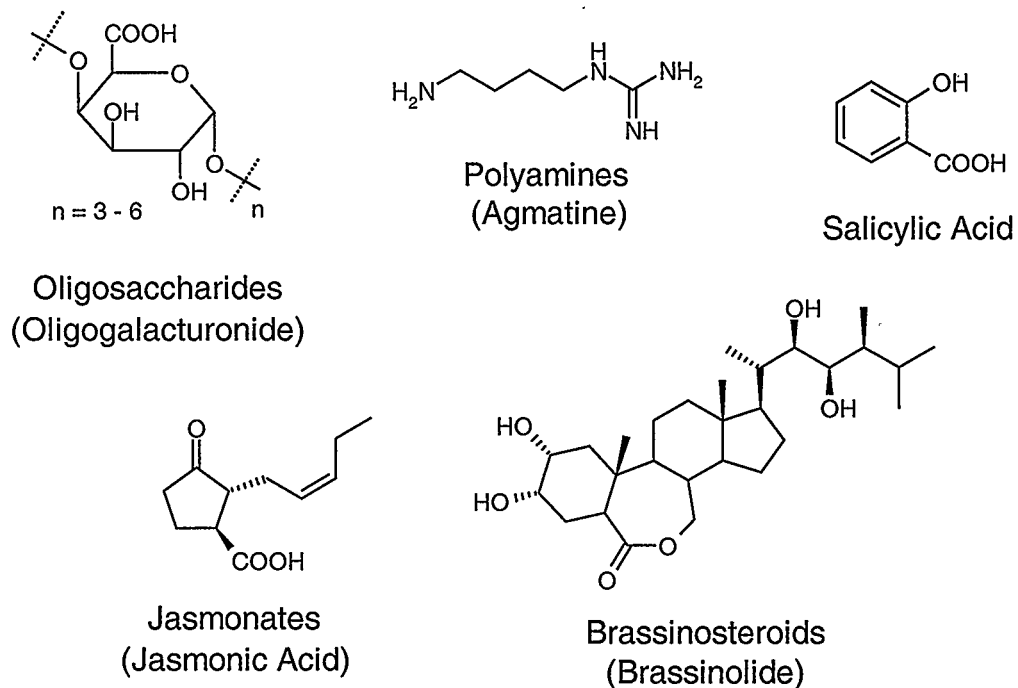
giberellins, cytokinins, ethylene, and abscisic acid. Examples of these five classes of phytohormones and their most important functions are given in Figure 1.1.⁷

Figure 1.1 Traditional Classes of Plant Hormones⁷



In recent years, several classes of nontraditional plant hormones have also been identified and studied with respect to their activity as plant growth regulators. The nontraditional plant hormones include: biologically derived oligosaccharides,⁸ polyamines,⁹ salicylic acid,¹⁰ jasmonates,⁸ and brassinosteroids.¹¹ A representative compound from each of the nontraditional classes of plant hormones is given in Figure 1.2.⁸⁻¹¹ Some of the physiological effects of the nontraditional plant hormones include: promotion of flowering, inhibition of leaf abscission and root growth, increase in insect and disease resistance, initiation of seed germination, influence on cell elongation and cell division, enhancement of stress resistance, and promotion of xylem differentiation.

Figure 1.2 Nontraditional Classes of Plant Hormones⁸⁻¹¹

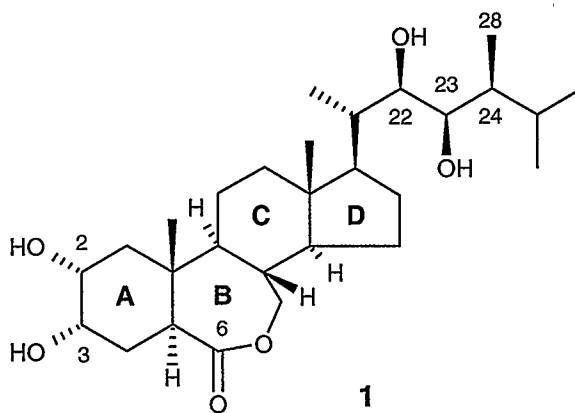


Recent research on the chemistry, physiology, and molecular biology of brassinosteroids now provides a convincing body of evidence that these steroidal plant hormones are essential regulators of plant growth and development.¹² Hence, brassinosteroids are now generally considered to represent a new sixth class of unique, naturally occurring steroidal plant hormones with high biological activity at very low concentrations.¹³⁻¹⁵ The remainder of this thesis deals with this new class of plant hormones and a novel class of synthetic brassinosteroid mimetics.

1.2 Brassinolide: History and Structural Elucidation

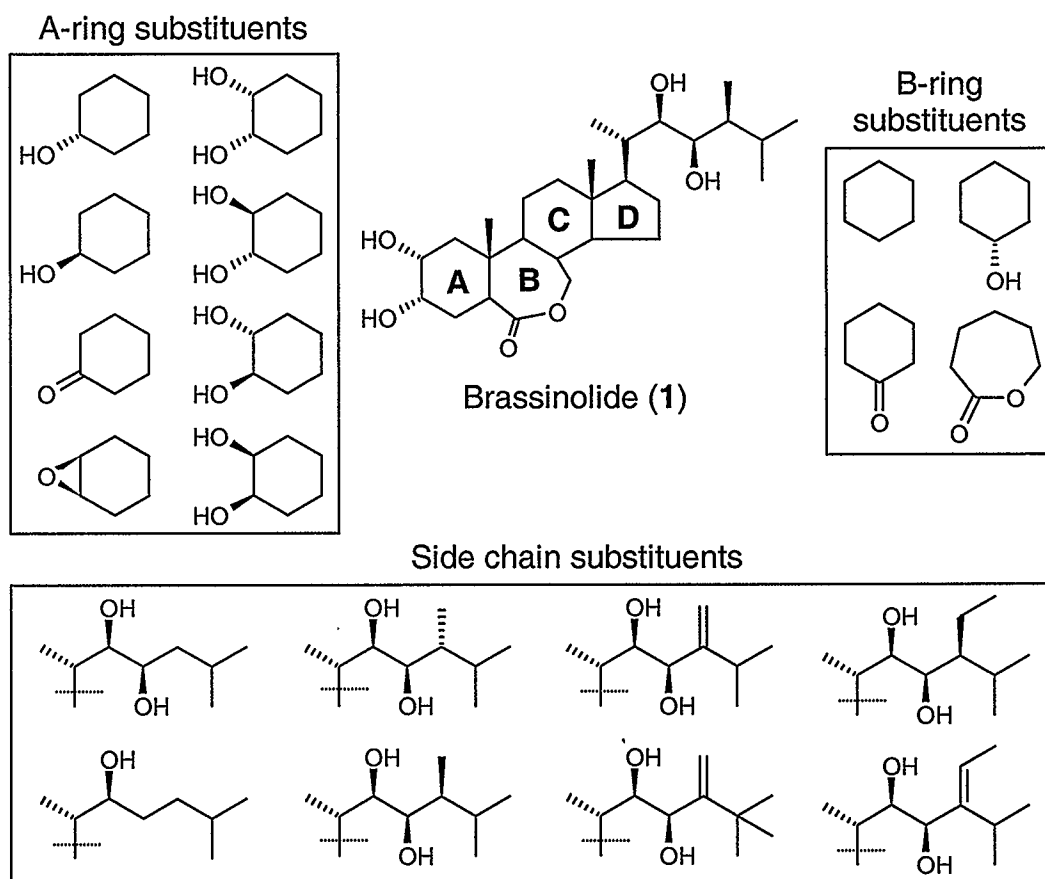
In 1970, Mitchell and coworkers¹⁶ were the first to report a naturally occurring group of plant growth promoting substances that had been obtained from rape pollen (*Brassica napus*), which they termed 'brassins'. Shortly thereafter, Grove and coworkers¹⁷ managed to characterize and isolate 4 mg of (22*R*,23*R*,24*S*)-2 α -3 α ,22,23-tetrahydroxy-24-methyl-B-homo-7-oxa-5 α -cholestan-6-one, which they named brassinolide (**1**) (Figure 1.3), from 40 kg of *B. napus* pollen.

Figure 1.3 Structure of Brassinolide



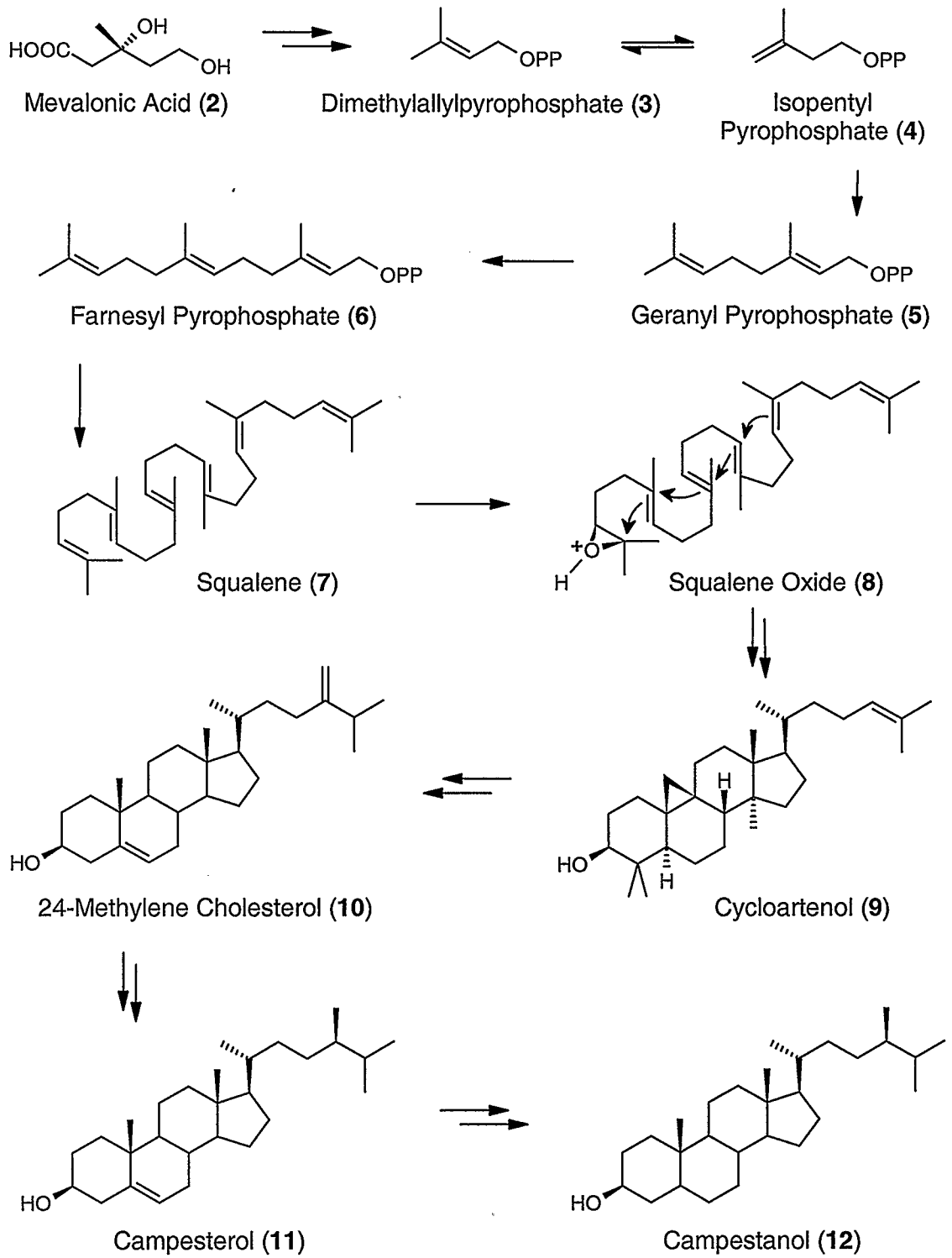
The structure of brassinolide was confirmed by X-ray crystallography¹⁷ and it was the first naturally occurring steroid known to contain a B-ring lactone.¹⁸ Since the groundbreaking work of Mitchell¹⁶ and Grove¹⁷ and their coworkers to isolate and identify brassinolide, it has been reported that, as of 2003, 54 brassinosteroids and 5 conjugates have been isolated from 58 different plant species.¹⁹ Figure 1.4 shows that there is substantial variety in the naturally occurring brassinosteroids.

Figure 1.4 Examples of Naturally Occurring Brassinosteroids¹⁹



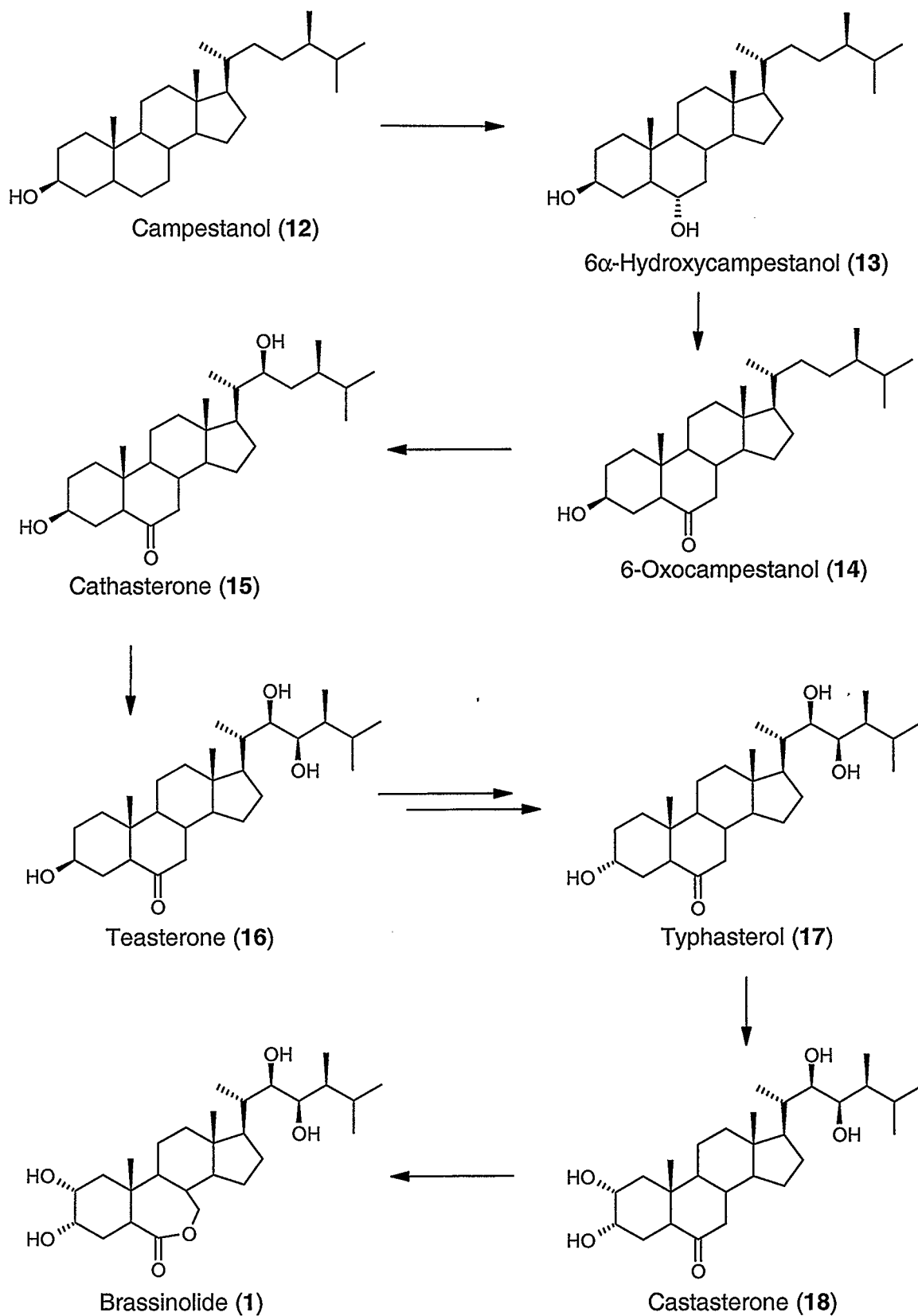
1.3 Biosynthesis of Brassinolide

In recent years, there has been considerable research activity²⁰⁻³¹ dedicated to elucidating the pathways of brassinosteroid biosynthesis. Biosynthesis of brassinosteroids has primarily been studied using cultured cells of *Catharanthus roseus*,²⁰ and it has been proposed that brassinolide, the most active naturally occurring brassinosteroid, is biosynthesized from campesterol (**11**) by two alternative pathways. These two pathways have been termed the early C6-oxidation pathway²¹ and the late C6-oxidation pathway,²²⁻²⁴ both of which can operate simultaneously in a wide variety of plants. The most recent findings on the biosynthesis of brassinosteroids suggests these two pathways can be connected at multiple steps making the brassinolide biosynthetic pathways highly networked (*vide infra*).²⁵ Although it has been established that campesterol (**11**) is the common starting point for each of the two pathways, it is important to recognize that **11** is a bulk sterol found in plant cell membranes and its role as a precursor to **1** is not its sole function.²⁶ Conversely, campestanol (**12**), the reduction product of campesterol, is recognized as being committed to brassinolide biosynthesis.²⁶ Downstream derivatives from campestanol are also recognized as intermediates that are committed to the biosynthesis of brassinolide. The biosynthesis of campestanol follows the mevalonic acid pathway and is given in Scheme 1.1.²⁷ Therefore, it follows that the biosynthesis of brassinolide starts from the conversion of campestanol via the early or late C6 oxidation pathway.²⁸ These two biosynthetic routes are described in more detail in Sections 1.3.1 and 1.3.2, respectively.

Scheme 1.1 Biosynthesis of Campesterol via the Mevalonic Acid Pathway²⁷

1.3.1 Biosynthesis of Brassinolide via Early C6 Oxidation

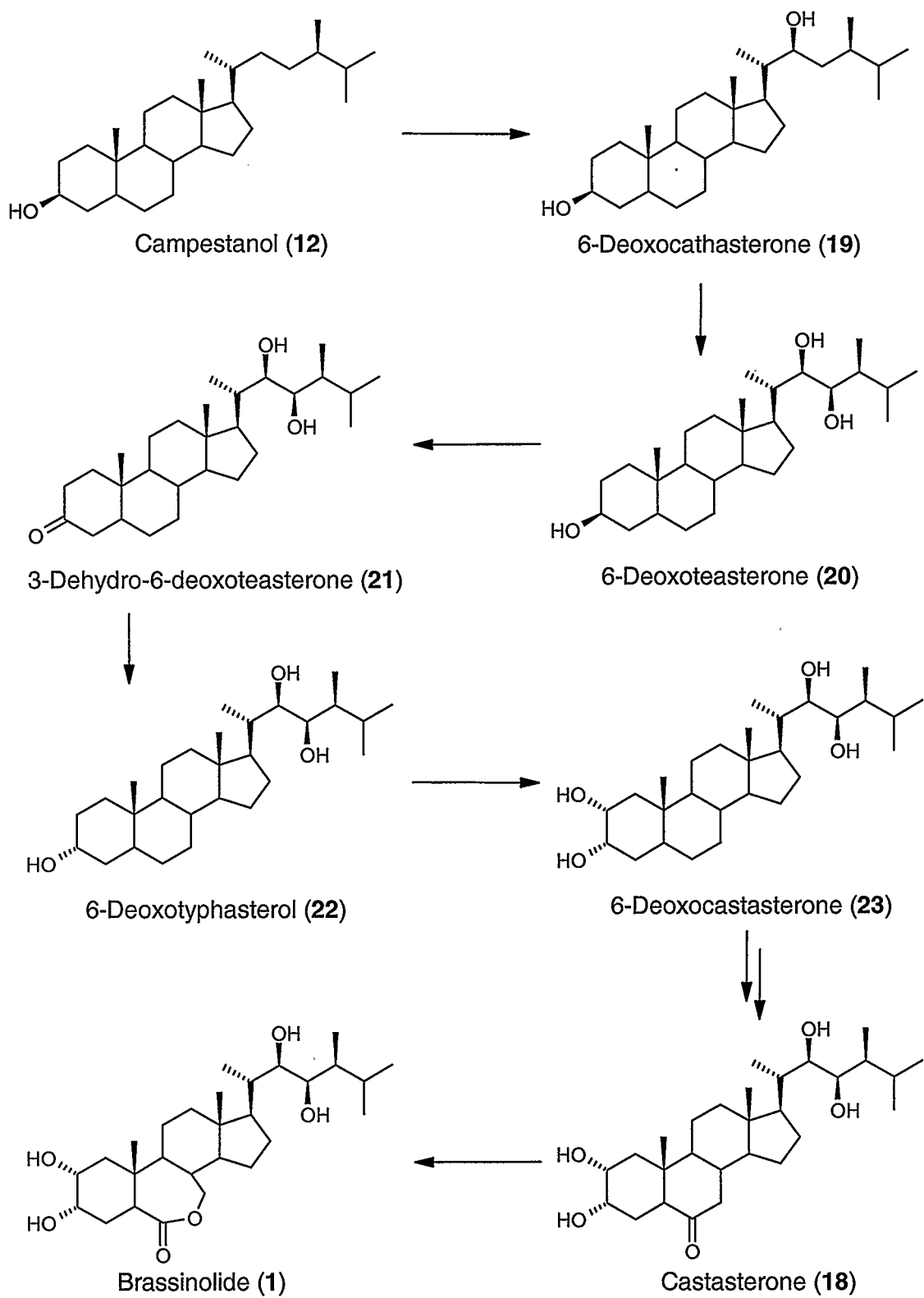
A biosynthetic pathway for brassinolide was demonstrated by Yokota *et al.*²⁹ in 1995. Yokota and coworkers established that campestanol is converted to teasterone (**16**) via oxidation at C-6, followed by several side-chain oxidation steps, then successive epimerization at C-3 to typhasterol (**17**), and oxidation to castasterone (**18**), and brassinolide. Yokota also noted that the biological activity increases as oxidation proceeds, giving greater credence to the suggested biosynthetic pathway. Yokota's biosynthetic pathway leading to brassinolide, known as the early C6 oxidation pathway, was demonstrated by employing isotopically labeled substrates in feeding experiments of *C. roseus*.²⁹ The early C6 oxidation pathway leading to brassinolide is illustrated in Scheme 1.2.³⁰ It is also interesting to note that the conversion of teasterone to typhasterol involves an intermediate with a ketone at the C3 position. The ketone is stereoselectively reduced to give the corresponding 3 α -hydroxy derivative typhasterol. Therefore, the early C6 oxidation pathway of brassinolide biosynthesis can be summarized as a series of hydroxylations and an epimerization after oxidation at C6 of the B-ring.

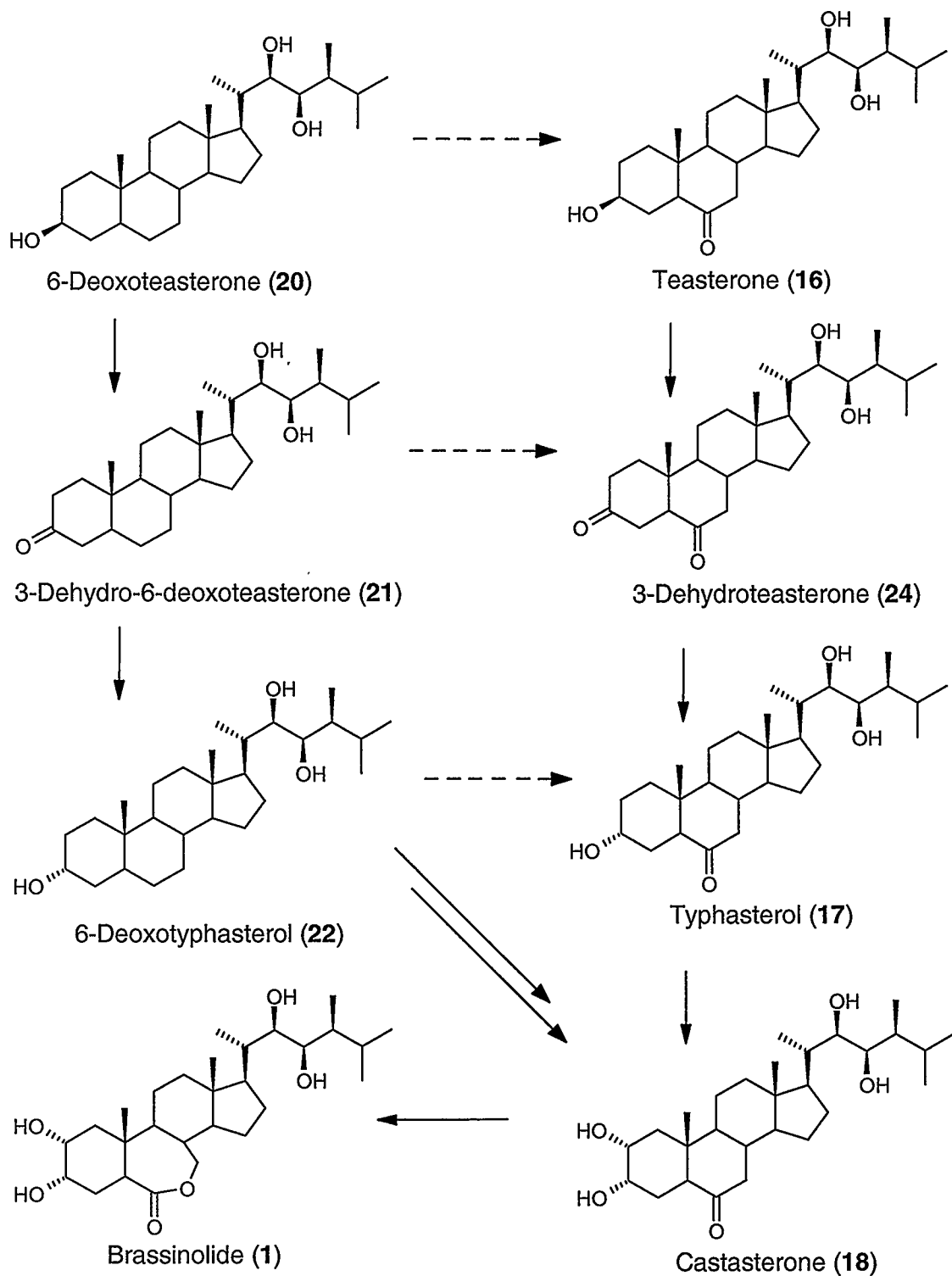
Scheme 1.2 Biosynthesis of Brassinolide via Early C6 Oxidation^{29,30}

1.3.2 Biosynthesis of Brassinolide via Late C6 Oxidation

Among natural brassinosteroids, attention was belatedly drawn to the 6-deoxo brassinosteroids such as 6-deoxocastasterone (**23**), since they are the least active among the brassinosteroids in known bioassays.^{22,23} They were initially considered to be dead-end products which were not converted to active brassinosteroids. However a feeding experiment revealed that deuterium labeled 6-deoxocastasterone was converted to castasterone and brassinolide in cultured cells of *Catharanthus roseus*.²² Subsequent feeding experiments²⁴ involving deuterium labeled substrates confirmed that the 6-deoxobrasinosteroids are involved in the biosynthesis of brassinolide by way of late C6 oxidation. The biosynthesis of brassinolide via the late C6 oxidation pathway is illustrated in Scheme 1.3.^{22-24,30} Therefore, the late C6 oxidation pathway is distinguished by the participation of brassinosteroids that lack oxidation at C6 until the penultimate step that gives rise to castasterone.

The major difference between the two biosynthetic pathways is the point at which the C6 position is oxidized. However, as mentioned earlier, the biosynthesis of brassinosteroids can be connected at multiple steps, making the brassinolide biosynthetic pathways highly networked.^{25,31} This suggests that the enzyme(s) responsible for oxidation at C6 can operate at any time during the biosynthetic pathway leading to brassinolide. The concept of pathway-independent C6 oxidation is illustrated in Scheme 1.4.^{25,31} Hence, multiple pathways in brassinolide biosynthesis, including interconnections, branches, and modified steps cannot be excluded because of the complex pattern of occurrence of brassinosteroids in plants:

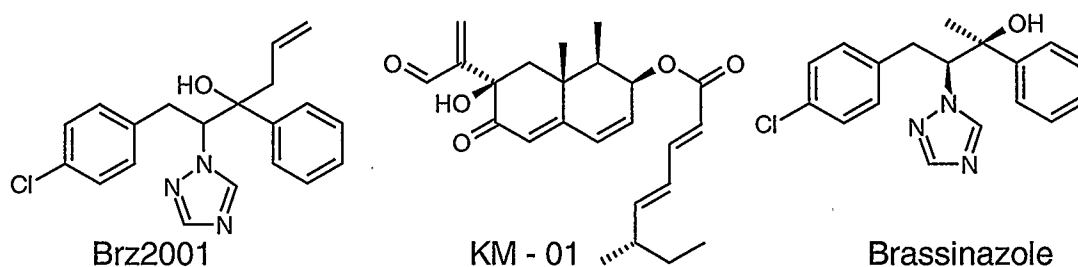
Scheme 1.3 Biosynthesis of Brassinolide via Late C6 Oxidation^{22-24,30}

Scheme 1.4 Brassinolide Biosynthesis via Pathway Independent C6 Oxidation^{25,31}

1.3.3 Inhibitors of Brassinolide Biosynthesis

Biosynthesis inhibitors that are specific in their action are useful in determining the physiological functions of endogenous substances. This is accomplished by observing morphological differences that arise in plants after treatment with an inhibitor of a specific biosynthetic step.³² Many steps of the brassinolide biosynthetic pathway are thought to be catalyzed by cytochrome P450 enzymes and the availability of inhibitors specific to the action of these enzymes provides an opportunity to inhibit a number of steps in brassinosteroid biosynthesis.³³ This should provide a new and complementary approach to understanding the physiological functions of brassinosteroids.³⁴ A number of such inhibitors have been recognized and a few examples are given in Figure 1.5.³²⁻³⁴

Figure 1.5 Inhibitors of Brassinolide Biosynthesis³²⁻³⁴



Another more modern way to determine the physiological functions of endogenous substances is to create mutant plants lacking genes needed for key biosynthetic steps.^{35,36} Such plants can subsequently be rescued by exogenous application of the hormone, i.e. brassinolide.

Elucidation of brassinosteroid biosynthetic pathways is fundamental to understanding how plants regulate the endogenous levels of active brassinosteroids for their proper growth and development. However, it is equally important to understand how plants regulate brassinosteroid levels through catabolic metabolism in order to gain a broad understanding of the physiological role played by this class of plant hormones.

1.4 Metabolism of Brassinosteroids

While it has been shown that brassinosteroid biosynthesis is highly regulated, so too is brassinosteroid metabolism and deactivation. Since it has now been determined that brassinosteroids are essential for normal plant growth and development, it seems highly likely that metabolic deactivation of brassinolide and other active brassinosteroids is an important mechanism for maintaining normal plant function. The available evidence indicates that plant hormones are in a state of constant flux, undergoing continual turnover. Thus, in order to maintain effective hormone concentrations there needs to be a balance between the rates of biosynthesis and metabolic deactivation.²⁸

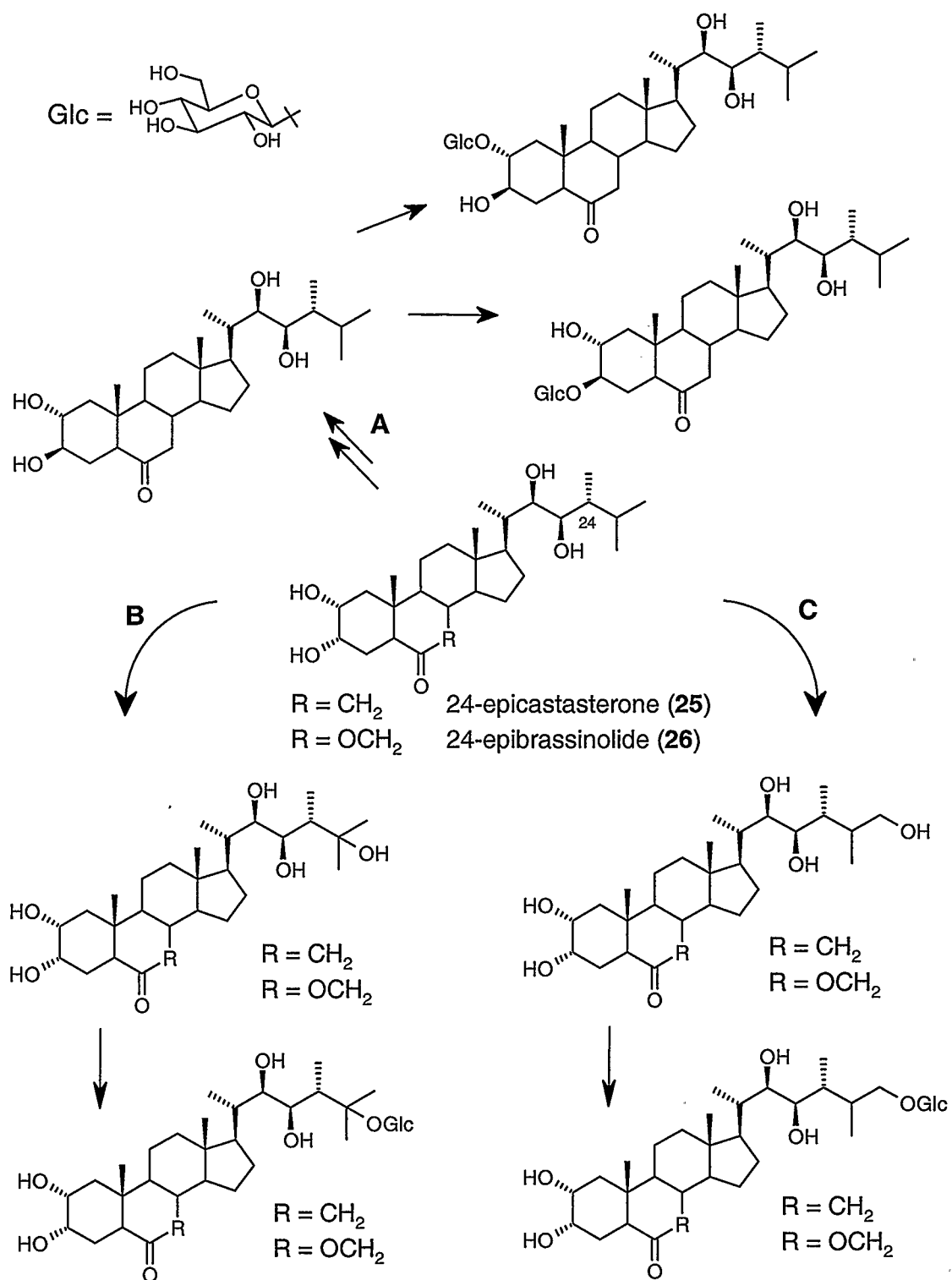
The metabolism of 24-epicastasterone (**25**) and 24-epibrassinolide (**26**) in *Lycopersicon esculentum*³⁷⁻³⁹ and *Ornithopus sativus*⁴⁰ has been investigated in detail and has been reviewed by Adam and Schneider.⁴¹ These studies employed the C24 epimer of castasterone and brassinolide because of the more facile synthesis of isotopically labeled analogs of these isomers, compared to labeled analogs of castasterone and brassinolide. To study the metabolism of natural products that occur in low concentrations, such as plant hormones in the plant cell, substrates labeled at high specific activity with

radioactive or heavy isotopes must be used in order to detect the small amounts of metabolites. This is done using very sensitive radiodetection or gas chromatography-mass spectrometry (GCMS).⁴¹ Most studies related to brassinosteroid metabolism have used ³H or ¹⁴C labeled substrates applied to cell cultures. Cell cultures have been extensively employed to study biogenetic and metabolic pathways of natural products, including plant hormones.⁴¹ Cell cultures also provide an aseptic environment (relatively free of microbes) and therefore allow investigation of metabolism without undue microbial influence. The use of cell cultures also facilitates the exposure of the cells to exogenous substances.

1.4.1 Metabolism of 24-Epicastasterone (25) and 24-Epibrassinolide (26) in Tomato Cell Cultures (*Lycopersicon esculentum*)

In order to establish the metabolic fate of 24-epicastasterone (25) and 24-epibrassinolide (26) in tomato cell cultures (*Lycopersicon esculentum*), radiolabeled analogs of 25 and 26 were applied to the cell cultures in their growth medium.³⁷⁻³⁹ The investigators found that glucosylation at C2 or C23, or epimerization of C3 followed by glucosylation, were major pathways. This is illustrated as pathway A in Scheme 1.5. It was also found that hydroxylation of the side chain at C25 or C26, followed by conjugation with a glucosyl moiety, was another major pathway of brassinosteroid deactivation. This is illustrated as pathways B and C in Scheme 1.5. It is generally accepted that metabolic glucosylation of brassinosteroids results in their deactivation.

Scheme 1.5 Metabolism of 24-Epicastasterone and 24-Epibrassinolide in Tomato Cell

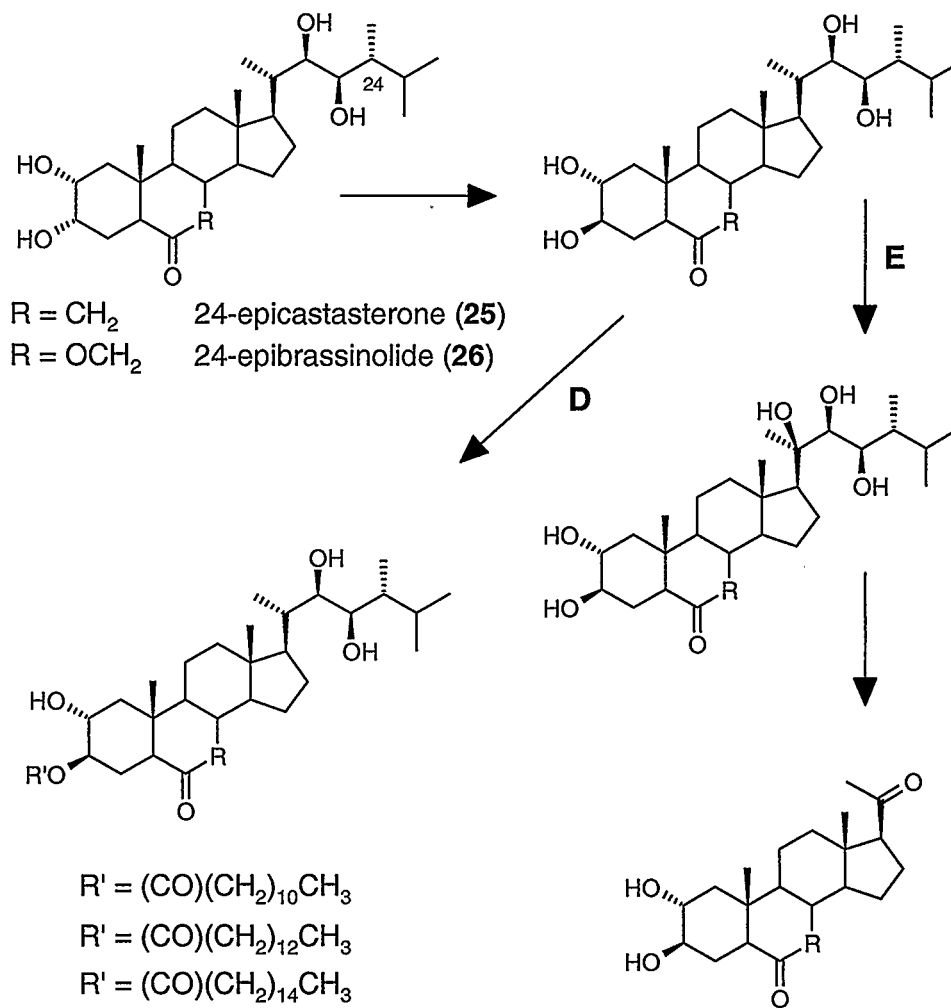
Cultures (*Lycopersicon esculentum*)³⁷⁻³⁹

1.4.2 Metabolism of 24-Epicastasterone (25) and 24-Epibrassinolide (26) in Serradella Cell Cultures (*Ornithopus sativus*)

Feeding studies using radiolabeled analogs of 24-epicastasterone (25) and 24-epibrassinolide (26) were also investigated in serradella cell cultures (*Ornithopus sativus*) to determine their metabolic fates.⁴⁰ Interestingly, there was no evidence of glucosylated metabolites in the growth medium. While this could imply an inability to secrete brassinosteroid conjugates, it could also mean that there is more than one general pathway of metabolic deactivation of brassinosteroids operating in plants. In fact, these investigators isolated metabolites from the culture medium that were identified as brassinosteroid lipophilic conjugates as illustrated in pathway D of Scheme 1.6.⁴⁰ The lipophilic conjugates were identified as fatty acyl esters of 24-epicastasterone (25) and 24-epibrassinolide (26). The culture medium also contained several nonconjugated brassinosteroid metabolites with side chain degradation as illustrated in pathway E of Scheme 1.6.⁴⁰

Thus, several catabolic pathways of metabolism have been established using cell cultures of tomato (*Lycopersicon esculentum*) and serradella (*Ornithopus sativus*). While obvious differences exist in these pathways, the common thread is side chain hydroxylation and conjugation both at the side chain and the A ring.⁴¹ These findings add support to the concept that several potential metabolic pathways exist in order for plants to regulate endogenous levels of brassinosteroids.

Scheme 1.6 Metabolism of 24-Epicastasterone (**25**) and 24-Epibrassinolide (**26**) in
Serradella Cell Cultures (*Ornithopus sativus*)⁴⁰



1.5 Bioassays for Brassinosteroids

Since the discovery of brassinosteroids by Grove *et al.*,¹⁷ there has been considerable interest in developing a reliable means to quantify their physiological effects. A bioassay is a biological system that is used to measure the effects of a known or suspected biologically active substance by utilizing a physiological response.⁴² Bioassays have also played a critical role in elucidating structure-activity relationships in the brassinosteroid family (see Section 1.6). There are four principal criteria that must be met in order for a bioassay to be useful:⁴²

1. It should be specific for the class of compound being assayed and not respond to other types of compounds.
2. It must be very sensitive in order to detect the small amounts of a given plant growth substance found in plant tissue.
3. The response time should be relatively short and the response of the plant tissue to the administered substance should be relatively easy to measure.
4. The substance being assayed must be present only at low levels or essentially be absent from the plant material.

A number of bioassays have been developed or adapted to study the physiological effects of exogenously applied brassinosteroids and brassinosteroid analogues. The wheat leaf-unrolling bioassay, the bean second internode bioassay, and the rice leaf lamina inclination bioassay will be discussed here.

1.5.1 Wheat Leaf-Unrolling Bioassay

Wada *et al.* reported that brassinosteroids show strong activity when subjected to the wheat leaf-unrolling bioassay.⁴³ This assay is quantified by the degree of unrolling of wheat leaf segments after a few days of incubation with the brassinosteroid. The general procedure for this bioassay begins by growing wheat seeds for 6 days, then removing the leaf segments. These leaf segments are then incubated in a growth medium containing various concentrations of the test substance, which, if active, results in unrolling of the wheat leaf. The degree of unrolling of the leaf segments was determined by measuring leaf width with a caliper. The widths of the control segments were observed to be about 2.0 cm while the widths of the leaf segments treated with brassinolide unrolled completely to about 3.6 cm. Although it was found that this is a reliable bioassay for brassinosteroids, it is only one-tenth as sensitive as the rice leaf lamina inclination bioassay which is discussed in section 1.5.3.

1.5.2 Bean Second Internode Bioassay

Mitchell *et al.*¹⁶ developed the bean second internode bioassay to determine the biological activity of their novel extract which they initially termed “brassins”. In this bioassay brassinosteroids evoke both cell elongation and cell division, resulting in characteristic morphological changes of the second internode.⁴⁴ In practice, this bioassay involves application of a lanolin-brassinosteroid paste to the second internode of 6 day old pinto bean seedlings (*Phaseolus vulgaris* L.). After an incubation period the second

internode shows not only elongation but also curvature, swelling, and splitting depending on the concentration of applied brassinosteroid. In particular, application of brassinolide at a dosage level of 10 ng per plant resulted in remarkable elongation, curvature, and swelling of the second internode.⁴⁴ Therefore, this bioassay is quantified by comparing differences in elongation of the internode between plants treated with brassinosteroids and control plants.

1.5.3 Rice Leaf Lamina Inclination Bioassay

The rice leaf lamina inclination bioassay was initially developed by Maeda⁴⁵ to study the physiological activity of auxins. The bioassay was later modified by Wada *et al.*⁴⁶ and then by Takeno and Pharis⁴⁷ to study the physiological effects of brassinosteroids. This bioassay involves the application of brassinosteroids to intact dwarf rice seedlings (*Oryza sativa* var. Tan-ginbozu is used in the Pharis lab) which results in a change in the inclination angle of the leaf lamina.⁴⁷ The procedure developed by Takeno and Pharis⁴⁷ begins by incubating dwarf rice seeds for three days under optimal growth conditions. Germinated seeds are then selected for consistent uniformity and planted in an appropriate growth medium and incubated for a further three days. Brassinosteroids are then applied to the seedlings in a variety of concentrations and the seedlings are incubated for a further three days under optimal growth conditions. Then, the angle between the second leaf lamina and its leaf sheath is measured using a protractor. Generally, control plants elicit an angle of approximately 165-175° (i.e. nearly upright), while plants treated with brassinosteroids elicit an angle as small as 50°,

depending on the activity of the particular brassinosteroid and the applied dose. Furthermore, it was established that the effects of brassinosteroids can be synergistically enhanced by the coapplication of the auxin indole-3-acetic acid (IAA) at a 1000 ng/plant concentration,⁴⁷ thereby increasing the detection limit of brassinosteroids. It is now generally accepted that the rice leaf lamina inclination bioassay⁴⁷ is an efficient, highly sensitive, and convenient method for detecting and quantifying the biological activity of brassinosteroids.

1.5.4 Extension to Field Applications

Care must be taken when choosing a bioassay to monitor the activity of brassinolide (and related analogues) when investigating their usefulness for agricultural applications, since compounds which show high activity in one or more bioassays may show little, if any, activity in field trials.⁴⁸ In the late 1980's three brassinosteroids [brassinolide, 24-epibrassinolide, and (22*S*,23*S*)-28-homobrassinolide], each of which was shown to elicit a strong response in bioassays, were selected as practical candidates for agricultural uses.

Field tests were carried out in China, Japan, and many other countries. However, there were conflicting reports regarding the success of the field trials. For example, in Japan, it was observed that as growth systems and environmental conditions changed, the plant growth-regulating effects of these brassinosteroids also varied considerably. On the other hand, researchers in China found that 24-epibrassinolide (**26**) accelerated the growth of cereals (wheat and corn), vegetables (watermelon, cucumber, and grape), and

tobacco.⁴⁹ Yields were also improved when 24-epibrassinolide (**26**) was applied at low concentration at specific growth stages of these plants.

While there are obvious discrepancies among the results of a number of different field trials, it is important to remember that there are many critical variables that must be considered when moving from the bioassay (a closed biological system where it is easy to maintain consistent environmental conditions) to the field. Several parameters must be investigated further (e.g. formulation, time, method of application) before the full potential of brassinosteroids for increasing the biomass and yield of crops, and for controlling the effects of diseases and environmental stress, can be realized.¹³

1.6 Structure-Activity Relationships of Brassinosteroids

A method to define the relationship between molecular structure and biological activity allows an investigator to demonstrate the activity of a biologically active compound based on inherent structural features. To date, the knowledge gained about structure-activity relationships of brassinosteroids has largely been due to biological activity data obtained from bioassay systems such as those described earlier. It is important to remember that the biological activity of a particular brassinosteroid may vary depending on the bioassay used. However, despite this caveat, it is accepted that structure-activity studies can provide useful information regarding the structural features needed for brassinosteroid activity.

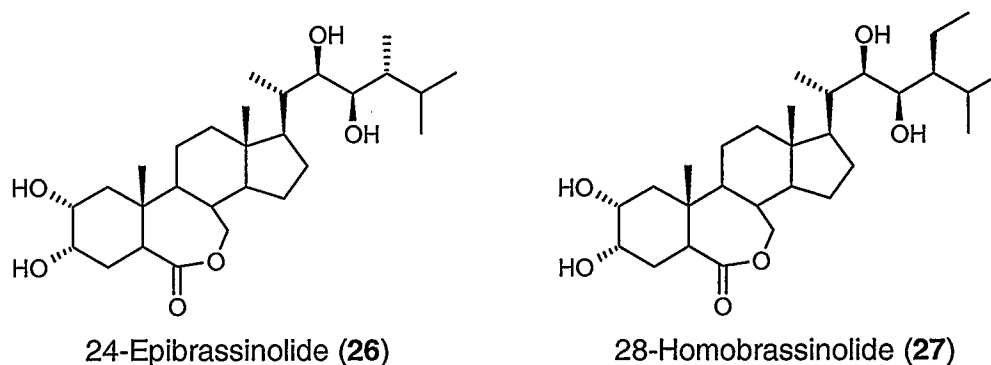
Therefore, structure-activity relationships of brassinosteroids have been studied in order to identify key features that are required for high biological activity.⁵⁰⁻⁷³ As a result

many qualitative structure-activity relationships have been established for the brassinosteroids. Such information is potentially useful, both for providing insight into possible brassinosteroid-receptor interactions and in the task of developing more effective and less expensive brassinosteroids for agricultural and horticultural applications.⁵⁰ A brief overview of brassinosteroid structure-activity relationships will be provided here.

1.6.1 Structure Activity Relationships in the Brassinosteroid Side Chain

Two examples of brassinosteroid analogues whose bioactivities were compared with **1** were 24-epibrassinolide (**26**)⁵¹ and 28-homobrassinolide (**27**),⁵² (Figure 1.6) both of which are more readily accessible than **1** from available starting materials. It is known that 24-epibrassinolide retains about one-tenth of the activity of brassinolide, while 28-homobrassinolide retains up to three-quarters of the activity of brassinolide at a variety of concentrations.^{52b}

Figure 1.6 The First Analogues of Brassinolide



Subsequently, a number of other side chain analogues of brassinolide were prepared (Figure 1.7) and subjected to structure activity studies in an effort to gain a greater understanding of the required constitution and stereochemistry of the side chain that is needed for maximum biological activity.⁵²⁻⁶¹ Takatsuto found that the *S*-configuration of an alkyl group at C-24 is required in order to retain high biological activity.⁵³ Furthermore, the *22R,23R*-relationship of the vicinal diol was shown to elicit much greater biological activity than the *22S,23S*-isomer (**29**), the *22R,23S*-isomer (**30**), and the *22S,23R*-isomer (**31**).^{53,54} It has recently been shown⁵⁵ that removal of the C-26 methyl group (**32**) results in weaker biological activity when compared to brassinolide.

It has also been shown that 25,26-bisnorbrassinolide (**33**),⁵⁶ 25-methylbrassinolide (**34**),⁵⁷ and 25-methoxybrassinolide (**35**)⁵⁸ all exhibit similar biological activity to that of brassinolide at equivalent dosage levels in the rice leaf lamina inclination bioassay. Interestingly, contrary to earlier reports,³⁸ 25-hydroxybrassinolide (**36**) exhibits no biological activity.⁶¹

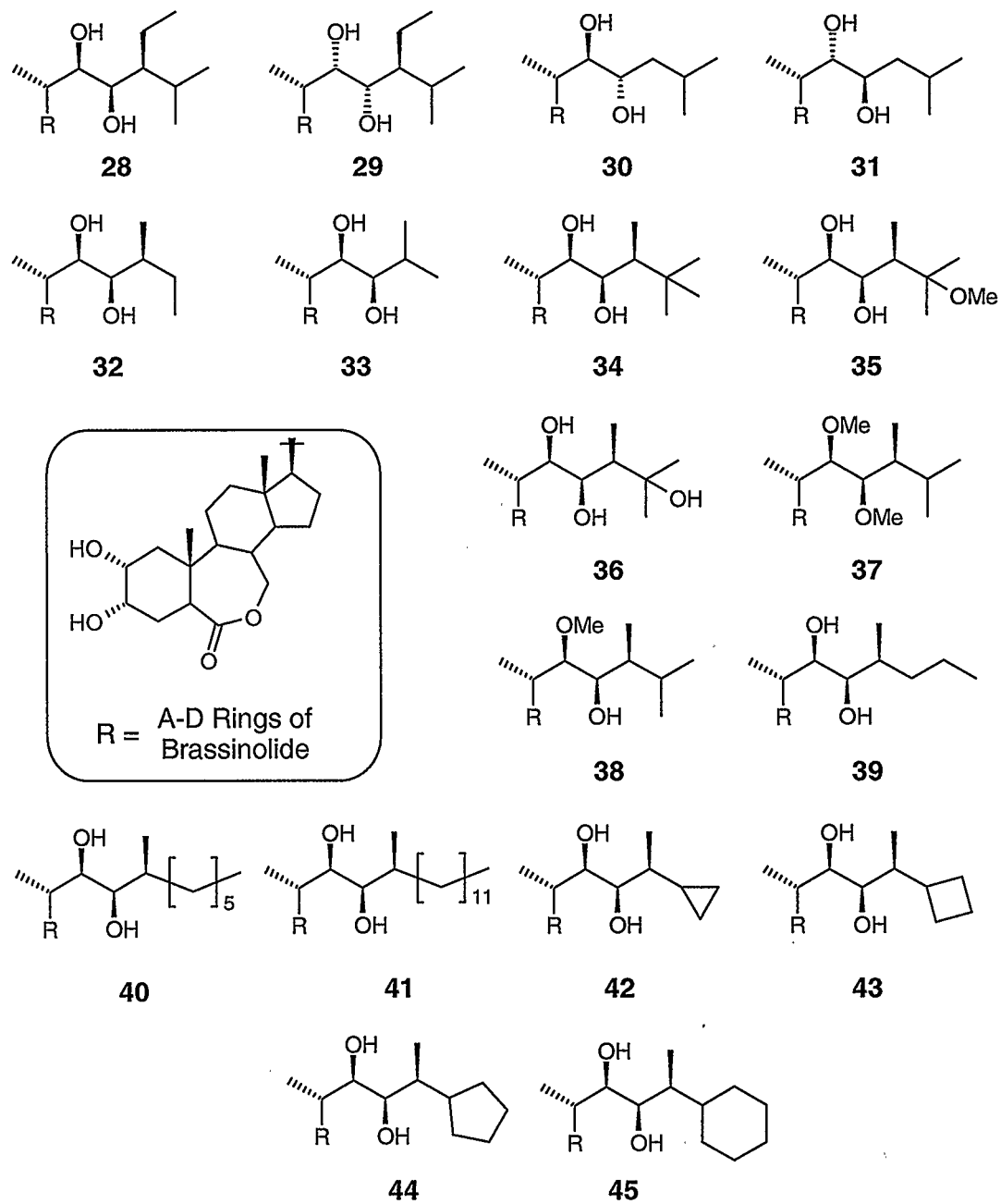
A number of recent studies by Back and Pharis and their coworkers⁵⁸⁻⁶¹ have further examined the effects of variation in the brassinolide side chain on biological activity. Brassinolide methyl ethers and the installation of other groups that could prevent metabolic deactivation were studied. Since it is known that metabolic deactivation is effected by glucosylation of free hydroxyl groups, the prospect of “protecting” certain hydroxyl groups was considered to be a potential way of increasing the persistence of brassinosteroids *in vivo*. Accordingly, Back and Pharis’ initial investigation into brassinolide side chain analogues revealed that 22,23-dimethyl ether (**37**) and to a lesser extent 22-methyl ether (**38**) had significant biological activity.⁵⁹ These results indicated

that free side chain hydroxyl functions are not essential for the characteristic brassinosteroid activity, suggesting that the interactions of brassinolide and its analogues with the putative receptor do not require hydrogen bond donation from the side chain hydroxyl groups.

Further investigations by Back and Pharis and their coworkers looked at a series of novel brassinolide analogues (Figure 1.7) that had different alkyl or cycloalkyl substituents in place of the isopropyl group at C-24.⁶⁰ In general, increasing activity was observed as the chain length or ring size of the C-24 substituent decreased. Remarkably, the novel cyclopropyl (42) and cyclobutyl (43) substituted analogues of brassinolide were approximately 5-7 times as active as **1** in the rice leaf lamina inclination bioassay. They appear to be the most potent brassinosteroids reported to date.⁶⁰ Meanwhile, the C-24 *n*-propyl (39) and cyclopentyl (44) derivatives had biological activity approaching or similar to that of brassinolide in the rice leaf lamina inclination bioassay. On the other hand, the cyclohexyl (45), *n*-hexyl (40), and *n*-dodecyl (41) derivatives showed lower or no biological activity. Interestingly, further enhancement of the biological activity of each of the active analogues was observed when the brassinosteroid was applied together with IAA (see Figure 1.1). This synergy between the brassinosteroids and IAA thus increased the biological activity of the novel brassinosteroids, including the extremely potent C-24 cyclopropyl and cyclobutyl substituted analogues, by 1-2 orders of magnitude. In summary, the salient structural features of the brassinolide side chain that are required for high biological activity are: 1) a vicinal diol or methyl ether thereof with 22*R*,23*R* stereochemistry; 2) *S* stereochemistry at C-24 and; 3) an appropriate alkyl

substituent at C-24 that is compact enough to fit into the recognition site of a putative receptor.

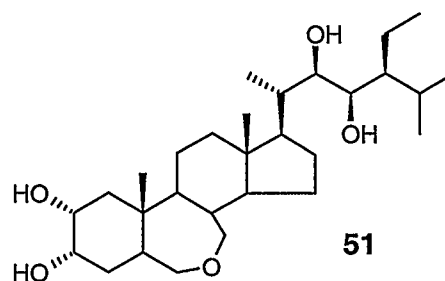
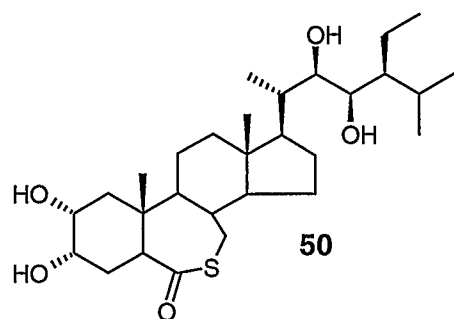
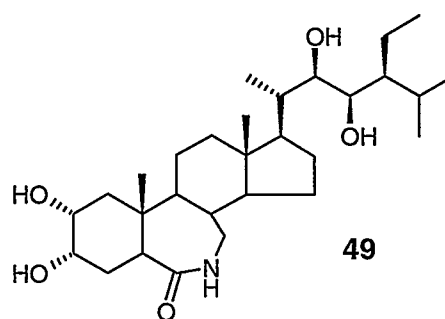
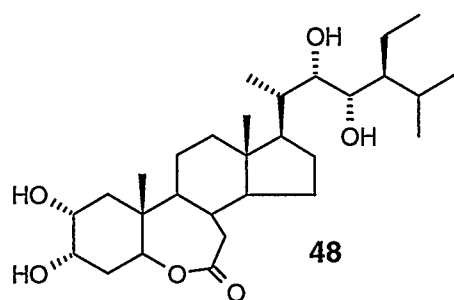
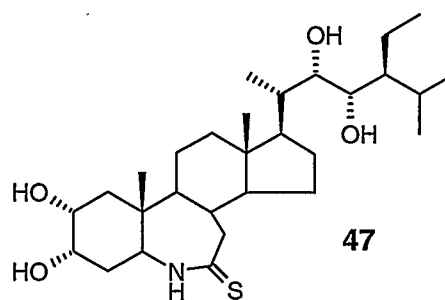
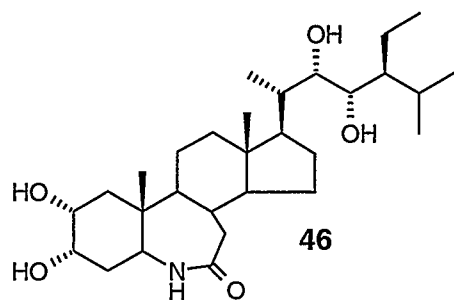
Figure 1.7 Side Chain Analogues of Brassinolide



1.6.2 Structure Activity Relationships in the Brassinosteroid Nucleus

There has been considerable interest in elucidating the structural requirements of the brassinolide nucleus, in particular the seven member B-ring (6-oxo-7-oxa) lactone and the $2\alpha,3\alpha$ vicinal diol moieties.⁶²⁻⁷³ Okada and Mori^{62a} were the first to report the effects of heteroatoms in the B-ring of the brassinosteroid framework, as illustrated in Figure 1.8. Among the brassinosteroid analogues that they developed were the 6-aza lactam **46**, 6-aza thiolactam **47**, and 6-oxa-7-oxo lactone **48**. However, only the 6-oxa-7-oxo lactone was biologically active. The 6-aza lactam was, as one would predict, the major regioisomer of the Beckmann rearrangement of the corresponding oxime. Anastasia *et al.*⁶³ were the first to report the anti-Beckmann 7-aza lactam **49** and Kishi *et al.*⁶⁴ showed that it was only weakly biologically active. Kishi *et al.*⁶⁴ also showed that 7-thiolactone **50** and the 6-deoxo derivative **51** exhibited only weak biological activity in the rice leaf lamina inclination bioassay. Unfortunately, it is difficult to make comparisons between these two structure activity studies because they used side chains containing different stereochemistry at C22 and C23, as shown in Figure 1.8. Moreover, all of these analogues contained the 28-homo side chain, making it difficult to make direct comparisons to the activity of brassinolide and other brassinosteroids containing the brassinolide side chain.

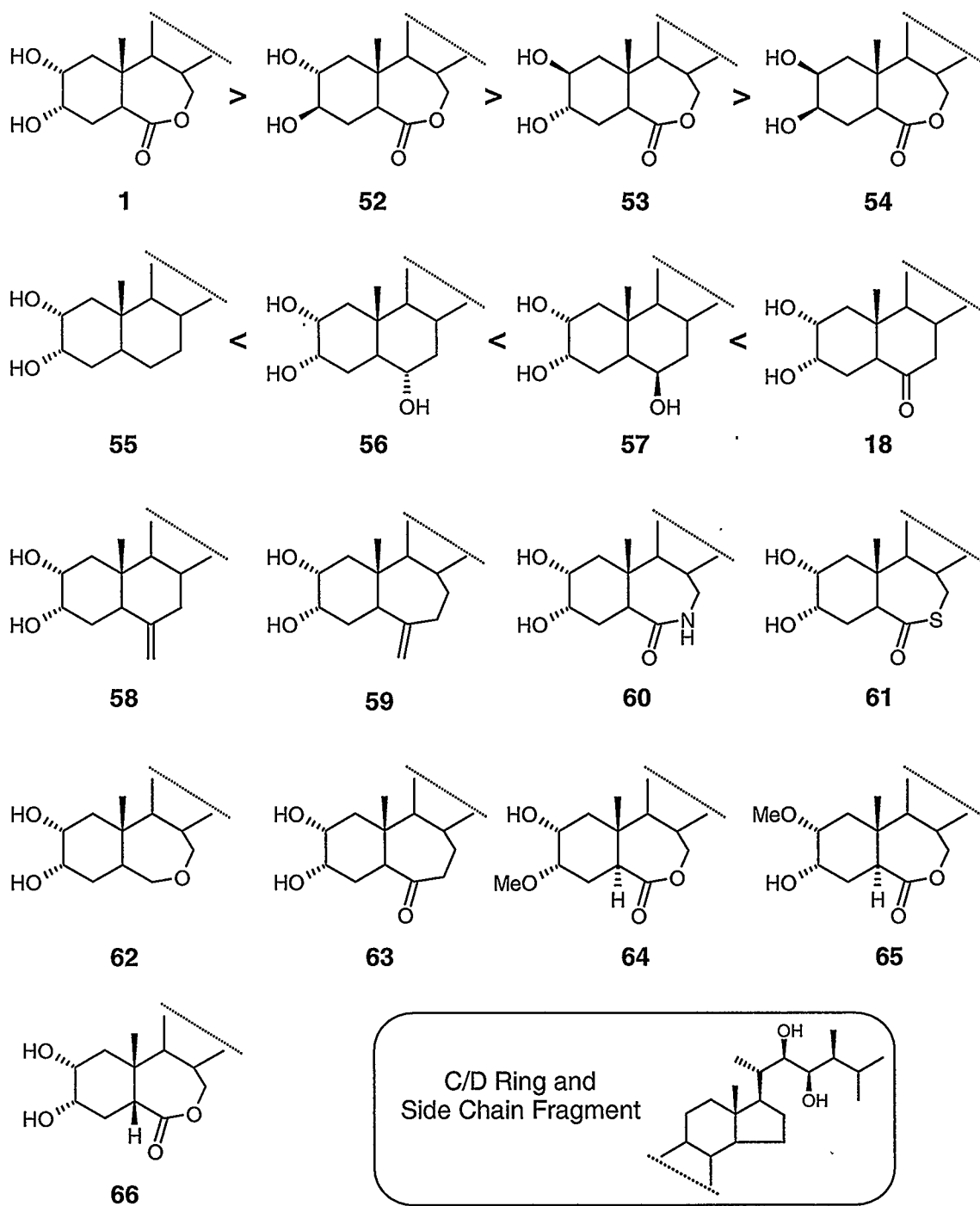
Figure 1.8 B-Ring Brassinosteroid Analogues



Hence, in an effort to draw solid conclusions about structure-activity relationships of the A and B rings of brassinolide, further investigations⁶⁷⁻⁷³ have used compounds containing the characteristic brassinolide side chain. For example, it was shown that the stereochemistry of the C2,C3 vicinal diol group is crucial in order to retain high biological activity.⁶⁷ The biological activity is greatest for the 2 α ,3 α isomer (**1**) but decreases substantially in the case of the 2 α ,3 β (**52**) and 2 β ,3 α (**53**) isomers, while in the case of the 2 β ,3 β (**54**) isomer there is essentially no observed biological activity (Figure 1.9). It is also known that as the oxidation state of the B ring system increases from the weakly active saturated B-ring analogue (**55**) to the comparably active C6 α and β -hydroxy analogues (**56** and **57** respectively) to castasterone, and finally to brassinolide, so does the biological activity (see Figure1.9).⁷²

Although brassinolide derivatives are more difficult to prepare than their 28-homo analogues, a new synthetic protocol (*vide infra*) has been developed by Back *et al.* that facilitates their preparation. Using this new protocol, Back and Pharis *et al.*^{69,72,73} prepared a number of novel brassinolide analogues containing the same side chain as brassinolide (Figure 1.9). It was found that the B-ring carbocycles 6-methylidenecastasterone (**58**) and 6-methylidene-B-homocastasterone (**59**) were completely inactive.⁶⁹ The heterocycles 7-azabracinolide (**60**), 7-thiabracinolide (**61**), 6-deoxybrassinolide (**62**), as well as B-homocastasterone (**63**), exhibited significant biological activity, but not as strong as that of brassinolide.

Figure 1.9 A/B Ring Analogues of Brassinolide



Back and Pharis *et al.* have also investigated the biological activity of brassinolide C2 and C3 methyl ethers.⁷³ They found that the 3-*O*-methyl derivative (**64**) (Figure 1.9) had modest biological activity at higher doses while the 2-*O*-methyl derivative (**65**) displayed only very weak biological activity and only at the highest doses.⁷³ Finally, Seto^{70,71} reported that the A/B *trans*-fused ring of brassinolide is an essential structural feature for high biological activity due to the fact that 5-epibrassinolide (**66**) had essentially no biological activity in the rice leaf lamina inclination bioassay. This was in contrast to an earlier report by Brosa *et al.*,⁶⁸ who claimed high activity for A/B-*cis* fused structures, but who employed less reliable single dose bioassays.

In summary, it has been established that the following structural features are required in the brassinolide nucleus for optimal biological activity: 1) the presence of the 2 α ,3 α vicinal diol moiety in the A ring; 2) the seven membered B-ring 6-oxo-7oxa lactone functionality; and 3) a *trans*-A/B ring junction.

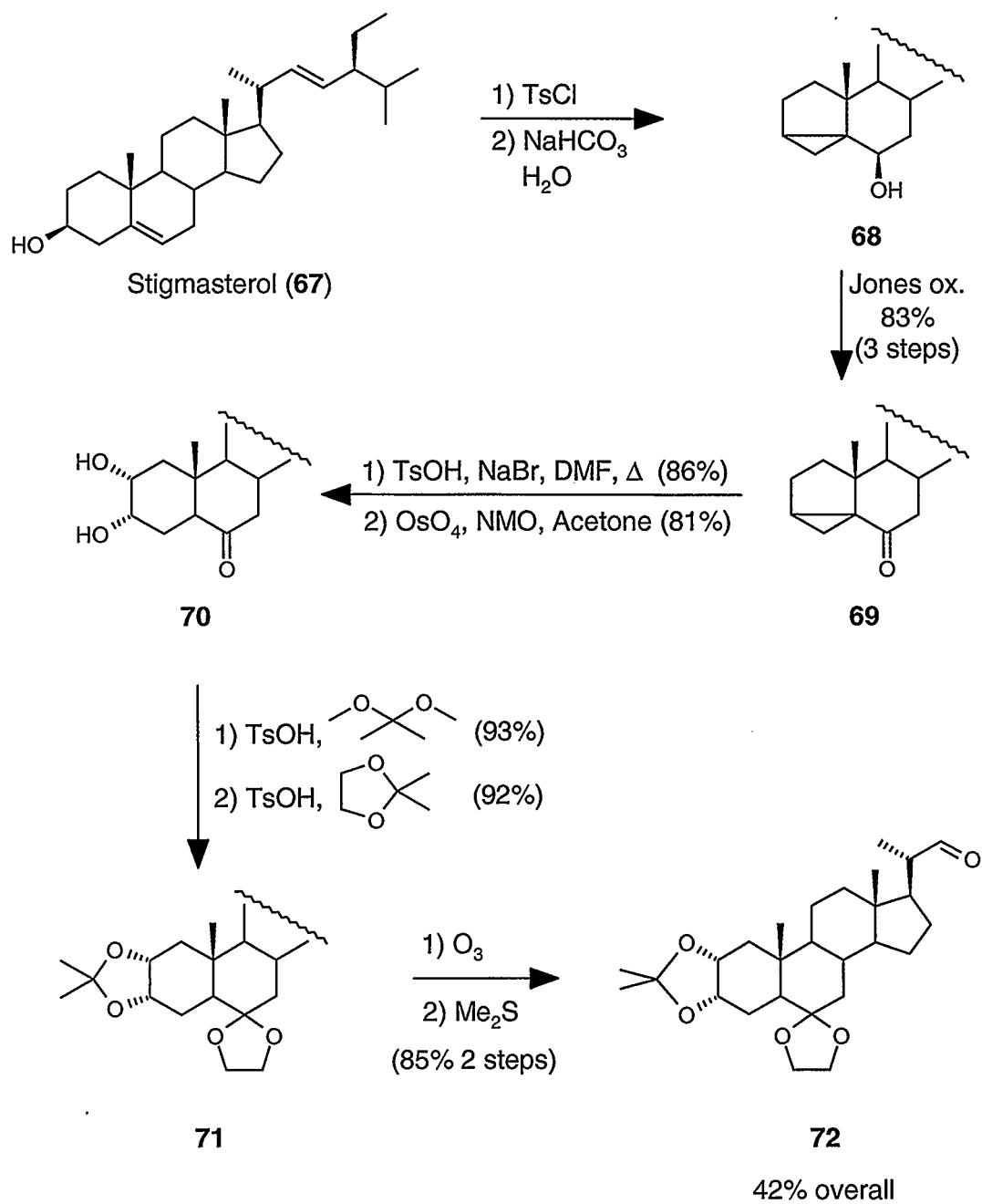
1.7 Synthesis of Brassinolide

Due to the potent activity of brassinolide as a plant-growth promoter and, accordingly, to its potential use in agriculture, brassinolide has given rise in recent years to a substantial amount of research towards the development of efficient ways to obtain this scarce material through various synthetic methods. The greatest challenge in the synthesis of brassinolide is the stereochemically demanding side chain that has four contiguous stereocenters, including a vicinal diol moiety. Unfortunately the existing syntheses of brassinolide are lengthy, expensive, and low yielding.

There are a number of reviews summarizing the state of the art of brassinolide synthesis.⁷⁴⁻⁷⁷ The most concise formal total synthesis to date has been developed by Back *et al.*⁷⁸ and gives brassinolide in ca. 10% overall yield in 12 steps from naturally occurring and commercially available stigmasterol (**67**). Since this is the most efficient method of brassinolide synthesis to date, it is the only one that will be considered here.

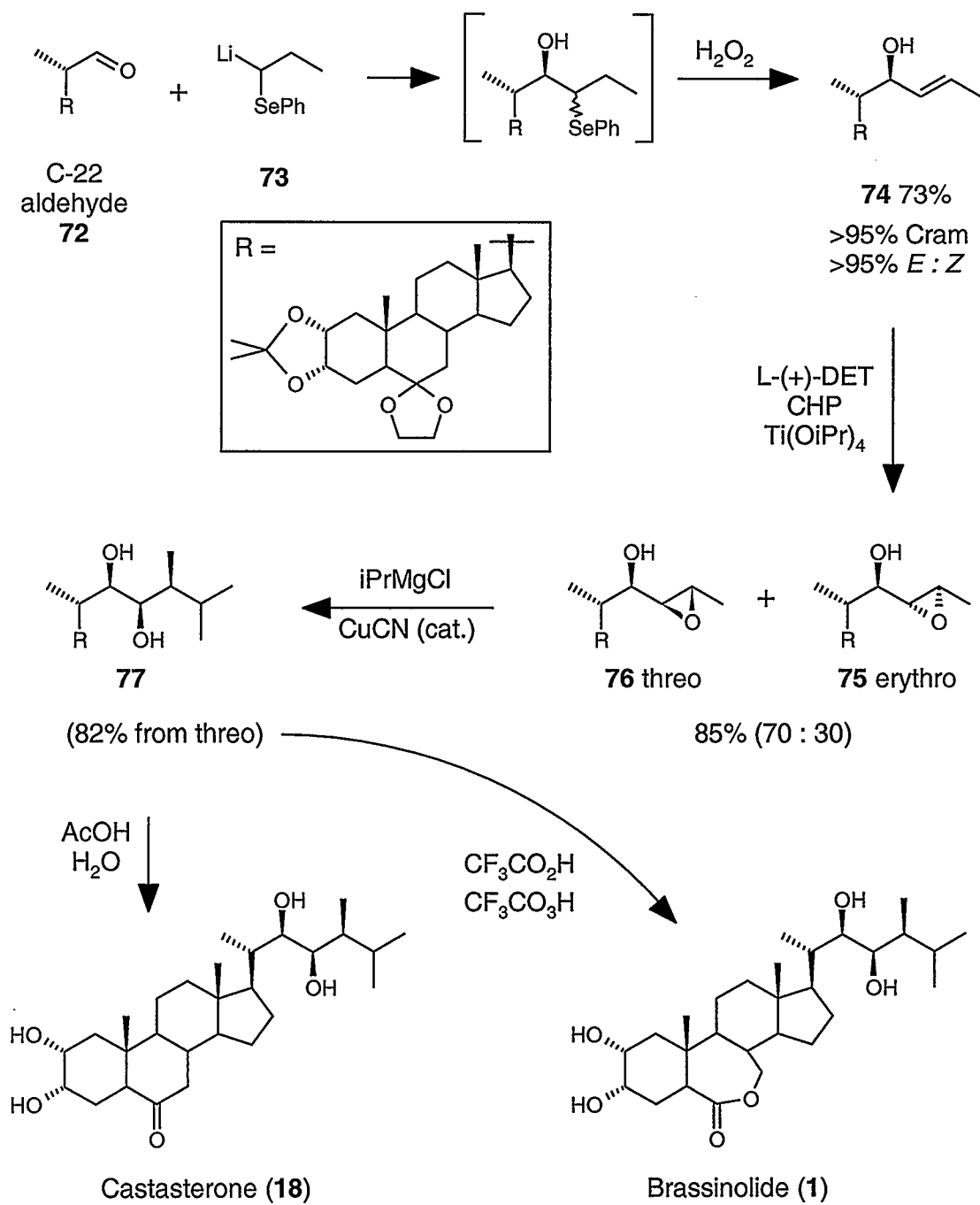
1.7.1 Back's Synthesis of Brassinolide

The efficient chemical synthesis of brassinolide and related analogues has been a major focus of the Back group in recent years.^{58,60,78,79} In 1997, Back and coworkers reported an improved procedure that provided excellent stereoselectivity and optimized yields that allow for the preparation of brassinolide on a multigram scale.⁷⁸ The synthesis begins from the abundant plant sterol stigmasterol (Scheme 1.7). Initially, stigmasterol was converted to its corresponding tosylate followed by solvolysis to give the 3,5-cyclosterol **68**. The resulting hydroxyl group was oxidized under conditions of the Jones oxidation to give the corresponding ketone **69**. Isomerization of the cyclopropyl group gave an unconjugated enone, which was subjected to dihydroxylation conditions with catalytic osmium tetroxide and stoichiometric NMO to give the α,α -*cis*-diol **70**. Protection of the diol and ketone functions by transketalization yielded bisketal **71**, which was suitable for ozonolysis of the double bond in the side chain. The ozonolysis reaction was worked up under reductive conditions with dimethyl sulfide to give the C-22 aldehyde **72**. Thus, the C-22 aldehyde was prepared in 42% overall yield by slightly modified literature procedures.^{80,81}

Scheme 1.7 Preparation of the C-22 Aldehyde **72**

Back's route to brassinolide starts with a highly selective Cram addition of selenium stabilized anion **73** to aldehyde **72**. The resulting epimeric mixture of selenides was immediately treated with hydrogen peroxide to effect an *in situ* selenoxide *syn* elimination that predominantly gave the *trans*-olefin. The *trans*-olefin was subjected to conditions of the Sharpless asymmetric epoxidation, which gave the epoxides **75** and **76** in the ratio of 70:30 in favor of the *threo* isomer. Treatment of the *threo* epoxide with isopropylmagnesium chloride gave the 22*R*,23*R* diol as the chief addition product. The completion of the synthesis was achieved in one step by treating diol **77** with trifluoroacetic and trifluoroperoxyacetic acids, which resulted in protecting group removal with concomitant Baeyer-Villiger oxidation to give brassinolide in 10% overall yield from the natural sterol stigmaterol. Castasterone can also be obtained by treating **77** with aqueous acetic acid.

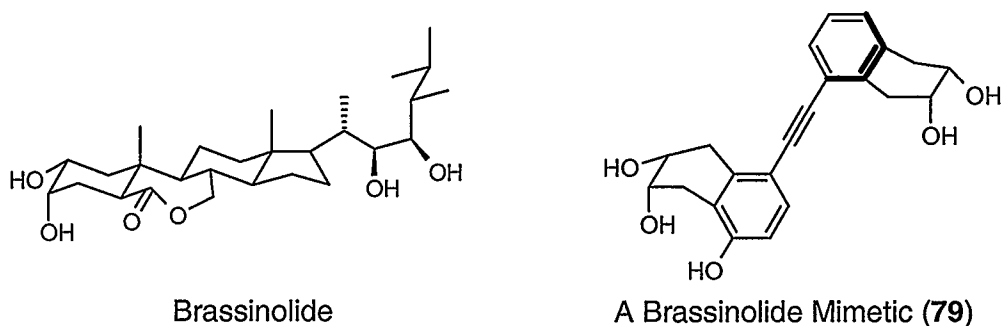
This provides an efficient, relatively high yielding, and highly stereoselective approach to this commercially valuable plant hormone. Unfortunately, the cost of preparing brassinolide on a large scale remains prohibitively expensive even with the use of Back's route.

Scheme 1.8 Back's Highly Selective and Efficient Route to Brassinolide⁷⁸

1.8 Design of Nonsteroidal Analogues

While Back's approach to brassinolide is highly selective and gives relatively good yields, it is still too costly for large-scale commercial applications. Although brassinosteroids are found widespread throughout the plant kingdom, natural sources are not considered a practical source of these compounds due to their low abundance in plants. Similarly, there are no known fermentation processes by which brassinosteroids can be prepared economically. Hence, the development of simple, easily available, and inexpensive compounds capable of mimicking the biological activity of natural brassinosteroids would be of considerable interest. Thus, based on a wide body of structure-activity information, Back and Pharis *et al.*⁸² set out to design nonsteroidal analogues consisting of two rigid subunits containing vicinal diol groups, joined by an appropriate linker, that would permit close superimposition of individual hydroxyl groups upon those of brassinolide. This concept is shown in Figure 1.10.

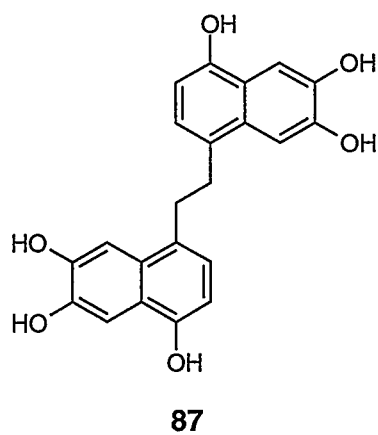
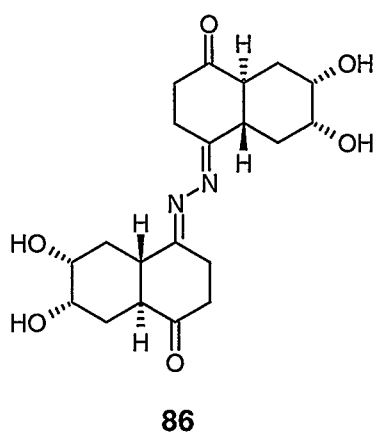
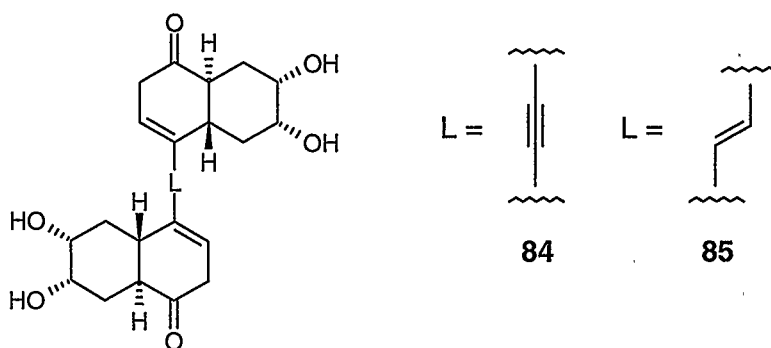
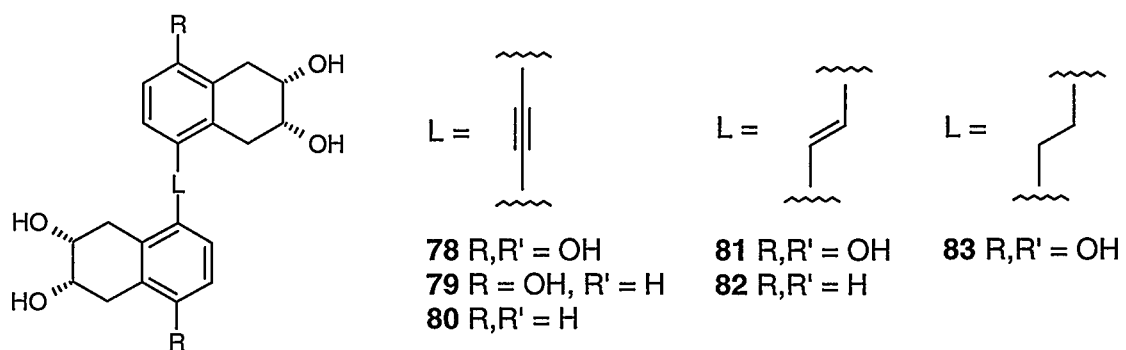
Figure 1.10 A Brassinolide Mimetic With Close Superimposition of Functionality

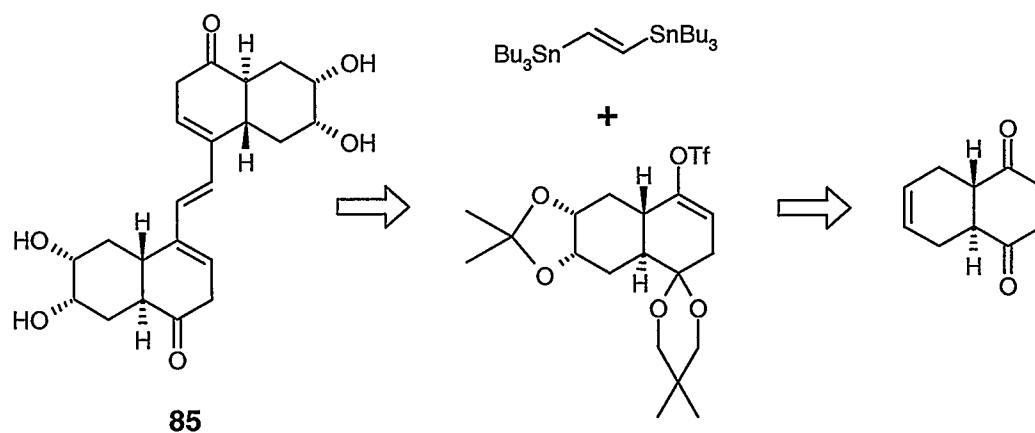
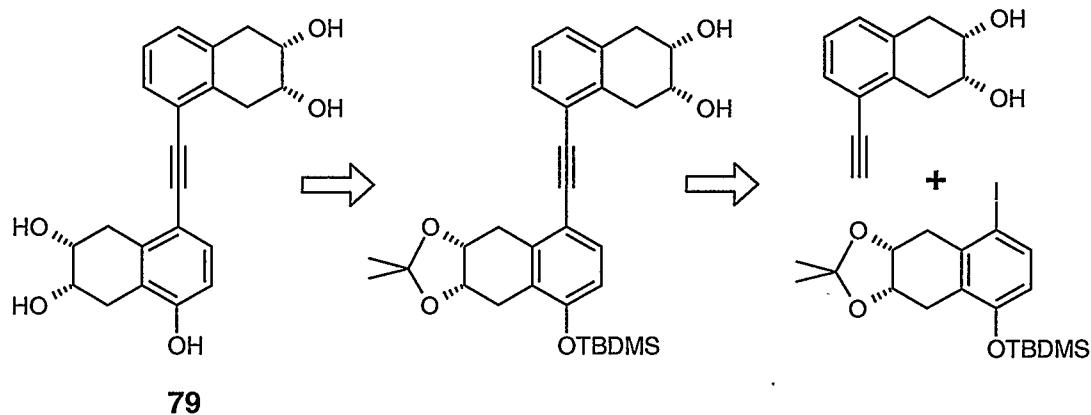


A series of bicyclic subunits containing the key diol groups, and generally an additional hydroxyl or ketone group to mimic the polar B-ring functionality of natural brassinosteroids, were linked by means of acetylene (**78-80, 84**), *trans*-alkene (**81, 82, 85**), -CH₂CH₂- (**83, 87**), or azine (**86**) groups (Figure 1.11).⁸² This afforded structures that superimposed relatively closely with brassinolide. Molecular modeling of several of the mimetics confirmed that there was considerable overlap of key functional features which made this work appear quite promising.

The mimetics were synthesized and subjected to the rice leaf lamina inclination bioassay. Most of the mimetics did not elicit significant biological activity. However, two of the mimetics (**79, 85**) elicited a substantial response, but only when coapplied with the auxin IAA, which is known to synergize brassinosteroid activity. Thus, acetylene **79** showed significant activity, while alkene **85** showed exceptional activity at doses as low as 0.001 ng per plant when appropriately formulated.⁸²

As mentioned earlier, these mimetics were strategically constructed by connecting the bicyclic subunits to an appropriate linker moiety. In all cases, the subunits were prepared as mixtures of diastereomers and enantiomers. In the non-aromatic systems, **84, 85**, and **86**, a *trans* geometry of the fused rings was maintained in all cases. A retrosynthetic analysis for the active acetylene **79** and alkene **85** is given in Scheme 1.9.⁸² These results therefore indicate that it is possible to prepare biologically active nonsteroidal analogues of **1** consisting of a relatively rigid scaffolding that holds key functional groups in the required spatial orientation to mimic the structure and geometry of brassinolide.

Figure 1.11 Nonsteroidal Mimetics⁸² of Brassinolide

Scheme 1.9 Retrosynthetic Analysis of Acetylene **79** and Alkene **85**

1.9 Objectives

There continues to be considerable interest in broadening the general understanding and commercial exploitation of the brassinosteroid family of plant growth hormones. Of particular interest is the development of nonsteroidal mimetics which could be synthesized from simple, easily available and inexpensive compounds, and which

would then be capable of mimicing the biological activity of natural brassinosteroids. Hence, there are two main objectives of the work described in this thesis. First, in an effort to develop more potent nonsteroidal analogues of brassinolide, we wished to prepare mimetic **79** as four individual stereoisomers in order to evaluate the effects of stereochemistry on biological activity. Secondly, a more general objective was to improve the efficiency of the synthesis of mimetic **79**. While similar efforts directed toward the more strongly bioactive mimetic **85** were also considered, **79** was finally selected for these studies because it is less stereochemically complex.

Chapter Two

Synthesis and Biological Evaluation of Nonsteroidal Brassinolide Mimetics

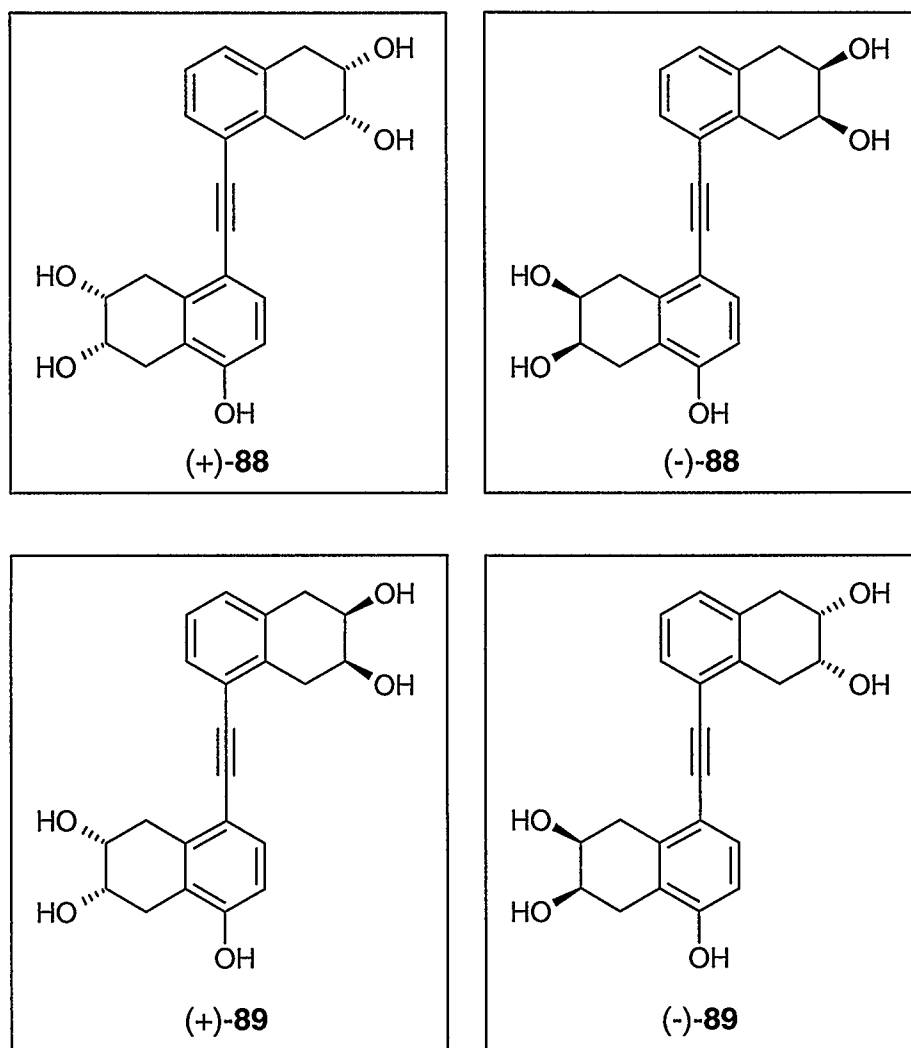
2.1 Introduction

It was mentioned in Chapter One that while there have been recent advances in the synthesis of brassinolide, any large scale production of this remarkable plant hormone remains impractical from an economical point of view. And, although brassinolide is found widespread throughout the plant kingdom, its extremely low natural abundance rules out extraction from plants as a potential commercial source of brassinolide. Hence, there is considerable value in the development of simple, easily available, and inexpensive compounds capable of mimicing the biological activity of natural brassinosteroids. As introduced in Chapter One, Back and Pharis *et al.*⁸² designed and synthesized a series of novel nonsteroidal brassinolide analogues consisting of two simple subunits, containing key structural features, joined by an appropriate linker (see Figure 1.11). These mimetics allowed close overlap of the vital structural features with those of brassinolide, presumably permitting recognition by the putative receptor. Remarkably, two of the mimetics (**79** and **85**) showed significant biological activity when coapplied with the auxin indole-3-acetic acid.⁸²

It is important to recall that these mimetics were initially prepared as mixtures of stereoisomers and were subjected to biological assay as such. In order to ascertain the effects of stereochemistry on the biological activity displayed by mimetic **79**, we were

interested in preparing each of the individual stereoisomers and subjecting them separately to the rice leaf lamina inclination bioassay.⁴⁷ This was undertaken with the hope of discovering one stereoisomer with increased biological activity relative to the mixture of stereoisomers. Therefore, the remainder of this thesis will focus on the preparation of mimetic **79** as individual stereoisomers (+)-**88**, (-)-**88**, (+)-**89**, and (-)-**89**, which are shown in Figure 2.1.

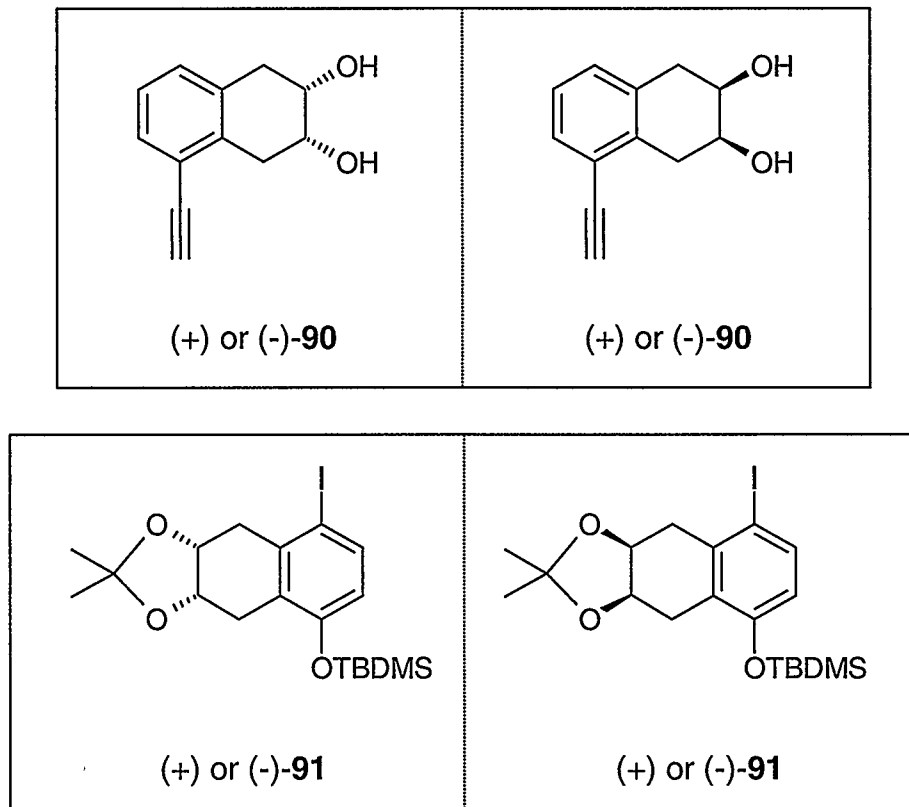
Figure 2.1 Mimetics (+)-**88**, (-)-**88**, (+)-**89**, and (-)-**89**.



2.2 Asymmetric Strategy

Since these mimetics are constructed from relatively simple building blocks (see Scheme 1.9) a logical starting point for an asymmetric synthesis would be to prepare the subunits as individual enantiomers. With enantiopure subunits, it would be possible to access all four of the stereoisomers (Figure 2.1) by coupling the appropriate combinations of the enantiomers, shown in Figure 2.2.

Figure 2.2 Required Chiral Subunits **90** and **91**

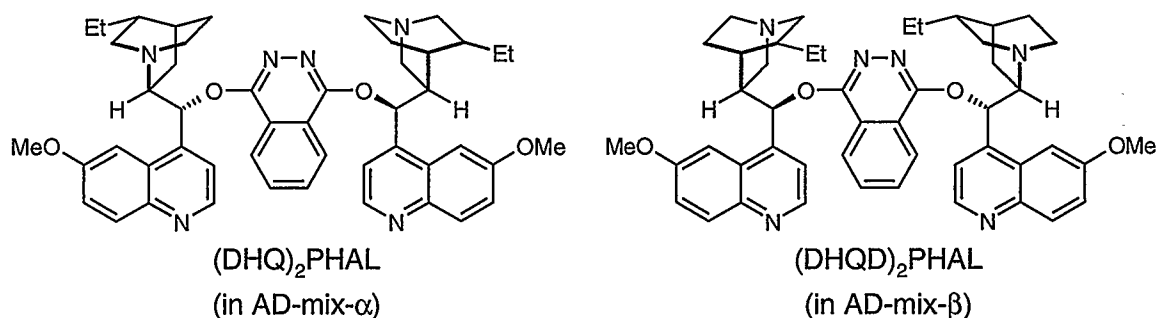


Hence it was necessary to develop a procedure that would allow access to each of the individual enantiomers of subunits **90** and **91** shown in Figure 2.2. Attempts to prepare the vicinal diol stereocenters of each subunit, potentially allowing access to each of the enantiomers, using catalytic asymmetric dihydroxylation (Sharpless dihydroxylation) are outlined in Section 2.3. A more successful approach to the individual enantiomers of each subunit was realized by conversion to diastereomers with a chiral resolving agent, followed by selective recrystallization of a single diastereomer, and cleavage of the chiral agent. This approach is discussed in Section 2.4. Synthesis of the fully functionalized enantiomeric subunits is outlined in Section 2.5 and the synthesis of mimetics (+)-**88**, (-)-**88**, (+)-**89**, and (-)-**89** is outlined in Section 2.6. Molecular modeling studies of the mimetics are discussed in Section 2.7. Measurements of biological activity were performed by Dr. R.P. Pharis and coworkers using the rice leaf lamina inclination bioassay,⁴⁷ and are presented in Section 2.8.

2.3 Sharpless Asymmetric Dihydroxylation

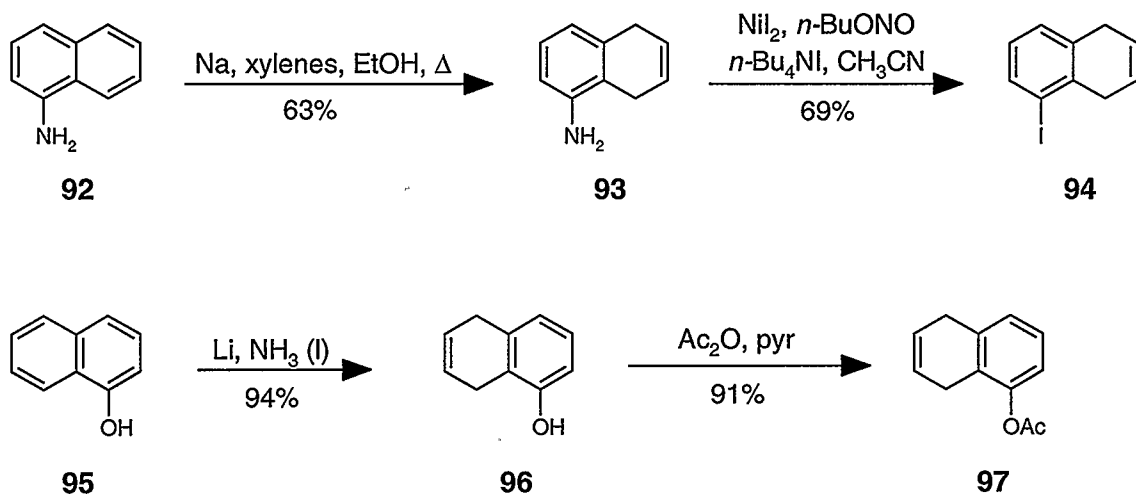
Osmium tetroxide-catalyzed asymmetric dihydroxylation of olefins using cinchona alkaloid derived ligands, also recognized as the Sharpless asymmetric dihydroxylation, is known for its broad scope and reliability for many types of substituted olefins on both the laboratory and industrial scale.⁸³ It is also known that the reaction is very easy to carry out since water and oxygen pose no problems. In fact, optimization studies have revealed that a 1:1 mixture of water and *t*-butyl alcohol is the solvent system of choice. Furthermore, it is possible to use a premix of all the necessary reactants [i.e. $K_2OsO_2(OH)_4$ as a nonvolatile OsO_4 source, chiral ligand (*vide infra*), K_2CO_3 , and $K_3Fe(CN)_6$].⁸³ This premix is commercially available as AD-mix- α or AD-mix- β depending on the chiral ligand present. The chiral ligand used in AD-mix- α is $(DHQ)_2PHAL$ while that in AD-mix- β is $(DHQD)_2PHAL$, both of which are shown in Figure 2.3. Note that DHQ and DHQD are diastereomers and not enantiomers, although ligands derived from these two “pseudoenantiomeric” alkaloids lead to diols of opposite configuration.

Figure 2.3 Cinchona Alkaloid Ligands in the AD-mix Reagents⁸³



Hence, the syntheses of olefins **94**^{84,85} and **97**^{86,87} were carried out according to literature procedures as outlined in Scheme 2.1.

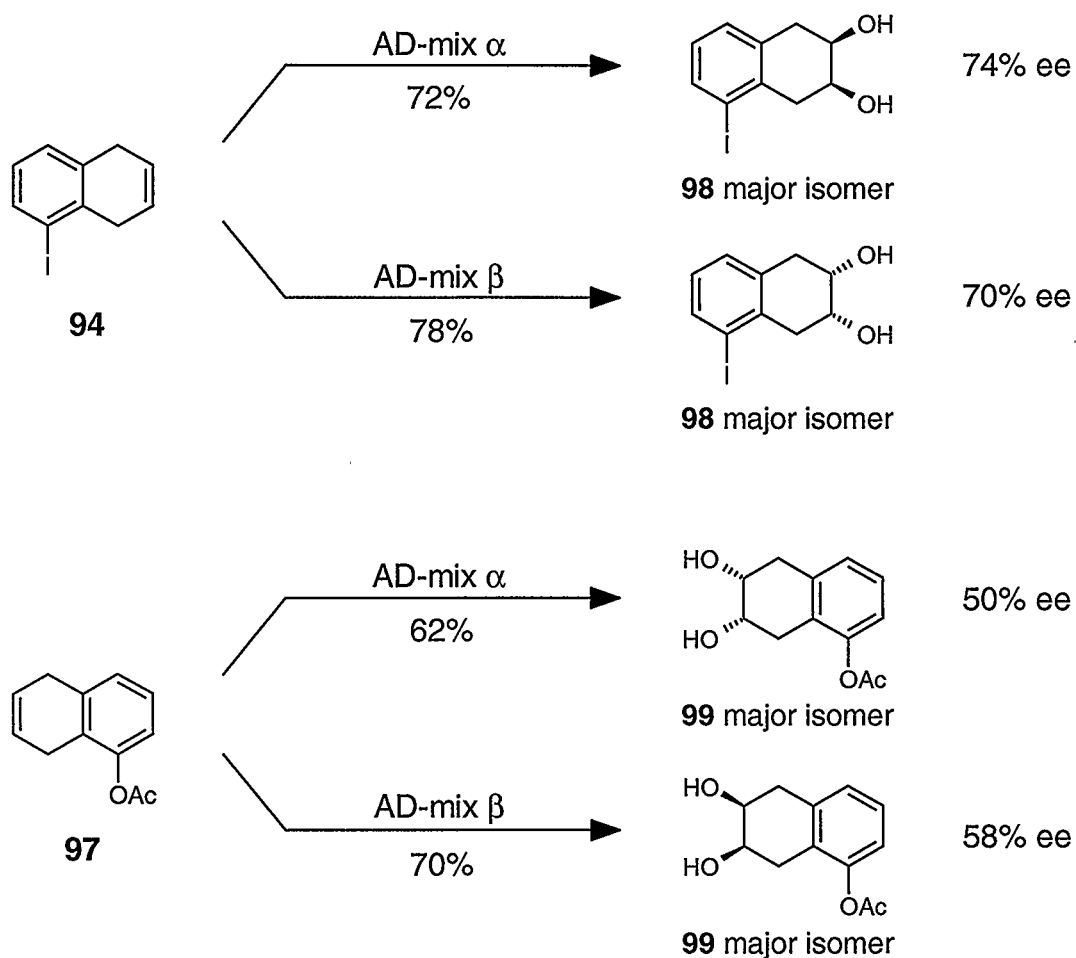
Scheme 2.1 Preparation of Olefins **94**^{84,85} and **97**^{86,87}



With olefins **94** and **97** in hand, we then subjected them to conditions of the Sharpless asymmetric dihydroxylation. Unfortunately, only marginal ee's were observed using this method. This is likely due to the diminished prochiral asymmetry inherent to both olefins resulting in only minimal enantiofacial selectivity during the course of the reaction.⁸⁸ These results were not surprising because it is generally recognized that *cis*-disubstituted olefins give diminished ee's compared to otherwise substituted olefins. The outcome of these studies is summarized in Scheme 2.2. The ee's were calculated from ¹H NMR integration of appropriate signals after converting the non-racemic diols to diastereomers (see Section 2.4). Absolute stereochemistry of the major isomer was

determined by single X-ray crystallography of the corresponding diastereomer (see Section 2.4).

Scheme 2.2 Results of the Sharpless Asymmetric Dihydroxylation

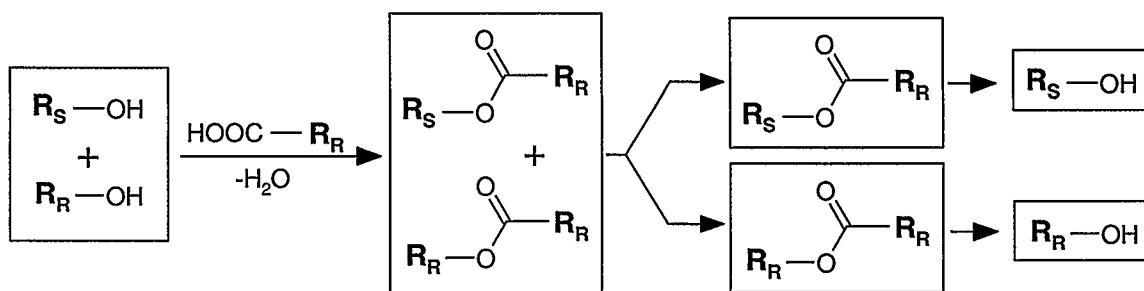


Clearly, this approach to the individual enantiomers of each subunit, on its own, was not suitable. Therefore, a second approach to obtain the subunits enantioselectively was undertaken by converting the mixture to diastereomers and resolving them by recrystallization.

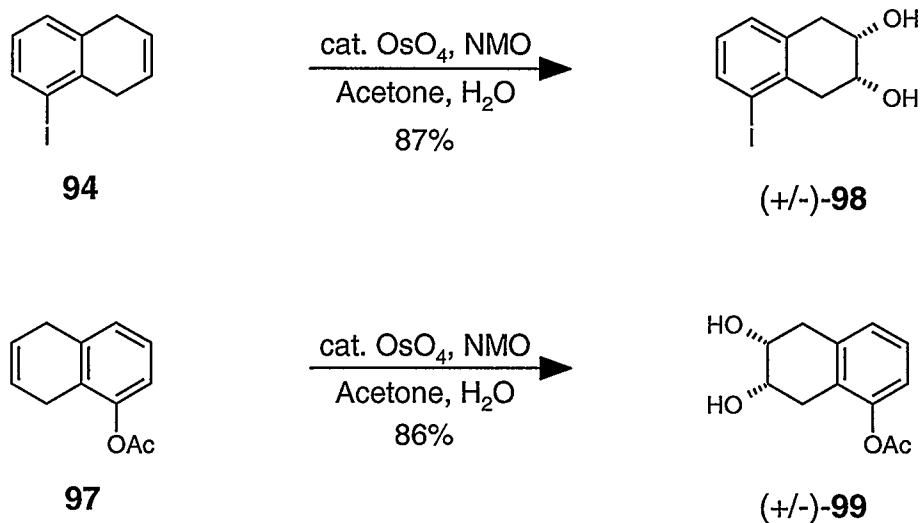
2.4 Conversion to Diastereomers

A mixture of enantiomers can be separated in several ways, the most common of which is conversion to diastereomers and separation of these by physical means, such as fractional recrystallization.^{89,90} The most common technique used to resolve alcohols involves formation of a covalent bond to a chiral resolving agent, such as a carboxylic acid, resulting in a diastereomeric mixture which may be separated by chromatography or fractional recrystallization. Removal of the chiral resolving moiety then completes the process. This concept is illustrated below in Scheme 2.3.

Scheme 2.3 Resolution of a Racemic Alcohol by Conversion to Diastereomeric Esters



It is conceivable that this concept could be extended to a racemic diol obtained from *cis*-dihydroxylation of olefins **94** and **97**. Dihydroxylation of these olefins following literature procedures gave racemic mixtures of *cis*-diols **98**⁸² and **99**⁹¹ as shown in Scheme 2.4.

Scheme 2.4 Preparation of Racemic *cis*-Diols **98**⁸² and **99**⁹¹

With the racemic diols **98** and **99** in hand, we wanted to investigate the reported usefulness^{92,93} of (*R*) and (*S*)-*O*-acetylmandelic acid⁹⁴ (**100**) as chiral resolving agents. Our investigations into the resolution of racemic *cis*-diols **98** and **99** using this chiral auxiliary are outlined in Sections 2.4.1 and 2.4.2 respectively.

2.4.1 Resolution of Racemic *cis*-Diol **98** with *O*-Acetylmandelic Acid

Dicyclohexylcarbodiimide⁹⁵ (DCC) has proven to be an exceptionally useful reagent in the field of synthetic organic chemistry. Among other synthetic applications, DCC has proven to be particularly useful in the formation of an ester from the condensation of an alcohol and a carboxylic acid.⁹⁶ In our studies, the DCC coupling was found to be highly efficient and practical in the conversion of racemic *cis*-diol **98** to a 1:1 diastereomeric mixture of the corresponding *bis*-(*R*)-*O*-acetylmandelate esters.

Conceivably, this diastereomeric mixture could then be separated into its individual diastereomers. Indeed, this was accomplished by recrystallization from absolute ethanol to give *bis*-ester (-)-**101** as a single diastereomer after several recrystallizations as shown in Scheme 2.5. NMR analysis failed to detect the other diastereomer. In order to confirm the absolute stereochemistry of C6 and C7 of ester (-)-**101**, a crystal was subjected to X-ray diffraction. The ester was found to have the *6R,7S* stereochemistry, as shown in Scheme 2.5. Details of the crystal structure of (-)-**101** are given in Appendix I and the ORTEP (Oak Ridge Thermal Ellipsoid Plot) diagram is shown in Figure 2.4.

Unfortunately, the more soluble diastereomer was not accessible from the mother liquor. This was due to the fact that (-)-**101** could not be entirely crystallized, leaving an unequal mixture of diastereomers in the mother liquor that could not be separated by flash chromatography or further crystallization. Thus, in order to access the remaining *6S,7R* stereoisomer of ester (-)-**101**, it was necessary to use (*S*)-*O*-acetylmandelic acid, the enantiomer of the chiral resolving agent used to prepare (-)-**101** (Scheme 2.5). For this reason, racemic *cis*-diol **98** was converted to a 1:1 diastereomeric mixture of the corresponding *bis*-(*S*)-*O*-acetylmandelate esters. Just as the mixture of diastereomers resulting from the (*R*) acid were resolved by recrystallization from absolute ethanol, so too was the diastereomeric mixture resulting from the (*S*) enantiomer. After several recrystallizations, *bis*-ester (+)-**101** was afforded as a single diastereomer as shown in Scheme 2.5. As expected, there was good agreement between the optical rotations of enantiomers (-)-**101** and (+)-**101**, thus confirming an enantiomeric relationship between the two stereoisomers.

Scheme 2.5 Preparation Of Esters (-)-101 and (+)-101

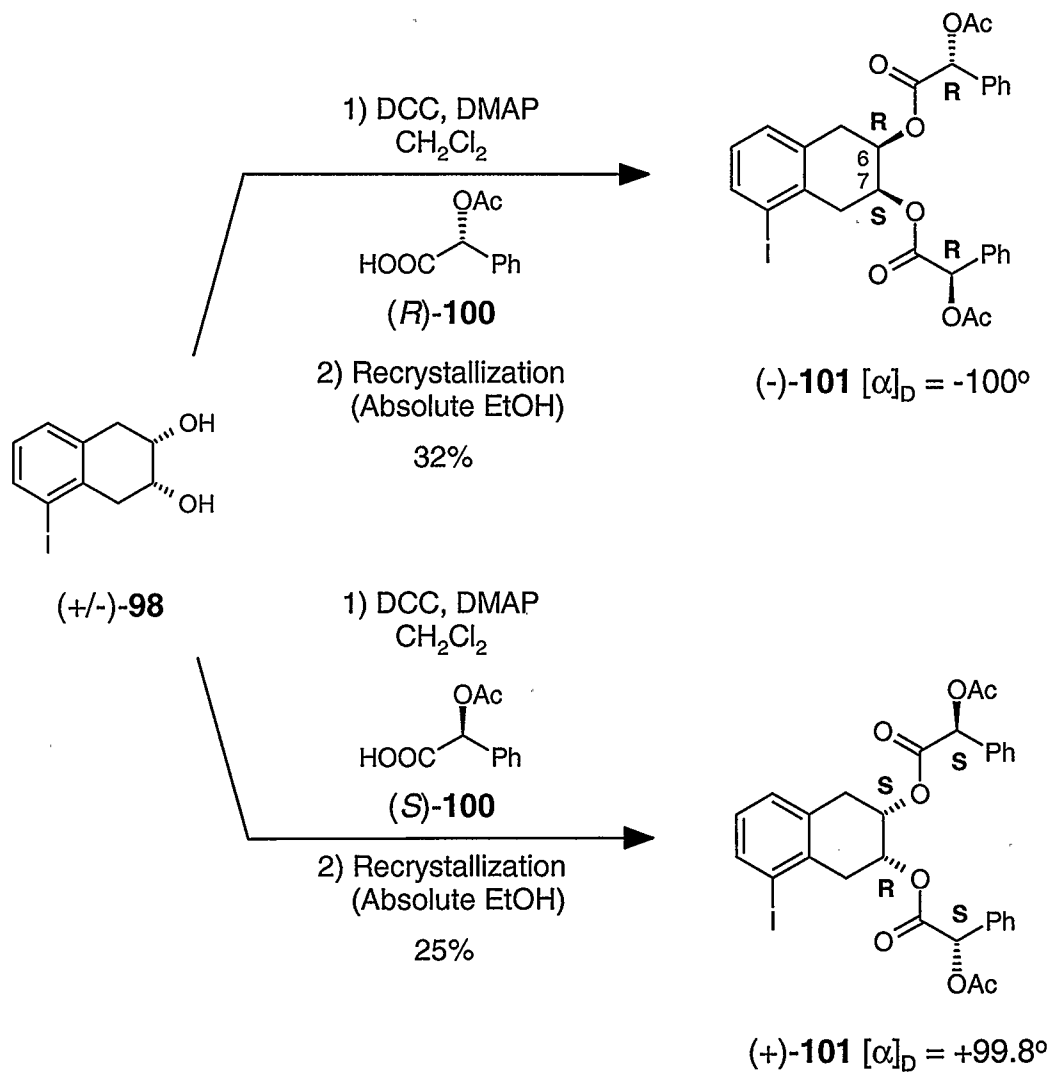
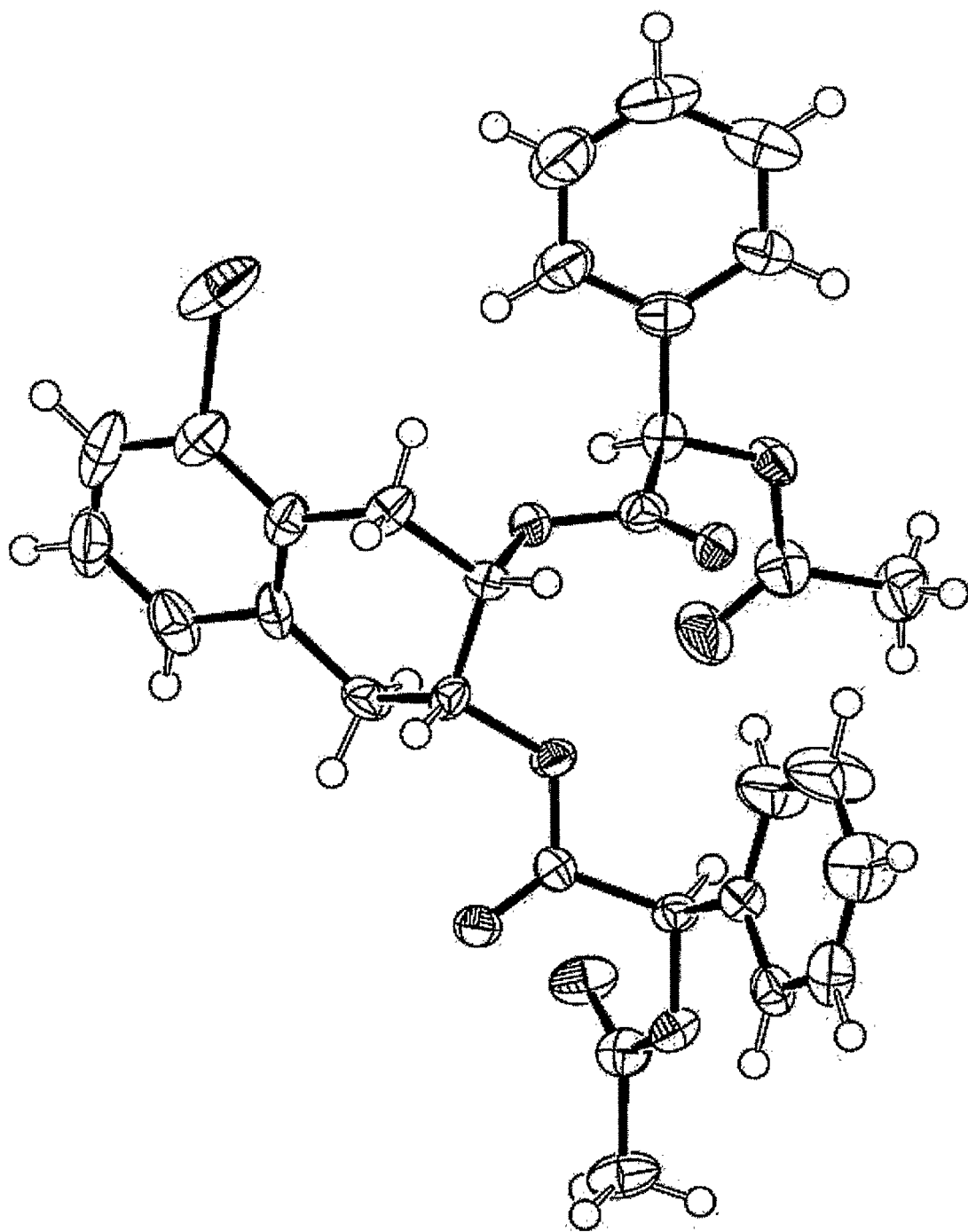


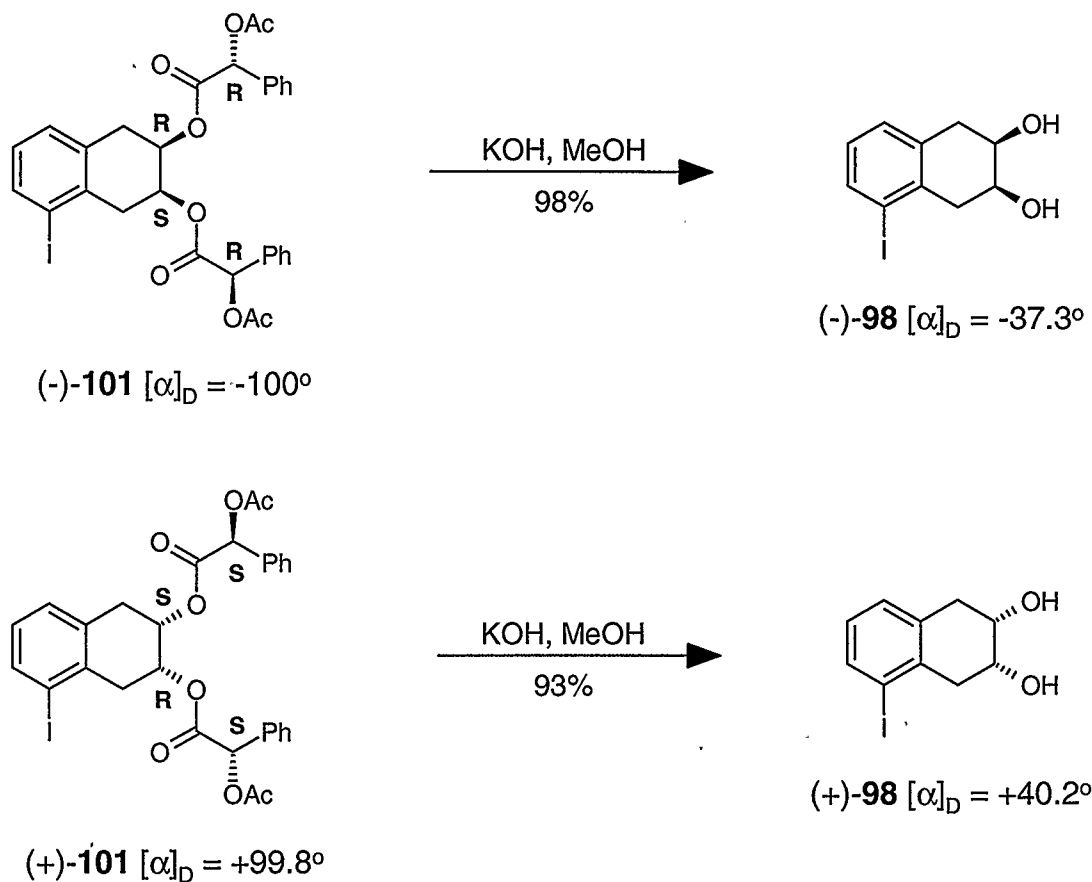
Figure 2.4 ORTEP Diagram of (-)-101



It is also interesting to note that although the mother liquors from each of the recrystallization procedures did not allow recovery of the other diastereomer, efforts were made to recycle the remaining iodide-functionalized subunit. This was effected by hydrolysis of the chiral auxiliary, recovery of the non-racemic diol, and condensation with the opposite chiral auxiliary, thereby facilitating selective recrystallization.

Furthermore, the same technique of attaching the matched chiral auxiliary to an enriched non-racemic mixture of diol **98**, in order to facilitate selective recrystallization, was applied to the enantioenriched *cis*-diols of **98** resulting from the Sharpless asymmetric dihydroxylation. Clearly, use of the appropriate chiral resolving agent would allow for an improved yield of the less soluble diastereomer upon recrystallization. Hence, this allowed for greater recovery of each enantiomeric subunit, as well as limiting the amount of the more soluble diastereomer remaining in the mother liquor.

With esters (-)-**101** and (+)-**101** in hand, containing opposite configurations at C6 and C7 of the subunit, cleavage of the mandelate moieties afforded each of the desired enantiomeric subunits. Treatment of the esters with KOH in methanol at room temperature gave each of the subunits, (-)-**98** and (+)-**98**, in excellent yield as outlined in Scheme 2.6. Close agreement between the optical rotations of each subunit once again indicated high enantiopurity.

Scheme 2.6 Cleavage of Resolving Agents to Yield (-)-**98** and (+)-**98**

2.4.2 Resolution of Racemic *cis*-Diol **99** with *O*-Acetylmandelic Acid

As a result of the successful resolution of diol **98**, a similar procedure for the resolution of racemic *cis*-diol **99** was envisioned using (*R*) and (*S*)-*O*-acetylmandelic acid. Therefore, in hopes of once again realizing selective recrystallization of a single diastereomer, racemic *cis*-diol **99** was converted to a 1:1 diastereomeric mixture of bis-(*R*)-*O*-acetylmandelate esters. Fortunately, several selective recrystallizations from methanol furnished bis-ester (-)-**102** as a single diastereomer as shown in Scheme 2.7.

Absolute stereochemistry of C6 and C7 of (-)-**102** was confirmed by single crystal X-ray diffraction and found to be *6R,7S*. Details of the crystal structure of (-)-**102** are given in Appendix II and the ORTEP diagram is shown in Figure 2.5.

Similarly to the first example in Section 2.4.1, the more soluble diastereomer was not accessible from the mother liquor. This was due to the fact that (-)-**102** could not be completely recovered from the mother liquor leaving an unequal mixture of diastereomers that could not be separated by chromatography or further crystallization. Thus, in order to access the remaining *6S,7R* stereoisomer of ester (-)-**102** it was again necessary to use (*S*)-*O*-acetylmandelic acid, the enantiomer of the chiral resolving agent used to prepare (-)-**102** (Scheme 2.7). Accordingly, racemic *cis*-diol (**99**) was converted to a 1:1 diastereomeric mixture of the corresponding *bis*-(*S*)-*O*-acetylmandelate esters. Following several recrystallizations from methanol, *bis*-ester (+)-**102** was recovered as a single diastereomer, as confirmed by ¹H NMR analysis, as shown in Scheme 2.7. Comparison of the optical rotation values of (+)- and (-)-**102** implied an enantiomeric relationship with high enantiopurity for each isomer.

As mentioned earlier, although the mother liquors from each of the recrystallization procedures leading to (+)- and (-)-**101** did not allow recovery of the other diastereomer, efforts were made to recycle the functionalized subunit. However, no effort was directed at recycling this series of subunit due to the fact that hydrolysis of the chiral resolving agent would also cleave the acetate group at C1, leaving a free phenol in place of the acetate group, which would make recycling of this product to the required diester problematic. It is also important to recall that the mother liquor could not be separated into each diastereomer by flash chromatography or further crystallization.

On the other hand, it was possible to make use of the enantioenriched *cis*-diols of **99** resulting from the Sharpless asymmetric dihydroxylation in order to facilitate selective recrystallization of a single diastereomer. Similar to the concepts mentioned in Section 2.4.1, use of the appropriate chiral auxiliary allowed for a greater recovery of the less soluble diastereomer and minimized the amount of the more soluble diastereomer remaining in the mother liquor.

Scheme 2.7 Preparation of Esters (-)-**102** and (+)-**102**

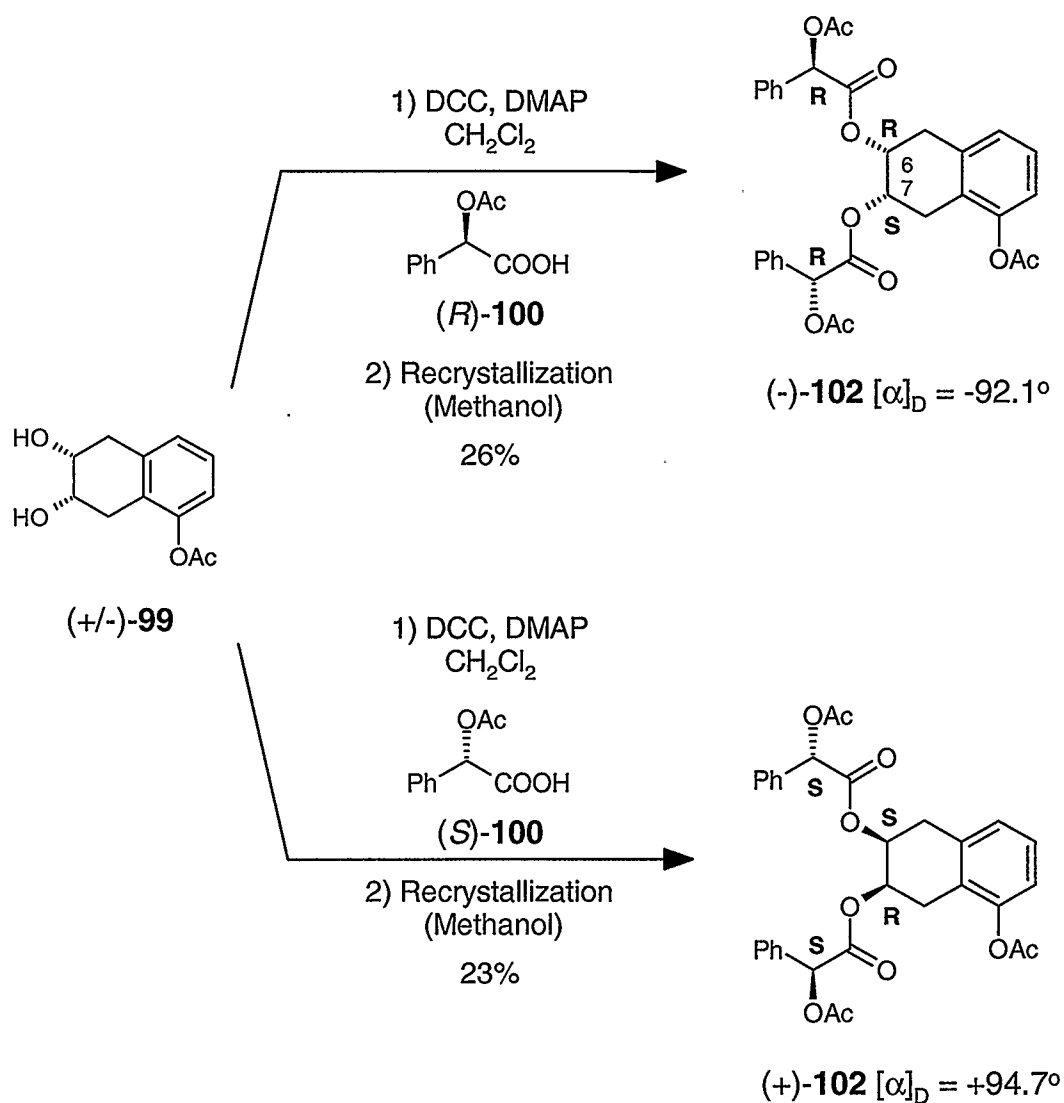
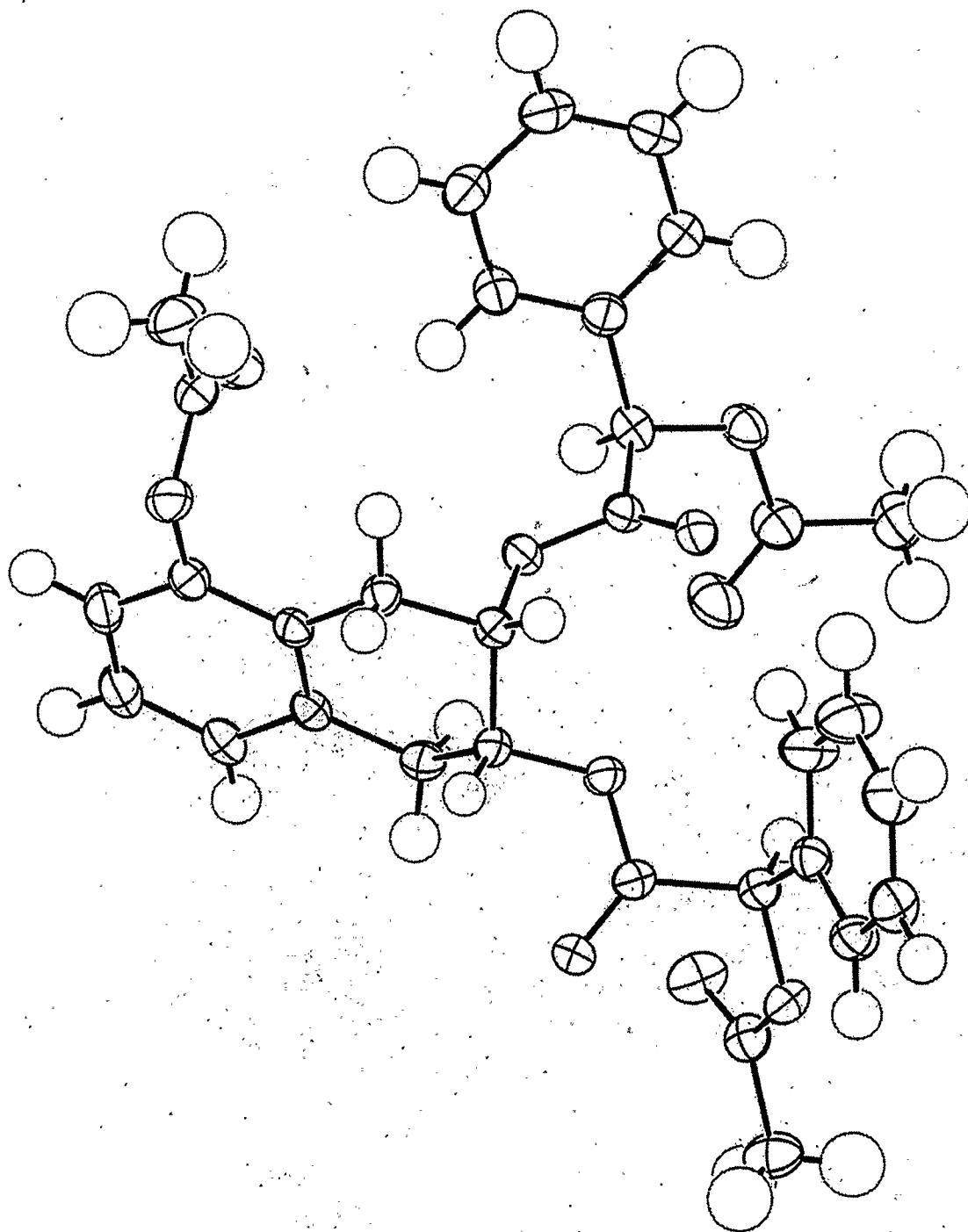
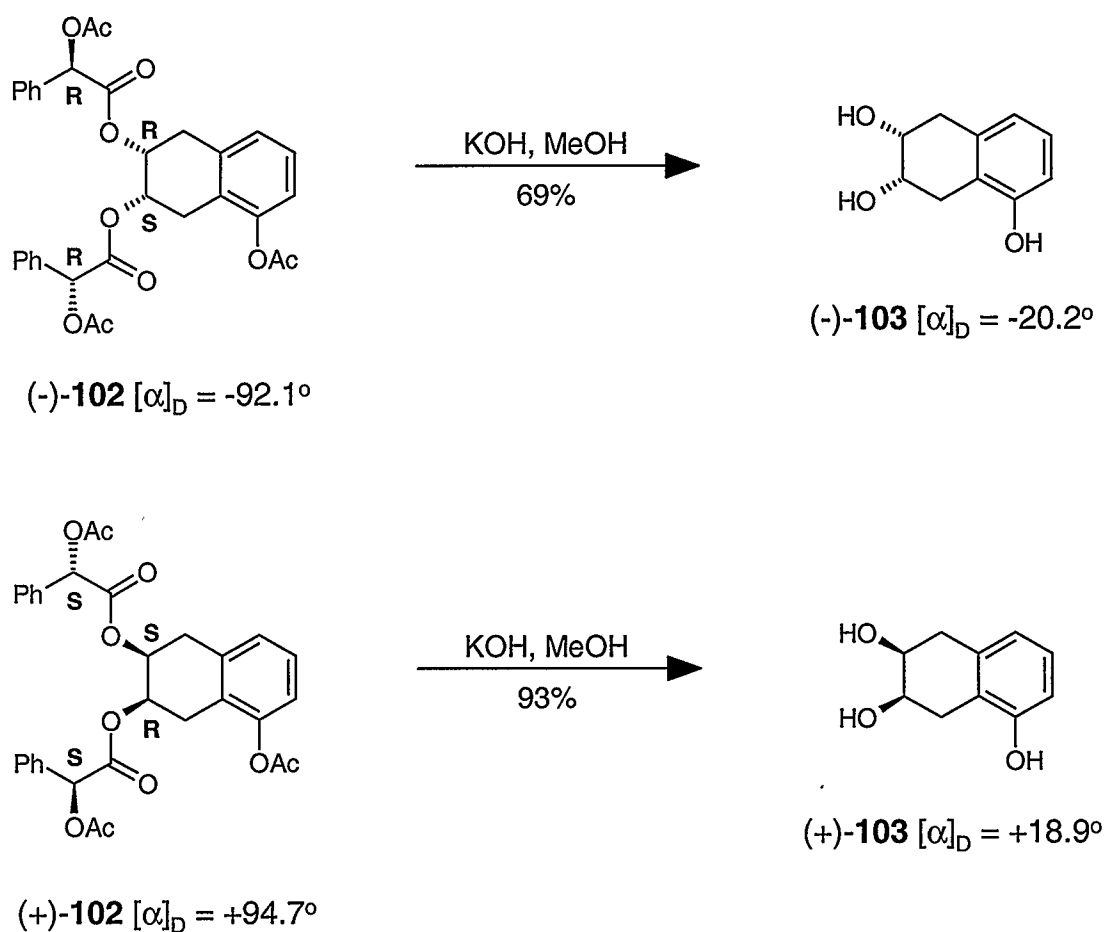


Figure 2.5 ORTEP Diagram of (-)-102



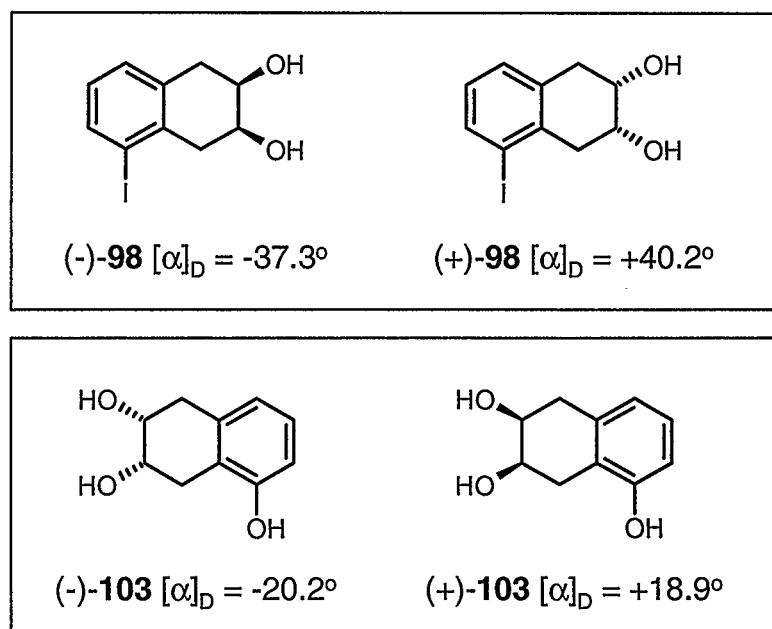
With esters (-)-**102** and (+)-**102** in hand, each containing the desired configurations at C6 and C7 of the subunit, cleavage of the mandelate moieties afforded each of the desired enantiomeric subunits. Treatment of the esters with KOH in methanol at room temperature gave triol subunits, (-)-**103** and (+)-**103**, in good yield as outlined in Scheme 2.8. Excellent agreement between the optical rotations of each diol indicated high enantiopurity.

Scheme 2.8 Cleavage of Resolving Agents to Yield (-)-**103** and (+)-**103**



With the preparation of each individual enantiomer of each vicinal diol subunit complete (Figure 2.6), all that remained was to functionalize the subunits for the Sonogashira reaction used to couple the subunits.

Figure 2.6 Summary of Vicinal Diol Subunits as Individual Enantiomers



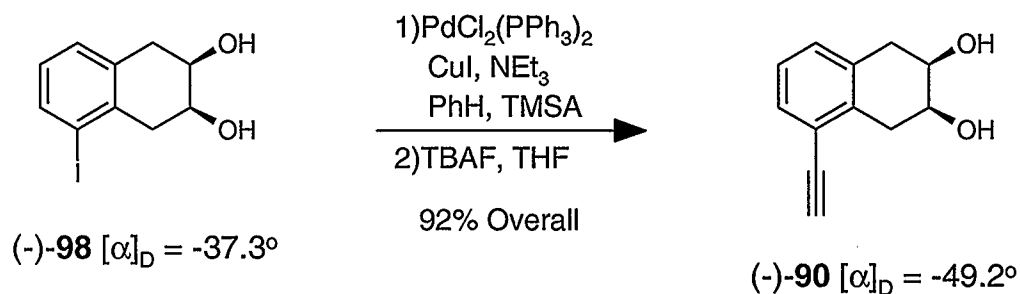
2.5 Synthesis of Enantiopure Subunits **90** and **91**

With the appropriate subunits available as their individual enantiomers, it was now possible to prepare them for the key cross-coupling reaction. This involves installation of appropriate protecting groups and, most importantly, the acetylenic linker that holds the subunits at the desired distance apart. The synthesis of both enantiomers of subunits **90** and **91** are outlined in Sections 2.5.1 and 2.5.2, respectively.

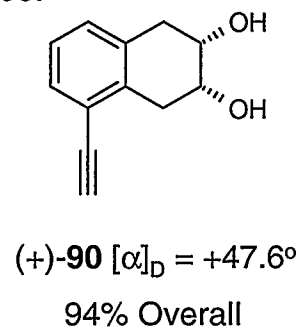
2.5.1 Synthesis of Subunits (-)-90 and (+)-90

Acetylenes (-)- and (+)-90 were prepared by slightly modified⁹⁷ literature procedures.⁸² Starting from iodide (-)-98, the iodide was subjected to a Sonogashira reaction with trimethylsilylacetylene (TMSA) as shown in Scheme 2.9. The resulting silylacetylene was immediately treated with tetra-*n*-butylammonium fluoride to reveal terminal acetylene (-)-90 in excellent yield over two steps. Similarly, acetylene (+)-90 was prepared from iodide (+)-98 (Scheme 2.9).

Scheme 2.9 Preparation of Acetylenes (-)-90 and (+)-90



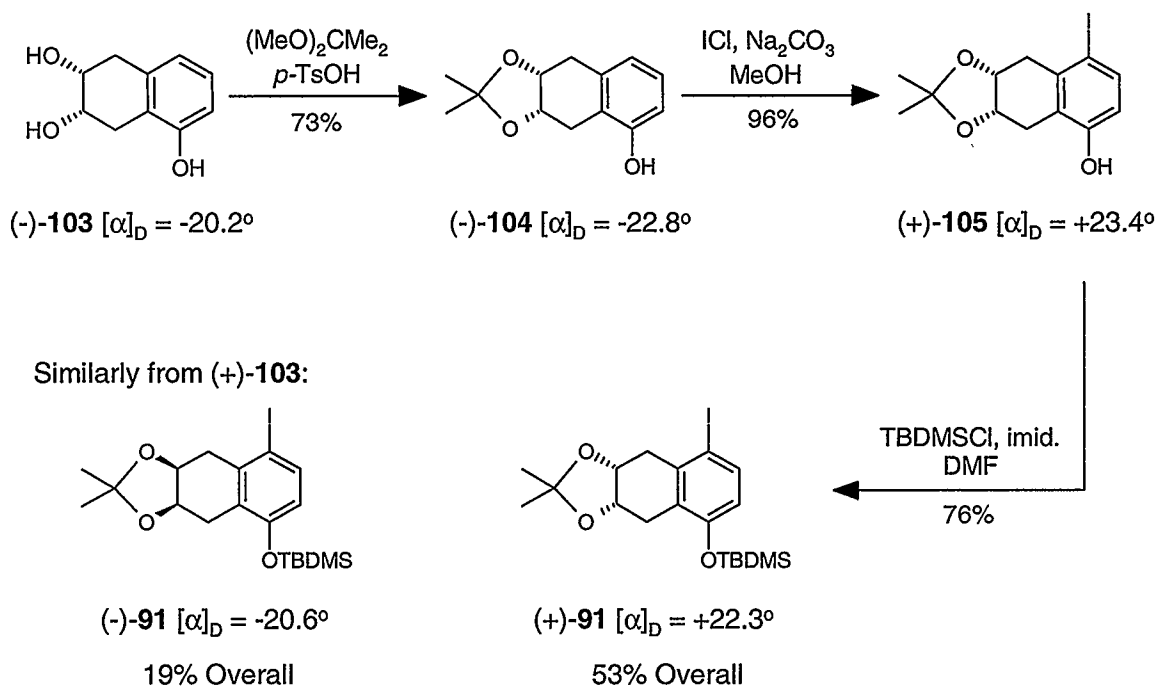
Similarly, from (+)-98:



2.5.2 Synthesis of Subunits (-)-91 and (+)-91

Following a literature procedure,⁸² triol (-)-103 was converted to phenol (-)-104 using dimethoxypropane and catalytic *p*-toluenesulfonic acid as outlined in Scheme 2.10. Phenol (-)-104 was then iodinated⁹⁸ using iodine monochloride to yield phenol (+)-105 in excellent yield. Finally, protection⁸² of the phenol using *t*-butyldimethylsilyl chloride gave the corresponding iodide (+)-91 in good yield as a pure enantiomer. Similarly, the enantiomer, (-)-91 was prepared following the same synthetic protocols starting from triol (+)-103 (Scheme 2.10).

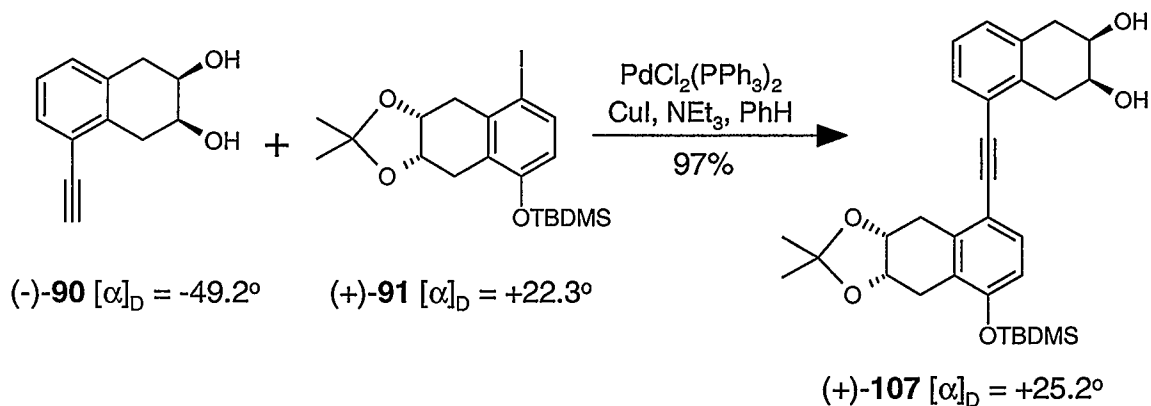
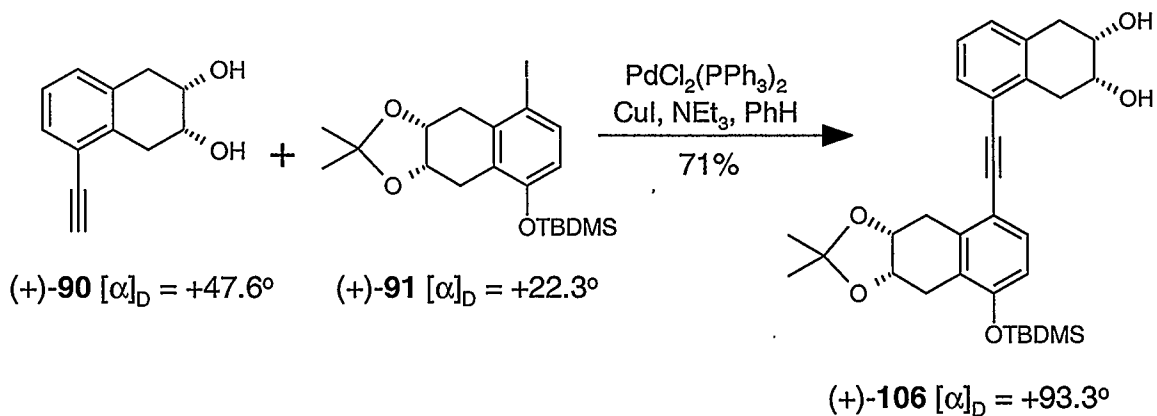
Scheme 2.10 Preparation of Iodide (-)-91 and (+)-91



2.6 Synthesis of Mimetics

With the desired chiral subunits in hand, each available as an individual enantiomer, all that remained was coupling of the appropriate subunits to realize the four stereoisomers of **88** and **89**. This was achieved using a Sonogashira reaction following slightly modified⁹² literature procedures,⁸² as outlined in Scheme 2.11. The preparation of enantiomers (-)-**106** (63%, $[\alpha]_D = -92.8^\circ$) and (-)-**107** (83%, $[\alpha]_D = -25.8^\circ$) was achieved using the corresponding subunits following the protocol described in Scheme 2.11.

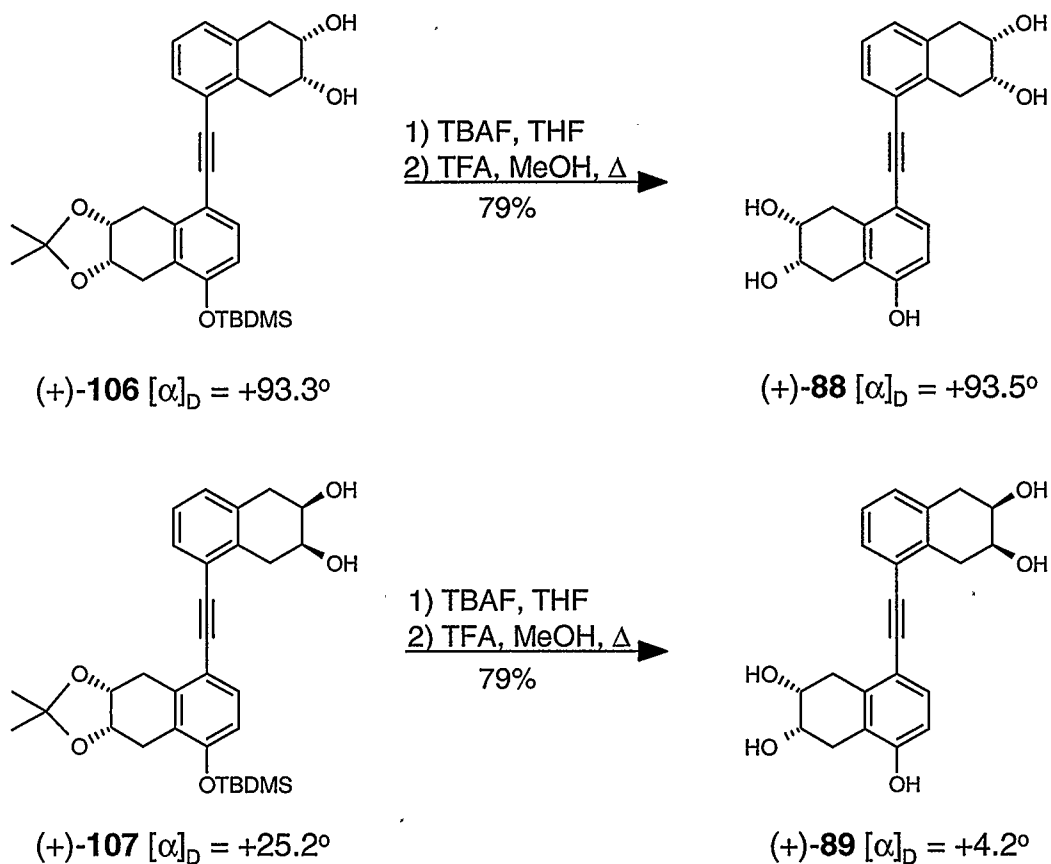
Scheme 2.11 Coupling of Subunits



It is worthwhile to mention that yields of this key cross-coupling step were substantially improved compared to the initial work⁸² when the mimetic was prepared as a mixture of enantiomers and diastereomers. The milder conditions reported by Grieco *et al.*⁹⁷ afforded the cross-coupled products (+)-**88**, (-)-**88**, (+)-**89**, and (-)-**89** in good to excellent yields (see Scheme 2.11), compared to the yield of 54% in the original work.⁸²

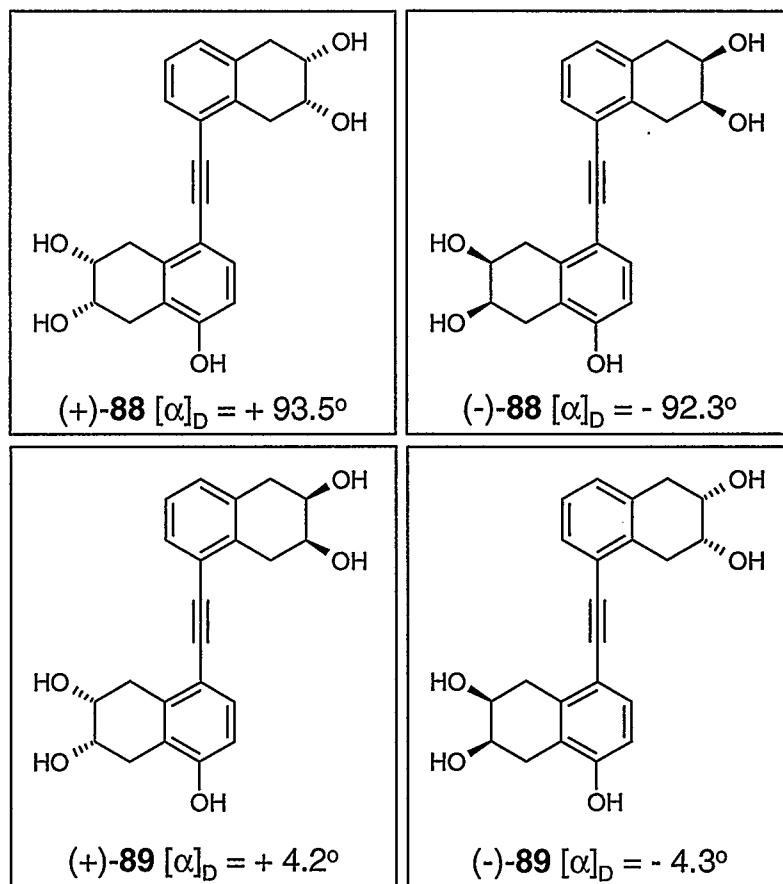
Deprotection of the coupled products afforded the desired mimetics (+)-**88** and (+)-**89** as described in Scheme 2.12. Although not shown here, enantiomers (-)-**88** (63%, $[\alpha]_D = -92.3^\circ$) and (-)-**89** (79%, $[\alpha]_D = -4.3^\circ$) were prepared from the corresponding compounds following the same procedures shown in Scheme 2.12.

Scheme 2.12 Deprotection of Mimetics



Good agreement between the optical rotation values for each set of enantiomers was observed and is consistent with high enantiopurity. A summary of the prepared mimetics is given below in Figure 2.7.

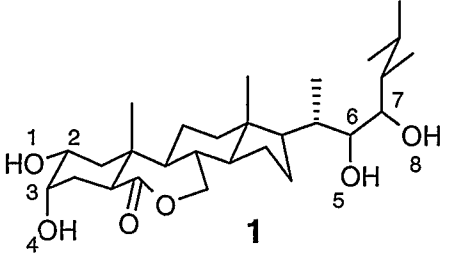
Figure 2.7 Nonsteroidal Brassinolide Mimetics



2.7 Molecular Modeling

Brassinolide was originally modeled by Andersen⁹⁹ using Spartan® software.¹⁰⁰ The molecular modeling studies were done at the semi-empirical level using an AM1 force field.¹⁰¹ Andersen's findings for brassinolide are summarized in Table 2.1.

Table 2.1 Selected Dihedral Angles and Interatomic Distances of Brassinolide⁹⁹

Compound ^a	Dihedral Angle (°)	Distances (Å)
 <p style="text-align: center;">1</p>	O1-C2-C3-O4 = -53.1	O1-O4 = 2.81
	O5-C6-C7-O8 = -55.6	O5-O8 = 2.67
	O1-C2-C6-O5 = -25.4	O1-O5 = 11.36
	O1-C2-C7-O8 = -50.9	O1-O8 = 13.77
	O4-C3-C6-O5 = -31.3	O4-O5 = 10.94
	O4-C3-C7-O8 = -0.6	O4-O8 = 13.94
E of Global Min = -1484.9 kJ/mol		

(a) Numbering scheme is for convenience and does not reflect IUPAC rules.

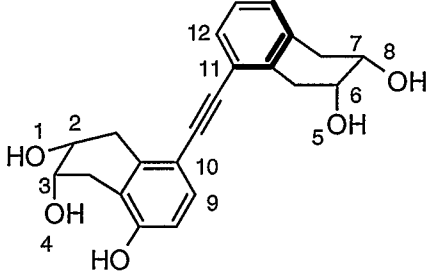
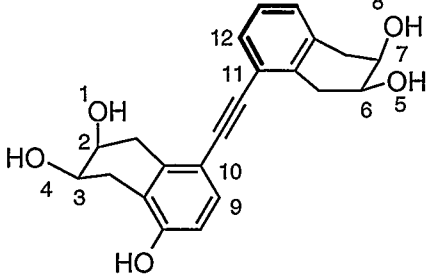
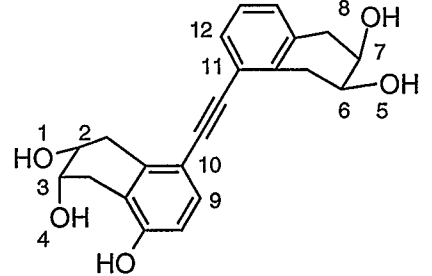
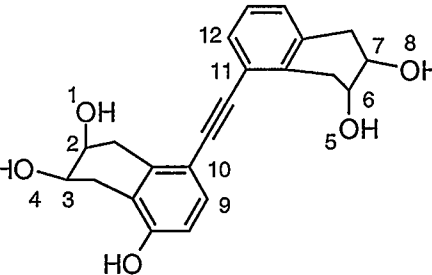
Since we had prepared each of the four individual stereoisomers of mimetic **79**, it was interesting to model each stereoisomer in order to provide a better understanding of the spatial orientation of key functionalities of the mimetics relative to the corresponding functionalities of brassinolide. Hence, compounds (+)-**88**, (-)-**88**, (+)-**89**, and (-)-**89** were subjected to similar molecular modeling studies, using Spartan® software, in order to establish how closely the vicinal diol groups of the mimetic stereoisomers superimpose with the vicinal diol groups of brassinolide.

In order to determine the conformer of each mimetic that superimposes closest with brassinolide, we postulated that the most important variable is rotation of the two aryl units around the acetylenic linker. For this reason, we constrained the C9-C10-C11-C12 dihedral angle (See Table 2.2) at 30° intervals and optimized the geometry of the constrained conformers at the semi-empirical level using an AM1 force field. The distances between O1-O5 and O4-O8 were measured for each constrained conformer, and were then compared to the same interatomic distances of brassinolide. The closest matching conformer for each mimetic relative to brassinolide, based on the O1-O5 and

O4-O8 interatomic distances, is shown in Table 2.2. Moreover, since each cyclohexane ring can exist as two possible half-chair conformations that interconvert pseudo-axial and pseudo-equatorial hydroxyl groups in each vicinal diol moiety, only those conformations that give the closest superimposition with brassinolide are included. The minimized energies for the unconstrained mimetic and constrained conformation are also given in Table 2.2. Full experimental details are provided in Chapter Three, Section 3.27.

As shown in Table 2.2, the O1-O5 distance for each of the mimetics, when in the desired conformation, is significantly shorter than that of brassinolide. The same is true for the O4-O8 distances, except in (-)-**89**, where it is close to that of brassinolide. Furthermore, a comparison of models of the mimetics with that of brassinolide indicates that (-)-**88** and (-)-**89** can at most superimpose three of the four diol hydroxyl groups with those of brassinolide regardless of the conformation. Thus, the interatomic distances between oxygen atoms provide only a very rough guide to the superimposability of these molecules with brassinolide. There is also a considerable difference between the minimum energy of the conformers shown in Table 2.2 and the global minimum energy for the unconstrained structures. This can be attributed to the fact that the global minimum energy conformation exists when there is an intramolecular hydrogen bond between the closest hydroxyl groups of each vicinal diol (i.e. where the dihedral angle C9-C10-C11-C12 = ca. 0°). Clearly this conformation, which bears little resemblance to brassinolide, is considerably different from the conformations shown in Table 2.2. Finally, it is also important to remember that the conformations of the mimetics and brassinolide may be quite different in an aqueous environment where hydrogen bonding to water molecules could have a substantial effect on the conformations of the mimetics.

Table 2.2 Selected Measurements of Mimetics in Conformations that Most Closely Resemble Brassinolide^a

 <p style="text-align: center;">(+)-88</p>	<p>Dihedral Angle: C9-C10-C11-C12 = 150°</p> <p>Interatomic Distances: O1-O5 = 10.44 Å O4-O8 = 12.68 Å</p> <p>Energy of Global Minimum: -703.2 kJ/mol</p> <p>Energy of Indicated Conformer: -671.8 kJ/mol</p>
 <p style="text-align: center;">(-)-88</p>	<p>Dihedral Angle: C9-C10-C11-C12 = 210°</p> <p>Interatomic Distances: O1-O5 = 10.58 Å O4-O8 = 12.72 Å</p> <p>Energy of Global Minimum: -703.2 kJ/mol</p> <p>Energy of Indicated Conformer: -675.5 kJ/mol</p>
 <p style="text-align: center;">(+)-89</p>	<p>Dihedral Angle: C9-C10-C11-C12 = 180°</p> <p>Interatomic Distances: O1-O5 = 10.72 Å O4-O8 = 11.68 Å</p> <p>Energy of Global Minimum: -703.6 kJ/mol</p> <p>Energy of Indicated Conformer: -691.9 kJ/mol</p>
 <p style="text-align: center;">(-)-89</p>	<p>Dihedral Angle: C9-C10-C11-C12 = 180°</p> <p>Interatomic Distances: O1-O5 = 10.46 Å O4-O8 = 13.77 Å</p> <p>Energy of Global Minimum: -703.6 kJ/mol</p> <p>Energy of Indicated Conformer: -692.7 kJ/mol</p>

a) Dihedral angles are measured by sighting from C-10 to C-11 and rotating the C11-C12 bond clockwise.

2.8 Biological Evaluation

In collaboration with R.P. Pharis and coworkers in the Department of Biological Sciences, brassinolide mimetics (+)-**88**, (-)-**88**, (+)-**89**, and (-)-**89** were subjected to the rice leaf lamina inclination bioassay⁴⁷ in an effort to quantify their biological activity. As mentioned earlier, the nonsteroidal mimetics of brassinolide, originally prepared as mixtures of stereoisomers, displayed biological activity only when coapplied with IAA.⁸² It was mentioned in Chapter One that the auxin IAA is known to synergize the effects of brassinosteroids in the rice leaf lamina inclination bioassay. All bioassays discussed below thus had IAA coapplied at 1000 ng per rice plant, unless stated otherwise. The biological activity of mimetic **79** (the mixture of (+/-)-**88** and (+/-)-**89**) is shown below in Figure 2.8.

Mimetics (+)-**88**, (-)-**88**, (+)-**89**, and (-)-**89** were applied across a range of doses in the rice leaf lamina inclination bioassay. However, only mimetics (+)-**89** and (-)-**89** showed modest and significantly promotive activity and this response was only observed at higher doses (Figures 2.9 and 2.10 respectively). It is perhaps noteworthy that (-)-**89**, which had the strongest promotive effect, also had interatomic distances between oxygen atoms most closely resembling those of brassinolide.

Interestingly, it was found that both mimetic (+)-**88** and (+)-**89** had an antagonistic effect on the ability of brassinolide to promote leaf lamina bending when these two mimetics were coapplied with brassinolide at 1000- and 10000-fold higher doses (Figures 2.11 and 2.12, respectively). Since the observed antagonistic effect was greatest for mimetic (+)-**89**, it was decided to concentrate additional bioassays on this

mimetic in order to acquire a greater understanding of this unusual antagonistic biological activity.

Subsequent bioassays showed that (+)-**89** could also significantly enhance (synergize) brassinolide's promotive effect on leaf lamina bending, depending on the dose of both the brassinolide and mimetic. As shown in Figures 2.13, using three different dosage levels of brassinolide, when mimetic (+)-**89** was coapplied at various concentrations for each brassinolide dose, there was a significant synergistic promotive effect followed by an antagonistic effect at higher doses of mimetic. A similar effect was seen for one dose of brassinolide and four doses of the mimetic in Figure 2.14. Recall that this antagonistic effect was also observed earlier for mimetic (+)-**89** as shown in Figure 2.12. The observed antagonistic effect of mimetic (+)-**88** and (+)-**89** could be attributed to effective binding of the mimetic to the putative receptor of brassinolide, but in doing so, eliciting only a limited response relative to that of brassinolide, while blocking the access of brassinolide to the receptor.

In summary, we have found that three of the mimetics [(+)-**88**, (+)-**89**, and (-)-**89**] yield a modest promotion of leaf lamina bending (Figures 2.9 – 2.14). Moreover, our results indicate that mimetics (+)-**88** and (+)-**89** have the ability to synergize the effect of brassinolide on leaf lamina bending at low doses and antagonize brassinolide at high doses (Figures 2.11 – 2.14). It's important to note that mimetic **79** (the mixture of stereoisomers) retained slightly greater biological activity when compared to the activity observed by the individual stereoisomers. This may be evidence that a certain combination of the mimetics may be optimal to promote leaf lamina bending in the bioassay.

These preliminary data suggest that the relationships between bioactivity, stereochemistry, and the dose of the mimetic are more complex than originally anticipated. Additional experiments will be required to corroborate these results and to ultimately provide a clearer understanding of their observed agonistic and antagonistic behavior.

Figure 2.8

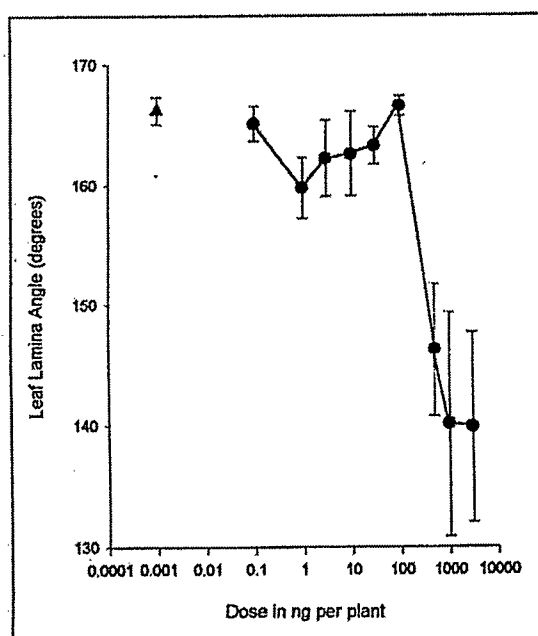


Figure 2.9

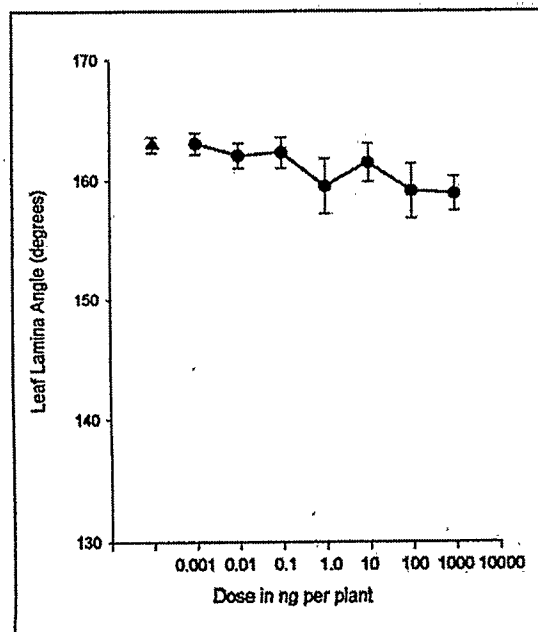


Figure 2.8 – Effect of mimetic **79**, applied in 0.5 μ L drops of 95% ethanol to dwarf rice cv. Tan-ginbozu plants pretreated with IAA. \blacktriangle = IAA control. \bullet = Varied doses of mimetic **79**. Mimetic **79** differed significantly from the IAA controls at 1, 500, 1000, and 3000 ng. Error bars represent standard error.

Figure 2.9 – Effect of mimetic (+)-**89** applied in 0.5 μ L drops of 2.5% aqueous solution of Atlas G-1086 to dwarf rice cv. Tan-ginbozu plants pretreated with IAA. \blacktriangle = IAA control + Atlas G-1086. \bullet = Varied doses of mimetic (+)-**89**. Only the highest dose of mimetic (+)-**89** differed significantly from the IAA control. Error bars represent standard error.

Figure 2.10

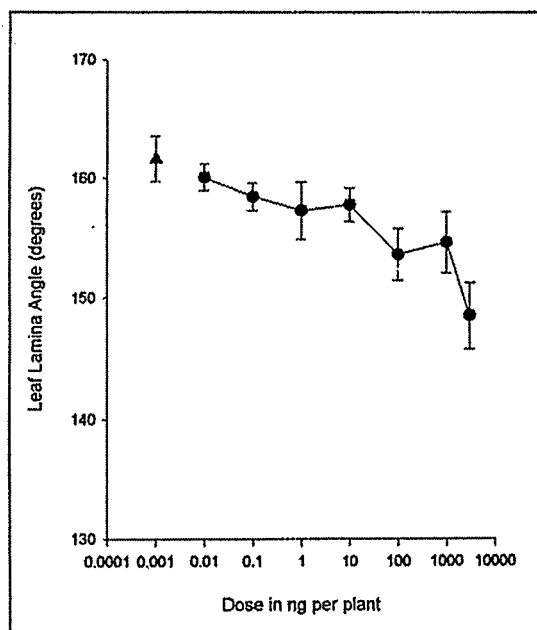


Figure 2.11

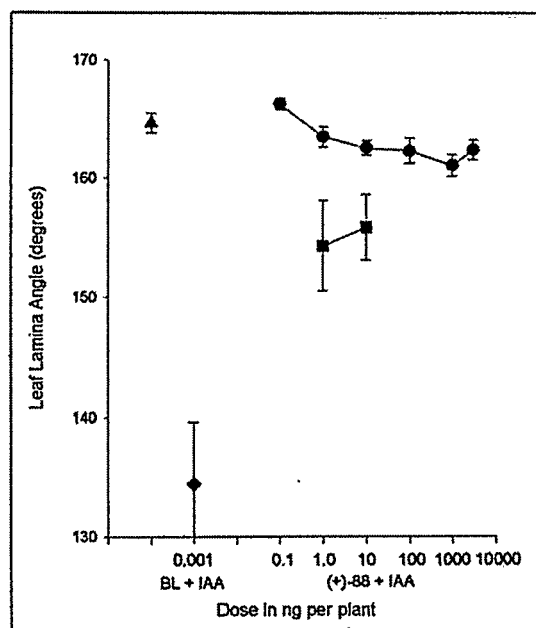


Figure 2.10 – Effect of mimetic (-)-89 applied in 0.5 μ L drops of 2.5% aqueous solution of Atlas G-1086 to dwarf rice cv. Tan-ginbozu plants pretreated with IAA. ▲ = IAA control, but without Atlas G-1086. ● = Varied doses of mimetic (-)-89. The three highest doses of mimetic (-)-89 showed significant or near-significant differences from the lowest dose of mimetic (-)-89. Additionally, “dose” was a significant variable for mimetic (-)-89 based on regression analysis as performed by R.P. Pharis. Error bars represent standard error.

Figure 2.11 – A highly significant and antagonistic effect of mimetic (+)-88 at two doses on the leaf lamina bending induced by 0.001 ng of brassinolide. Applications of IAA alone and mimetic (+)-88 alone were made as stated in Figure 2.10 above. Applications of brassinolide at 0.001 ng were made in 0.5 μ L microdrops of 2.5% Atlas G-1086. Additionally, mimetic (+)-88 was applied to rice plants that were subsequently treated with 0.001 ng of brassinolide at 1 and 10 ng doses (of mimetic), which were 1,000- and 10,000-fold higher than the dose of brassinolide. ▲ = IAA control + Atlas G-1086. ◆ = Brassinolide 0.001 ng + IAA. ● = Varied doses of mimetic (+)-88 + IAA. ■ = Brassinolide, 0.001 ng, coapplied with varied doses of (+)-88 + IAA. Error bars represent standard error.

Figure 2.12

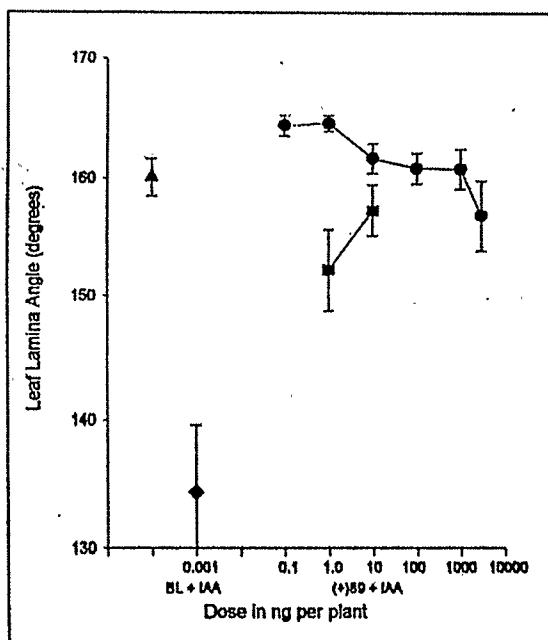


Figure 2.13

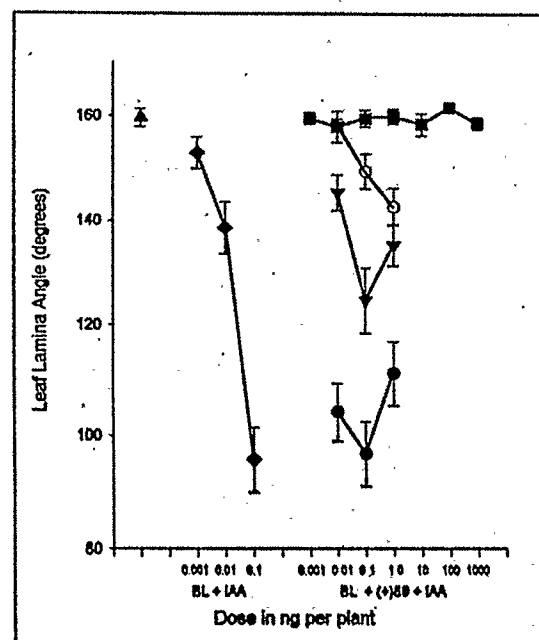


Figure 2.12 – A highly significant and antagonistic effect of mimetic (+)-89 at two doses on the leaf lamina bending induced by 0.001 ng of brassinolide. Applications of IAA alone and mimetic (+)-89 alone were made as stated in Figure 2.10 above. Applications of brassinolide were made in 0.5 μ L microdrops of 2.5% Atlas G-1086. Additionally, mimetic (+)-89 was applied to rice plants that were subsequently treated with 0.001 ng of brassinolide at 1 and 10 ng doses (of mimetic), which were 1,000- and 10,000-fold higher than the dose of brassinolide. ▲ = IAA control + Atlas G-1086. ◆ = Brassinolide 0.001 ng + IAA. ● = Varied doses of mimetic (+)-89 + IAA. ■ = Brassinolide, 0.001 ng, coapplied with varied doses of (+)-89 + IAA. Error bars represent standard error.

Figure 2.13 – September 26, 2003 bioassay. Promotive and antagonistic effects of mimetic (+)-89 on the leaf lamina bending induced by three doses of brassinolide (0.001, 0.01, 0.1 ng). Applications of IAA alone and mimetic (+)-89 alone were made as stated in Figure 2.10 above. Applications of brassinolide were made in 0.5 μ L microdrops of 2.5% Atlas G-1086. Additionally, mimetic (+)-89 was applied to rice plants that were subsequently treated with each of the three doses of brassinolide. Here, mimetic (+)-89 dose ranged from 0.1 to 10-fold (lower curve), 1.0 to 100-fold (middle curve) and 10- to 1,000-fold (upper curve) of the dose of brassinolide. ▲ = IAA control + Atlas G-1086. ◆ = Varied doses of brassinolide + IAA. ■ = Varied doses of mimetic (+)-89 + IAA. ● = Brassinolide, 0.1 ng, coapplied with varied doses of (+)-89 + IAA. ▼ = Brassinolide, 0.01 ng, coapplied with varied doses of (+)-89 + IAA. ○ = Brassinolide, 0.001 ng, coapplied with varied doses of (+)-89 + IAA. Error bars represent standard error. The synergistic (promotive) effect of (+)-89 was significant at the highest dose (1 ng) of (+)-89 for 0.001 and middle dose of (+)-89 for 0.01 ng doses of brassinolide. The antagonistic effect of (+)-89 approached significance for the highest dose (1 ng) of (+)-89 when brassinolide dose was 0.1 ng (lower curve).

Figure 2.14

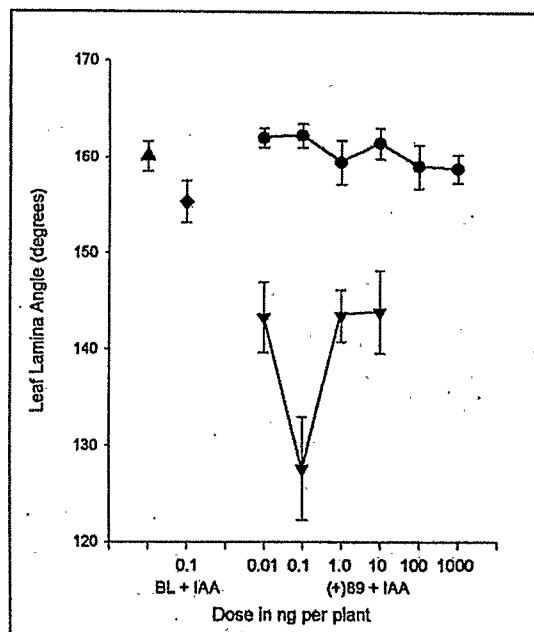


Figure 2.14 – October 3, 2003 bioassay. Synergistic (promotive) effects of mimetic (+)-**89** on the leaf lamina bending induced by brassinolide at 0.1 ng. Applications of IAA alone and mimetic (+)-**89** alone were made as stated in Figure 2.10 above. Applications of brassinolide were made in 0.5 μ L microdrops of 2.5% Atlas G-1086. Additionally, mimetic (+)-**89** was applied at four doses (of mimetic) to rice plants that were subsequently treated with brassinolide at 0.1 ng. These four doses of mimetic were 0.1, 1.0, 10 and 100-fold the dose of brassinolide. ▲ = IAA control + Atlas G-1086. ◆ = Brassinolide 0.001 ng + IAA. ● = Varied doses of mimetic (+)-**89** + IAA. ▼ = Brassinolide, 0.1 ng, coapplied with varied doses of (+)-**89** + IAA. Error bars represent standard error. A significant and synergistic promotion of the bending induced by 0.1 ng of brassinolide occurred at all four doses of (+)-**89** relative to brassinolide alone. The antagonism of the two highest doses of (+)-**89**, relative to the 0.1 ng dose of (+)-**89**, was also significant.

2.9 Conclusions

A nonsteroidal brassinolide mimetic (**79**) with proven biological activity was originally prepared as a mixture of enantiomers and diastereomers. The individual stereoisomers [(+)-**88**, (-)-**88**, (+)-**89**, and (-)-**89**] have now been synthesized in order to determine the effect of stereochemistry on biological activity. The mimetics are based on tetrahydronaphthalene subunits that contain vicinal diol groups, which have been shown to be required functional groups for the remarkable biological activity of brassinolide.

In order to quantify the effects of these nonsteroidal analogues, the mimetics were subjected to the rice leaf lamina inclination bioassay.⁴⁷ We found that three of the mimetics [(+)-**88**, (+)-**89**, and (-)-**89**] displayed modest promotive biological activity at relatively high doses when coapplied with IAA. Furthermore, mimetics (+)-**88** and (+)-**89** displayed an antagonistic effect of the brassinolide response, but only at higher concentrations. This effect was determined by coapplication of the nonsteroidal analogue with brassinolide and IAA followed by observation that the mixture has decreased activity relative to that of brassinolide plus IAA alone.

Molecular modeling studies were undertaken in an effort to help explain the observed biological activity. It was found that while certain conformations of mimetics (+)-**88**, (-)-**88**, (+)-**89**, and (-)-**89** retain similar geometrical characteristics compared to brassinolide, the nonsteroidal mimetics are not a perfect match of the natural plant hormone. It is possible that this imperfect match to brassinolide is causing the antagonism to the brassinolide response by competition of the intrinsically less active mimetic with

brassinolide for the receptor site, resulting in lower bioactivity due to blocked access of the more strongly active brassinosteroid.

Future work in this area may include investigations into the preparation of individual stereoisomers of mimetic **85**, which was also originally prepared as a mixture of stereoisomers. This would be of particular interest because mimetic **85** was found to have greater biological activity than **79**. In fact, mimetic **85** had biological activity approaching that of brassinolide in the rice leaf lamina inclination bioassay. However, the preparation of **85** as individual stereoisomers would pose a formidable challenge due to its inherent stereochemical complexity.

Chapter Three

Experimental Section

3.1 General Comments

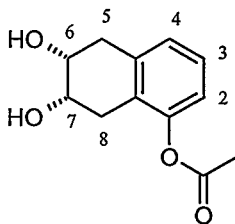
The ^1H and ^{13}C NMR spectra were obtained using a Bruker ACE 200 (^1H , 200 MHz; ^{13}C , 50 MHz) spectrometer in deuterated chloroform unless otherwise stated. Chemical shifts are expressed in parts per million (δ) using residual solvent signals as the internal standard. Coupling constants (J) are given in Hertz (Hz) and splitting patterns are specified as s (singlet), d (doublet), t (triplet), and m (multiplet). Optical rotation measurements were obtained using a Rudolph Research Autopol IV polarimeter at a wavelength of 589 nm and a temperature of 21.6 – 22.8 °C. IR spectra were obtained using a Nicolet Nexus 470 FTIR ESP spectrometer. Melting points were determined on an A.H. Thomas hot-stage apparatus. X-ray structure determinations were performed by Dr. Masood Parvez using a Nonius Kappa CCD diffractometer with graphite monochromated Mo-K α radiation. Complete details of the X-ray structures of compounds (-)-101 and (-)-102 are provided in Appendices I and II, respectively. The data contained in the Appendices was provided verbatim by Dr. M. Parvez. Low and high resolution mass spectra were obtained by Ms. Q. Wu or Ms. D. Fox. Elemental analyses were obtained by Ms. R. Smith. Analytical TLC was performed on aluminum sheets coated with silica gel 60 F-254. The spots were visualized with ultraviolet light, or by

dipping in a solution consisting of 9% ammonium molybdate (VI) tetrahydrate solution in 16% aqueous sulfuric acid, followed by a few moments of gentle heating.

Flash chromatography was carried out using silica gel, 230-400 mesh. Aqueous solutions of NaCl (brine), Na₂CO₃, NaHCO₃, and NH₄Cl used for working up organic reactions were saturated unless noted otherwise. Structures drawn in this section are numbered for convenience and do not necessarily reflect IUPAC rules.

5,8-Dihydro-1-naphthol,⁸⁴ 5,8-dihydro-1-naphthyl acetate,⁸² 5-iodo-1,4-dihydronaphthalene,^{86,87} and (+/-)-5-iodo-1,2,3,4-tetrahydro-2 α ,3 α -naphthalenediol⁸² were prepared according to literature procedures. All other reagents were purchased commercially and used without further purification. Anhydrous THF was obtained by distillation from lithium aluminum hydride. Benzene and triethylamine were purified by distillation from calcium hydride, sparged with argon, and stored over molecular sieves.

3.2 (+/-)- *cis*-6,7-Dihydroxy-5,6,7,8-tetrahydro-1-naphthyl acetate (**99**)

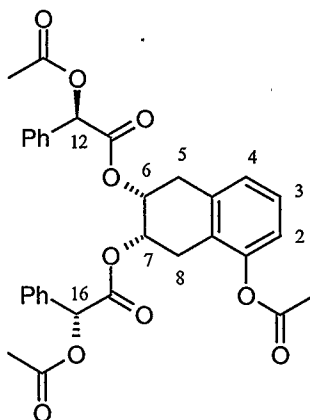


99

Osmium tetroxide (156 μL of a 0.39 M solution in *t*-butanol, 0.061 mmol), *N*-methylmorpholine *N*-oxide (1.57 g, 13.4 mmol), and water (220 μL , 12.2 mmol) were added to a solution of 5,8-dihydro-1-naphthyl acetate⁸² (2.29 g, 12.2 mmol) in acetone (75 mL). The solution was allowed to stir for 18 h at which point sodium thiosulfate (250 mg) and Florisil (500 mg) were added. Stirring was continued for a further 3 h before the mixture was filtered through Celite. The filtrate was evaporated in vacuo and the residue was subjected to flash chromatography (elution with 50% ethyl acetate-hexanes) to give 2.33 g (86%) of diol **99**. An analytical sample was prepared by recrystallization from acetone-benzene: mp 144-145 $^{\circ}\text{C}$; IR (Nujol) 3339, 3044, 1744, 1077, 1050 cm^{-1} ; ^1H NMR (CD_3OD) δ 7.15 (t, $J = 8.4$ Hz, 1 H, H-3), 7.00 (d, $J = 8.2$ Hz, 1 H, H-2 or H-4), 6.84 (d, $J = 8.2$ Hz, 1 H, H-2 or H-4), 4.03 (m, 2 H, H-6 and H-7), 3.11-2.63 (m, 4 H, H-5 and H-8), 2.30 (s, 3 H, CH_3); ^{13}C NMR (CD_3OD) δ 173.4, 153.1, 139.7, 130.3, 130.2, 130.1, 123.0, 72.4, 72.1, 37.8, 32.4, 23.2; mass spectrum, m/z (relative intensity, %) 222 (M^+ , 5), 204 ($\text{M}^+ - \text{H}_2\text{O}$, 6), 180 ($\text{M}^+ - \text{CH}_3\text{C}=\text{O}$, 43), 162 ($\text{M}^+ - \text{CH}_3\text{CO}_2$, 100), 133 (24), 120

(38). Atomic composition calculated for $C_{12}H_{14}O_4$: C, 64.85%; H, 6.35%. Found: C, 64.71%; H, 6.12%.

3.3 (-)-(6*R*,7*S*)-6,7-Bis-[(*R*)-*O*-acetylmandeloxyl]-5,6,7,8-tetrahydro-1-acetoxy-naphthalene [(-)-102]

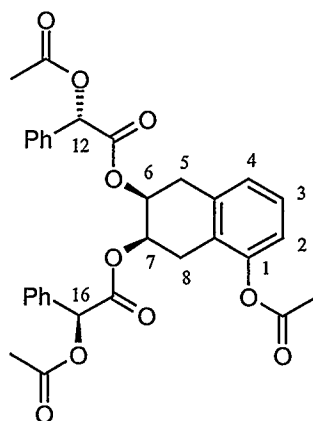


(-)-102

Diol **99** (2.73 g, 12.3 mmol), 4-dimethylaminopyridine (150 mg, 1.23 mmol), and (*R*)-(-)-*O*-acetylmandelic acid (5.01 g, 25.8 mmol) were added to a 250 mL round bottom flask. Methylene chloride (125 mL) was added and the resulting slurry was cooled in an ice/water bath. Dicyclohexylcarbodiimide (5.32 g, 25.8 mmol) in methylene chloride (65 mL) was added dropwise over 1 h. The reaction mixture was allowed to reach ambient temperature while stirring overnight. The resulting slurry was filtered to remove the urea byproduct and the filtrate was washed with Na_2CO_3 solution, brine, dried ($MgSO_4$), and evaporated in vacuo to leave a colorless solid foam. The solid foam was subjected to multiple recrystallizations (methanol) to furnish 1.81 g (26%) of ester (-)-**102** as white

needles. The absolute configurations of C-6 and C-7 were determined by x-ray crystallography (see appendix I): $[\alpha]_D = -92.1^\circ$ (c 1.0, $\text{CH}_3(\text{CO})\text{CH}_3$); mp 142-144 °C; IR (KBr, thin film) 3066, 3028, 2940, 1749, 1230, 1209, 1050, 1028 cm^{-1} ; ^1H NMR δ 7.41-7.30 (m, 10 H, Ar), 7.19 (t, $J = 8.2$ Hz, 1 H, H-3), 6.98 (d, $J = 8.1$ Hz, 1 H, H-2 or H-4), 6.91 (d, $J = 8.1$ Hz, 1 H, H-2 or H-4), 5.84 (s, 1 H, H-12 or H-16), 5.75 (s, 1 H, H-12 or H-16), 5.31 (m, 2 H, H-6 and H-7), 3.18 (m, 2 H, H-5 or H-8), 2.65 (m, 2 H, H-5 or H-8), 2.27 (s, 3 H, CH_3), 2.16 (s, 3 H, CH_3), 1.98 (s, 3 H, CH_3); ^{13}C NMR δ 170.2, 169.9, 168.6, 168.0, 167.8, 149.0, 133.9, 133.5, 133.5, 129.1, 128.8, 128.7, 128.6, 127.5, 127.4, 127.2, 126.5, 124.4, 119.9, 74.5, 70.0, 69.6, 31.3, 26.3, 20.7, 20.5, 20.2; mass spectrum, m/z (relative intensity, %) 575 (M^+ , <1), 515 ($\text{M}^+ - \text{CH}_3\text{CO}_2$, 9), 472 (12), 320 (7), 186 ($\text{M}^+ - (\text{mandelate} \times 2)$, 14), 145 (100), 115 (91), 79 (29). Atomic composition calculated for $\text{C}_{32}\text{H}_{30}\text{O}_{10}$: C, 66.89%; H, 5.26%. Found: C, 66.95%; H, 5.09%.

3.4 (+)-(6*S*,7*R*)-6,7-Bis-[(*S*)-*O*-acetylmandeloxy]-5,6,7,8-tetrahydro-1-acetoxy-naphthalene [(+)-102]

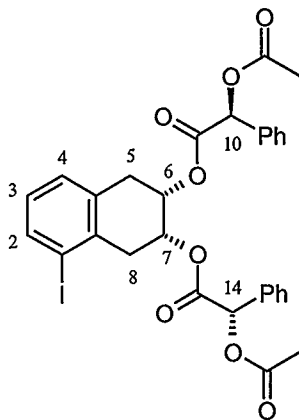


(+)-102

Diol **99** (3.40 g, 15.3 mmol), 4-dimethylaminopyridine (187 mg, 1.60 mmol), and (*S*)-(-)-*O*-acetylmandelic acid (6.24 g, 32.1 mmol) were added to a 250 mL round bottom flask. Methylene chloride (125 mL) was added and the resulting slurry was cooled in an ice/water bath. Dicyclohexylcarbodiimide (6.63 g, 32.1 mmol) in methylene chloride (75 mL) was added dropwise over 1 h. The reaction mixture was allowed to reach ambient temperature while stirring overnight. The resulting slurry was filtered to remove the urea byproduct and the filtrate was washed with Na₂CO₃ solution, brine, dried (MgSO₄), and evaporated in vacuo to leave a colorless solid foam. The solid foam was subjected to multiple recrystallizations (methanol) to furnish 2.02 g (23%) of ester (+)-**102** as white needles: $[\alpha]_D^{25} = +94.7^\circ$ (c 1.0, CH₃(CO)CH₃); mp 142-144 °C; IR (KBr, thin film) 3066, 3028, 2940, 1749, 1230, 1209, 1050, 1028 cm⁻¹; ¹H NMR δ 7.41-7.30 (m, 10 H, Ar), 7.19 (t, *J* = 8.2 Hz, 1 H, H-3), 6.98 (d, *J* = 8.1 Hz, 1 H, H-2 or H-4), 6.91 (d, *J* = 8.1 Hz, 1 H, H-2 or H-4), 5.84 (s, 1 H, H-12 or H-16), 5.75 (s, 1 H, H-12 or H-16), 5.31 (m, 2 H, H-6

and H-7), 3.18 (m, 2 H, H-5 or H-8), 2.65 (m, 2 H, H-5 or H-8), 2.27 (s, 3 H, CH₃), 2.16 (s, 3 H, CH₃), 1.98 (s, 3 H, CH₃); ¹³C NMR δ 170.2, 169.9, 168.6, 168.0, 167.8, 149.0, 133.9, 133.5, 133.5, 129.1, 128.8, 128.7, 128.6, 127.5, 127.4, 127.2, 126.5, 124.4, 119.9, 74.5, 70.0, 69.6, 31.3, 26.3, 20.7, 20.5, 20.2; mass spectrum, *m/z* (relative intensity, %) 575 (M⁺, <1), 515 (M⁺-CH₃CO₂, 5), 472 (8), 320 (3), 186 (M⁺-(mandelate x 2), 8), 145 (100), 115 (67), 79 (14). Atomic composition calculated for C₃₂H₃₀O₁₀: C, 66.89%; H, 5.26%. Found: C, 66.59%; H, 5.07%.

3.5 (+)-(6*S*,7*R*)-1-Iodo-5,6,7,8-tetrahydro-6,7-bis-[(*S*)-*O*-acetylmandeloxy] naphthalene [(+)-101]

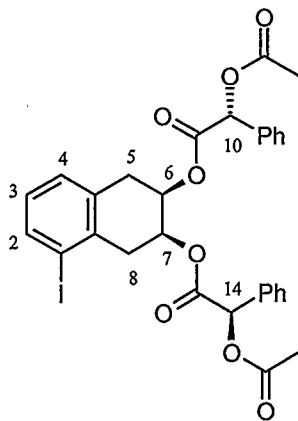


(+)-101

To a 250 mL round bottom flask was charged (+/-)-5-iodo-1,2,3,4-tetrahydro-2 α ,3 α -naphthalenediol⁸² (2.65g, 9.13 mmol), 4-dimethylaminopyridine (167 mg, 15 mol%), and (*S*)-(-)-*O*-acetylmandelic acid (3.90 g, 20.1 mmol). Methylene chloride (125 mL) was added and the resulting slurry was cooled in an ice/water bath.

Dicyclohexylcarbodiimide (4.15 g, 20.1 mmol) in methylene chloride (50 mL) was added dropwise over 1 h. The reaction mixture was allowed to reach ambient temperature while stirring overnight. The resulting slurry was filtered to remove the urea byproduct and the filtrate was washed with Na₂CO₃ solution, brine, dried (MgSO₄), and evaporated in vacuo to leave a colorless solid foam. The solid foam was subjected to multiple recrystallizations (absolute ethanol) to furnish 1.48 g (25%) of ester (+)-**101** as white needles: $[\alpha]_D = +99.8^\circ$ (c 1.0, CH₃OH); mp 113-115 °C; IR (KBr, thin film) 3066, 3033, 2935, 1749, 1230, 1056 cm⁻¹; ¹H NMR δ 7.69 (d, $J = 8.7$ Hz, 1 H, H-2 or H-4), 7.45-7.28 (m, 10 H, Ar), 7.08 (d, $J = 8.7$ Hz, 1 H, H-2 or H-4), 6.87 (t, $J = 8.6$ Hz, 1 H, H-3), 5.86 (s, 1 H, H-10 or H-14), 5.77 (s, 1 H, H-10 or H-14), 5.37-5.21 (m, 2 H, H-6 and H-7), 3.19-3.11 (m, 2 H, H-5 or H-8), 2.87-2.58 (m, 2 H, H-5 or H-8), 2.18 (s, 3 H, CH₃), 2.07 (s, 3 H, CH₃); ¹³C NMR δ 170.2, 169.8, 168.0, 167.8, 137.4, 134.5, 133.8, 133.4, 129.2, 129.1, 128.7, 128.6, 128.0, 127.4, 127.3, 101.7, 74.4, 74.3, 70.6, 70.1, 38.1, 32.0, 20.5, 20.3; mass spectrum, m/z (relative intensity, %) 388 (16), 254 (20), 203 (29), 178 (17), 128 (100), 79 (11). Atomic composition calculated for C₃₀H₂₇IO₈: C, 56.09%; H, 4.24%. Found: C, 56.14%; H, 3.94%.

3.6 (-)-(6*R*,7*S*)-1-Iodo-5,6,7,8-tetrahydro-6,7-bis-[(*R*)-*O*-acetylmandeloxy] naphthalene [(-)-101]

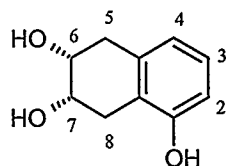


(-)-101

To a 250 mL round bottom flask was charged (+/-)-5-iodo-1,2,3,4-tetrahydro-2 α ,3 α -naphthalenediol⁸² (816 mg, 2.81 mmol), 4-dimethylaminopyridine (34 mg, 10 mol%), and (*R*)-(-)-*O*-acetylmandelic acid (1.15 g, 5.92 mmol). Methylene chloride (40 mL) was added and the resulting slurry was cooled in an ice/water bath. Dicyclohexylcarbodiimide (1.22 g, 5.91 mmol) in methylene chloride (15 mL) was added dropwise over 1 h. The reaction mixture was allowed to reach ambient temperature while stirring overnight. The resulting slurry was filtered to remove the urea byproduct and the filtrate was washed with Na₂CO₃ solution, brine, dried (MgSO₄), and evaporated in vacuo to leave a colorless solid foam. The solid foam was subjected to multiple recrystallizations (absolute ethanol) to furnish 580 mg (32%) of ester (-)-101 as white needles. The absolute configurations of C-6 and C-7 were determined by x-ray crystallography (see appendix II): [α]_D = -100° (c 1.0, CH₃OH); mp 113-115 °C; IR

(KBr, thin film) 3066, 3033, 2935, 1749, 1230, 1056 cm^{-1} ; ^1H NMR δ 7.69 (d, $J = 8.7$ Hz, 1 H, H-2 or H-4), 7.45-7.28 (m, 10 H, Ar), 7.08 (d, $J = 8.7$ Hz, 1 H, H-2 or H-4), 6.87 (t, $J = 8.6$ Hz, 1 H, H-3), 5.86 (s, 1 H, H-10 or H-14), 5.77 (s, 1 H, H-10 or H-14), 5.37-5.21 (m, 2 H, H-6 and H-7), 3.19-3.11 (m, 2 H, H-5 or H-8), 2.87-2.58 (m, 2 H, H-5 or H-8), 2.18 (s, 3 H, CH_3), 2.07 (s, 3 H, CH_3); ^{13}C NMR δ 170.2, 169.8, 168.0, 167.8, 137.4, 134.5, 133.8, 133.4, 129.2, 129.1, 128.7, 128.6, 128.0, 127.4, 127.3, 101.7, 74.4, 74.3, 70.6, 70.1, 38.1, 32.0, 20.5, 20.3; mass spectrum, m/z (relative intensity, %) 388 (5), 254 (6), 203 (9), 178 (6), 128 (100), 79 (16). Atomic composition calculated for $\text{C}_{30}\text{H}_{27}\text{IO}_8$: C, 56.09%; H, 4.24%. Found: C, 56.12%; H, 3.98%.

3.7 (-)-(6*R*,7*S*)-5,6,7,8-Tetrahydro-1,6,7-naphthalenetriol [(-)-103]

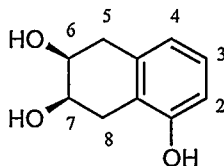


(-)-103

Potassium hydroxide (1.94 g, 34.6 mmol) was added to a slurry of ester (-)-102 (1.81 g, 3.15 mmol) in methanol (40 mL). Stirring was effected for 2 h at which point the homogeneous solution was evaporated in vacuo. The residue was taken up in NaHCO_3 solution and extracted several times with ethyl acetate. The combined organic layers were washed with brine, dried (Na_2SO_4), and evaporated in vacuo to give a crude residue that was recrystallized (ethanol-water) to give 392 mg (69%) of triol (-)-103 as a white

solid: $[\alpha]_D = -20.2^\circ$ (c 0.46, $\text{CH}_3(\text{CO})\text{CH}_3$); mp 184-186 °C (lit.⁹⁹ mp for the racemic mixture 185-187 °C); $^1\text{H NMR}$ ($\text{CD}_3(\text{CO})\text{CD}_3\text{-D}_2\text{O}$) δ 6.85 (t, $J = 7.8$ Hz, 1 H, H-3), 6.57 (d, $J = 7.9$ Hz, 1 H, H-2 or H-4), 6.51 (d, $J = 7.6$ Hz, 1 H, H-2 or H-4), 4.06-3.91 (m, 2 H, H-6 and H-7), 2.95-2.61 (m, 4 H, H-5 and H-8). Spectroscopic data were in agreement with those of the racemic mixture of triol (-)-**103** reported in the literature.⁸²

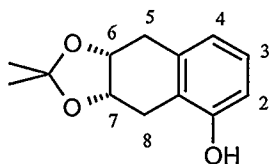
3.8 (+)-(6*S*,7*R*)-5,6,7,8-Tetrahydro-1,6,7-naphthalenetriol [(+)-**103**]



(+)-**103**

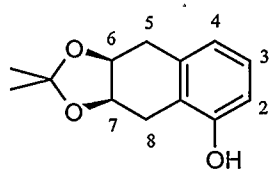
Potassium hydroxide (1.30 g, 23.2 mmol) was added to a slurry of ester (+)-**102** (1.21g, 2.11mmol) in methanol (40 mL). Stirring was effected for 2 h at which point the homogeneous solution was evaporated in vacuo. The residue was taken up in NaHCO_3 solution and extracted several times with ethyl acetate. The combined organic layers were washed with brine, dried (Na_2SO_4), and evaporated in vacuo to give a crude residue that was recrystallized (ethanol-water) to give 352 mg (93%) of triol (+)-**103** as a white solid: $[\alpha]_D = +18.9^\circ$ (c 0.38, $\text{CH}_3(\text{CO})\text{CH}_3$); mp 184-186 °C (lit.⁸² mp for the racemic mixture 185-187 °C). $^1\text{H NMR}$ spectrum was identical to that of triol (-)-**103** and the racemic mixture of the triol reported in the literature.⁹⁹

3.9 (-)-(6*R*,7*S*)-6,7-(Isopropylidenedioxy)-5,6,7,8-tetrahydro-1-naphthol [(-)-104]



(-)-104

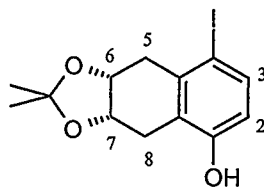
Catalytic *p*-toluenesulfonic acid (41.5 mg, 10 mol%) was added to a slurry of triol (-)-103 (392 mg, 2.18 mmol) and 2,2-dimethoxypropane (1.61 mL, 13.1 mmol). Stirring was effected for 2 h at ambient temperature at which time the homogeneous solution was diluted with methylene chloride and washed with NaHCO₃ solution and brine, dried (Na₂SO₄), and evaporated in vacuo to give an off-white solid. The crude residue was subjected to flash chromatography (elution with 20% ethyl acetate-hexanes) to give 352 mg (73%) of phenol (-)-104 as a white solid: $[\alpha]_D = -22.8^\circ$ (c 0.64, CHCl₃); ¹H NMR δ 7.04 (t, $J = 7.7$ Hz, 1 H, H-3), 6.79 (d, $J = 7.4$ Hz, 1 H, H-2 or H-4), 6.69 (d, $J = 8.0$ Hz, 1 H, H-2 or H-4), 4.63 (m, 2 H, H-6 and H-7), 3.17-2.58 (m, 4 H, H-5 and H-8), 1.35 (s, 3 H, CH₃), 1.17 (s, 3 H, CH₃); ¹³C NMR δ 153.1, 137.1, 126.8, 121.3, 120.9, 113.7, 108.1, 74.2, 74.0, 34.2, 26.3, 26.0, 24.5. Spectroscopic data were in agreement with those of the racemic mixture of phenol 104 reported in the literature.⁸²

3.10 (+)-(6*S*,7*R*)-6,7-(Isopropylidenedioxy)-5,6,7,8-tetrahydro-1-naphthol [(+)-104]**(+)-104**

Catalytic *p*-toluenesulfonic acid (30.4 mg, 10 mol%) was added to a slurry of triol (+)-**103** (288 mg, 1.60 mmol) and 2,2-dimethoxypropane (1.20 mL, 9.76 mmol). Stirring was effected for 2 h at ambient temperature at which time the homogeneous solution was diluted with methylene chloride and washed with NaHCO₃ solution and brine, dried (Na₂SO₄), and evaporated in vacuo to give an off-white solid. The crude residue was subjected to flash chromatography (elution with 20% ethyl acetate-hexanes) to give 293 mg (83%) of phenol (+)-**104** as a white solid: $[\alpha]_D = +25.6^\circ$ (c 0.59, CHCl₃). ¹H and ¹³C NMR spectra were identical to that of phenol (-)-**104** and the racemic mixture of the phenol reported in the literature.⁸²

3.11 (+)-(6*R*,7*S*)-4-Iodo-6,7-(isopropylidenedioxy)-5,6,7,8-tetrahydro-1-naphthol

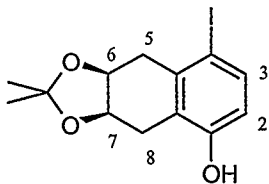
[(+)-105]



(+)-105

A slurry of phenol (-)-104 (1.75 g, 7.94 mmol), Na₂CO₃ (8.42 g, 79.4 mmol), and methanol (100 mL) was chilled to 0 °C. Slow addition of iodine monochloride (1.35 g, 8.31 mmol) was effected over 45 minutes. The slurry was allowed to reach ambient temperature and continue stirring for 3 h, at which time the reaction was filtered and evaporated in vacuo to give 2.64 g (96%) of iodide (+)-105. A portion was subjected to flash chromatography (elution with 20% ethyl acetate-hexanes) to give iodide (+)-105 as a white solid: $[\alpha]_D = +23.4^\circ$ (c 0.44, CH₃OH); mp 173-175 °C (lit.⁸² mp for the racemic mixture 172-175 °C); ¹H NMR δ 7.56 (d, $J = 8.5$ Hz, 1 H, H-3), 6.49 (d, $J = 8.5$ Hz 1 H, H-2), 4.88 (s, 1 H, OH), 4.66-4.55 (m, 2 H, H-6 and H-7), 3.26-3.10 (m, 2 H, H-5 and/or H-8), 2.83-2.52 (m, 2 H, H-5 and/or H-8), 1.33 (s, 3 H, CH₃), 1.15 (s, 3 H, CH₃). Spectroscopic data were in agreement with those of the racemic mixture of iodide 105 reported in the literature.⁸²

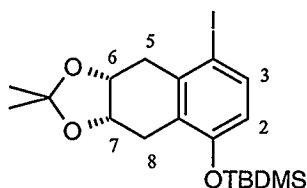
**3.12 (-)-(6*S*,7*R*)-4-Iodo-6,7-(isopropylidenedioxy)-5,6,7,8-tetrahydro-1-naphthol
[(-)-105]**



(-)-105

A slurry of phenol (+)-104 (25.0 mg, 0.113 mmol), Na₂CO₃ (120 mg, 1.13 mmol), and methanol (10 mL) was chilled to 0 °C. Slow addition of iodine monochloride (19.3 mg in 10 mL of methanol, 0.119 mmol) was effected over 45 minutes. The slurry was allowed to reach ambient temperature and continue stirring for 3 h, at which time the reaction was filtered, evaporated in vacuo, and subjected to flash chromatography (elution with 20% ethyl acetate-hexanes) to give 24 mg (62%) of iodide (-)-105 as a white solid: $[\alpha]_D = -24.8^\circ$ (c 0.77, CH₃OH); mp 172-175 °C (lit.⁸² mp for the racemic mixture 172-175 °C). ¹H NMR spectrum was identical to that of iodide (+)-105 and the racemic mixture of the iodide reported in the literature.⁸²

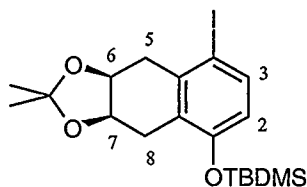
3.13 (+)-(6*R*,7*S*)-1-*t*-Butyldimethylsilyloxy-4-iodo-6,7-(isopropylidenedioxy)-5,6,7,8-tetrahydro-1-naphthol [(+)-91]



(+)-91

Imidazole (2.26 g, 33.3 mmol) and *t*-butyldimethylsilyl chloride (2.52 g, 16.7 mmol) were added to a solution of iodide (+)-**105** (2.64 g, 7.63 mmol) in DMF (42 mL). The reaction was allowed to stir overnight at which point the reaction was diluted with water and extracted several times with ethyl acetate. The organic layers were combined, dried (MgSO₄), and evaporated in vacuo. The crude residue was purified by flash chromatography (elution with 2% ethyl acetate-hexanes) to give 2.67 g (76%) of silyl ether (+)-**91**: [α]_D = +22.3° (c 0.75, CH₃(CO)CH₃); mp 71-73 °C (lit.⁸² mp for the racemic mixture 72-73 °C); ¹H NMR δ 7.53 (d, *J* = 8.6 Hz, 1 H, H-3), 6.49 (d, *J* = 8.6 Hz, 1 H, H-2), 4.59-4.45 (m, 2 H, H-6 and H-7); 3.16-2.67 (m, 4 H, H-5 and H-8), 1.32 (s, 3 H, CH₃), 1.20 (s, 3 H, CH₃), 1.04 (s, 9 H, Si(CH₃)₂*t*-Bu) 0.21 (s, 6 H, Si(CH₃)₂-Bu). Spectroscopic data were in agreement with those of the racemic mixture of silyl ether **91** reported in the literature.⁸²

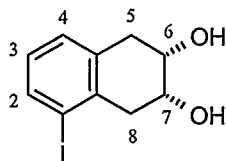
3.14 (-)-(6*S*,7*R*)-1-*t*-Butyldimethylsilyloxy-4-iodo-6,7-(isopropylidenedioxy)-5,6,7,8-tetrahydro-1-naphthol [(-)-91]



(-)-91

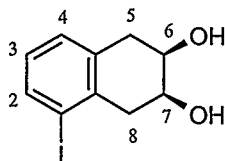
Imidazole (2.58 g, 37.9 mmol) and *t*-butyldimethylsilyl chloride (2.86 g, 19.0 mmol) were added to a solution of iodide (-)-**105** (3.01 g, 8.69 mmol) in DMF (44 mL). The reaction was allowed to stir overnight at which point the reaction was diluted with water and extracted several times with ethyl acetate. The organic layers were combined, dried (MgSO₄), and evaporated in vacuo. The crude residue was purified by flash chromatography (elution with 2% ethyl acetate-hexanes) to give 1.48 g (37%) of silyl ether (-)-**91**: $[\alpha]_D = -20.6^\circ$ (c 0.95, CH₃(CO)CH₃); mp 72-73 °C (lit.⁸² mp for the racemic mixture 72-73 °C). ¹H NMR spectrum was identical to that of silyl ether (+)-**91** and the racemic mixture of the silyl ether reported in the literature.⁸²

3.15 (+)-(6*S*,7*R*)-1-Iodo-5,6,7,8-tetrahydro-6,7-naphthalenediol [(+)-**98**]



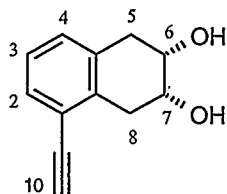
(+)-**98**

Potassium hydroxide (295 mg, 5.25 mmol) was added to a slurry of ester (+)-**101** (416 mg, 0.647 mmol) in methanol (25 mL). Stirring was effected for 2 h at which time the homogeneous solution was evaporated in vacuo. The residue was taken up in NaHCO₃ solution and extracted several times with ethyl acetate. The combined organic layers were washed with brine, dried (Na₂SO₄), evaporated in vacuo, and subjected to flash chromatography (elution with 80% ethyl acetate-hexanes) to give 175 mg (93%) of diol (+)-**98** as a white solid: $[\alpha]_D = +40.2^\circ$ (c 0.93, CH₃OH); mp 138-140 °C (lit.⁸² mp for the racemic mixture 139-141 °C); ¹H NMR δ 7.71 (d, $J = 7.7$ Hz, 1 H, H-2 or H-4), 7.10 (d, $J = 7.6$ Hz, 1 H, H-2 or H-4), 6.86 (t, $J = 7.7$ Hz, 1 H, H-3), 4.17 (m, 2 H, H-6 and H-7), 3.01 (m, 4 H, H-5 and H-8), 2.08 (br s, 2 H, OH). Spectroscopic data were in agreement with those of the racemic mixture of diol **98** reported in the literature.⁸²

3.16 (-)-(6*R*,7*S*)-1-Iodo-5,6,7,8-tetrahydro-6,7-naphthalenediol [(-)-98]**(-)-98**

Potassium hydroxide (1.64 g, 29.2 mmol) was added to a slurry of ester (-)-101 (2.35 g, 3.66 mmol) in methanol (45 mL). Stirring was effected for 2 h at which time the homogeneous solution was evaporated in vacuo. The residue was taken up in NaHCO₃ solution and extracted several times with ethyl acetate. The combined organic layers were washed with brine, dried (Na₂SO₄), evaporated in vacuo, and subjected to flash chromatography (elution with 80% ethyl acetate-hexanes) to give 1.04 g (98%) of diol (-)-98 as a white solid: $[\alpha]_D = -37.3^\circ$ (c 1.0, CH₃OH); mp 138-140 °C (lit.⁸² mp for the racemic mixture 139-141 °C). ¹H NMR spectrum was identical to that of diol (+)-98 and the racemic mixture of the diol reported in the literature.⁸²

3.17 (+)-(6*S*,7*R*)-1-Ethynyl-5,6,7,8-tetrahydro-6,7-naphthalenediol [(+)-90]

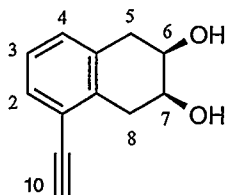


(+)-90

Diol (+)-98 (647 mg, 2.23 mmol), dichlorobis(triphenylphosphine)palladium(II) (78 mg, 5 mol%), and copper(I) iodide (42 mg, 10 mol%) were placed in an oven dried 100 mL round bottom flask. The flask was purged (argon) and benzene (65 mL), triethylamine (15 mL), and trimethylsilylacetylene (410 μ L, 2.9 mmol) were added via syringe. Stirring was effected overnight at which point the reaction was quenched with brine and extracted several times with ethyl acetate. The combined organic layers were dried (MgSO_4) and evaporated in vacuo leaving a crude residue that was used immediately in the next step. Hence, the residue was taken up in THF (20 mL), chilled to 0°C , and treated with tetrabutylammonium fluoride (3.1 mL of a 1.0 M solution in THF, 3.1 mmol). Stirring was effected for 2 h before addition of NH_4Cl solution, followed by extracting several times with ethyl acetate. The combined organic layers were washed with brine, dried (MgSO_4), evaporated in vacuo, and subjected to flash chromatography (elution with 55% ethyl acetate-hexanes) to yield 396 mg (94%) of acetylene (+)-90: $[\alpha]_D = +47.6^\circ$ (c 0.72, CH_3OH); mp $134\text{-}136^\circ\text{C}$ (lit.⁸² mp for the racemic mixture $133\text{-}136^\circ\text{C}$); $^1\text{H NMR}$ δ 7.36 (m, 1 H, H-3), 7.12 (m, 2 H, H-2 and H-4), 4.18 (m, 2 H, H-6 and

H-7), 3.32 (s, 1 H, H-10), 3.22-3.01 (m, 4 H, H-5 and H-8), 2.19 (br s, 2 H, OH). Spectroscopic data were in agreement with those of the racemic mixture of acetylene **90** reported in the literature.⁸²

3.18 (-)-(6*R*,7*S*)-1-Ethynyl-5,6,7,8-tetrahydro-6,7-naphthalenediol [(-)-90**]**

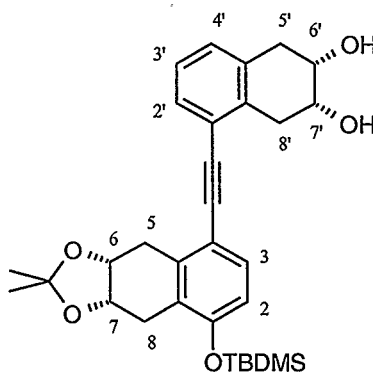


(-)-90****

Diol (-)-**98** (1.04 g, 3.60 mmol), dichlorobis(triphenylphosphine)palladium(II) (63 mg, 2.5 mol%), and copper(I) iodide (34 mg, 5 mol%) were placed in an oven dried 100 mL round bottom flask. The flask was purged (argon) and benzene (105 mL), triethylamine (25 mL), and trimethylsilylacetylene (710 μ L, 5.04 mmol) were added via syringe. Stirring was effected overnight at which point the reaction was quenched with brine and extracted several times with ethyl acetate. The combined organic layers were dried (MgSO_4) and evaporated in vacuo leaving a crude residue that was used immediately in the next step. Hence, the residue was taken up in THF (50 mL), chilled to 0 $^\circ\text{C}$, and treated with tetrabutylammonium fluoride (4.3 mL of a 1.0 M solution in THF, 4.3 mmol). Stirring was effected for 2 h before addition of NH_4Cl solution, followed by extracting several times with ethyl acetate. The combined organic layers were washed with brine, dried (MgSO_4), evaporated in vacuo, and subjected to flash chromatography

(elution with 55% ethyl acetate-hexanes) to yield 624 mg (92%) of acetylene (-)-**90**: $[\alpha]_D = -49.2^\circ$ (c 0.84, CH₃OH); mp 134-137 °C (lit.⁸² mp for the racemic mixture 133-136 °C). ¹H NMR spectrum was identical to that of acetylene (+)-**90** and the racemic mixture of the acetylene reported in the literature.⁸²

3.19 (+)-(6*R*,7*S*,6'*S*,7'*R*)-1-[6,7-(Isopropylidenedioxy)-4-*t*-butyldimethylsilyloxy-5,6,7,8-tetrahydronaphthyl]-2-[6',7'-dihydroxy-5',6',7',8'-tetrahydronaphthyl]ethyne [(+)-106**]**

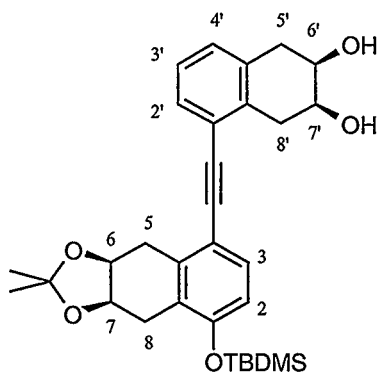


(+)-106

Acetylene (+)-**90** (219 mg, 1.16 mmol), iodide (+)-**91** (562 mg, 1.22 mmol), dichlorobis(triphenylphosphine)palladium(II) (41 mg, 5 mol%), and copper (I) iodide (22 mg, 10 mol%) were placed in an oven dried 100 mL round bottom flask. The flask was purged (argon) and sealed with a rubber septum prior to addition of benzene (46 mL) and triethylamine (11 mL) by syringe. Stirring was effected overnight at which point the reaction was quenched with brine and extracted several times with ethyl acetate. The

combined organic layers were washed with brine, dried (MgSO_4), evaporated in vacuo, and subjected to flash chromatography (elution with 50-100% ethyl acetate-hexanes) to give 430 mg (71%) of acetylene (+)-**106** as a solid foam: $[\alpha]_D = +93.3^\circ$ (c 0.94, CHCl_3); $^1\text{H NMR } \delta$ 7.41-7.27 (m, 2 H, Ar), 7.18-7.02 (m, 2 H, Ar), 6.71 (d, $J = 8.4$ Hz, 1 H, H-2 or H-3), 4.63-4.46 (m, 2 H, H-6 and H-7), 4.23-4.11 (m, 2 H, H-6' and H-7'), 3.30-2.73 (m, 8 H, H-5, H-8, H-5', and H-8'), 2.48 (br s, 2 H, OH), 1.34 (s, 3 H, CH_3), 1.25 (s, 3 H, CH_3) 1.03 (s, 9 H, $\text{Si}(\text{CH}_3)_2\text{t-Bu}$), 0.24 (s, 6 H, $\text{Si}(\text{CH}_3)_2\text{t-Bu}$); $^{13}\text{C NMR } \delta$ 153.2, 138.9, 134.9, 133.4, 130.5, 129.6, 128.9, 126.3, 125.8, 123.4, 117.2, 115.4, 108.2, 93.1, 90.1, 74.0, 73.7, 69.1, 68.8, 34.4, 33.6, 32.4, 27.0, 26.5, 25.8, 24.4, 18.3, -4.1, -4.2. Spectroscopic data were in agreement with those of the mixture of two (+/-) pairs of acetylene **106** reported in the literature.⁸²

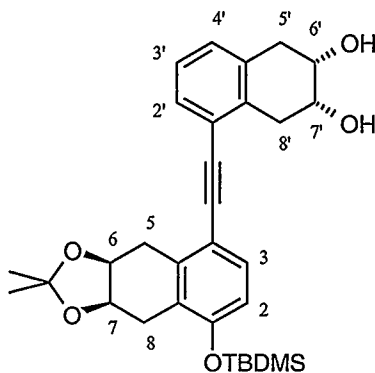
3.20 (-)-(6*S*,7*R*,6'*R*,7'*S*)-1-[6,7-(Isopropylidenedioxy)-4-*t*-butyldimethylsilyloxy-5,6,7,8-tetrahydronaphthyl]-2-[6',7'-dihydroxy-5',6',7',8'-tetrahydronaphthyl]ethyne [(-)-106]



(-)-106

Acetylene (-)-**90** (329 mg, 1.75 mmol), iodide (-)-**91** (871 mg, 1.89 mmol), dichlorobis(triphenylphosphine)palladium(II) (31 mg, 2.5 mol%), and copper (I) iodide (17 mg, 5 mol%) were placed in an oven dried 100 mL round bottom flask. The flask was purged (argon) and sealed with a rubber septum prior to addition of benzene (80 mL) and triethylamine (20 mL) by syringe. Stirring was effected overnight at which point the reaction was quenched with brine and extracted several times with ethyl acetate. The combined organic layers were washed with brine, dried (MgSO₄), evaporated in vacuo, and subjected to flash chromatography (elution with 50-100% ethyl acetate-hexanes) to give 573 mg (63%) of acetylene (-)-**106** as a solid foam: $[\alpha]_D = -92.8^\circ$ (c 1.28, CHCl₃). Spectroscopic data was identical to that of acetylene (+)-**106** and the mixture of two (+/-) pairs of the acetylene reported in the literature.⁸²

3.21 (-)-(6*S*,7*R*,6'*S*,7'*R*)-1-[6,7-(Isopropylidenedioxy)-4-*t*-butyldimethylsilyloxy-5,6,7,8-tetrahydronaphthyl]-2-[6',7'-dihydroxy-5',6',7',8'-tetrahydronaphthyl] ethyne [(-)-107]

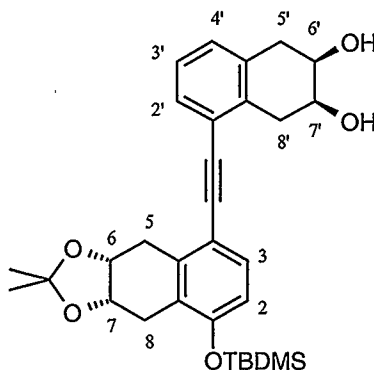


(-)-107

Acetylene (+)-**90** (203 mg, 1.08 mmol), iodide (-)-**91** (520 mg, 1.13 mmol), dichlorobis(triphenylphosphine)palladium(II) (38 mg, 5 mol%), and copper (I) iodide (21 mg, 10 mol%) were placed in an oven dried 100 mL round bottom flask. The flask was purged (argon) and sealed with a rubber septum prior to addition of benzene (43 mL) and triethylamine (10 mL) by syringe. Stirring was effected overnight at which point the reaction was quenched with brine and extracted several times with ethyl acetate. The combined organic layers were washed with brine, dried (MgSO₄), evaporated in vacuo, and subjected to flash chromatography (elution with 50-100% ethyl acetate-hexanes) to give 465 mg (83%) of acetylene (-)-**107** as a solid foam: $[\alpha]_D = -25.8^\circ$ (c 1.04, CHCl₃). ¹H NMR δ 7.41-7.27 (m, 2 H, Ar), 7.18-7.02 (m, 2 H, Ar), 6.71 (d, $J = 8.4$ Hz, 1 H, H-2 or H-3), 4.63-4.46 (m, 2 H, H-6 and H-7), 4.23-4.11 (m, 2 H, H-6' and H-7'), 3.30-2.73

(m, 8 H, H-5, H-8, H-5', and H-8'), 2.19 (br m, 2 H, OH), 1.34 (s, 3 H, CH₃), 1.25 (s, 3 H, CH₃) 1.03 (s, 9 H, Si(CH₃)₂t-Bu), 0.24 (s, 6 H, Si(CH₃)₂t-Bu); ¹³C NMR δ 153.2, 138.9, 134.9, 133.4, 130.5, 129.6, 128.9, 126.3, 125.8, 123.4, 117.2, 115.4, 108.2, 93.1, 90.1, 74.0, 73.7, 69.1, 68.8, 34.4, 33.6, 32.4, 27.0, 26.5, 25.8, 24.4, 18.3, -4.1, -4.2. Spectroscopic data were in agreement with those of the mixture of two (+/-) pairs of acetylene **107** reported in the literature.⁸²

3.22 (+)-(6*R*,7*S*,6'*R*,7'*S*)-1-[6,7-(Isopropylidenedioxy)-4-*t*-butyldimethylsilyloxy-5,6,7,8-tetrahydronaphthyl]-2-[6',7'-dihydroxy-5',6',7',8'-tetrahydronaphthyl] ethyne [(+)-107**]**

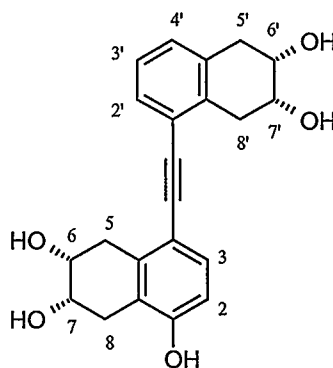


(+)-107

Acetylene (-)-**90** (225 mg, 1.20 mmol), iodide (+)-**91** (561 mg, 1.22 mmol), dichlorobis(triphenylphosphine)palladium(II) (21 mg, 2.5 mol%), and copper (I) iodide (24 mg, 10 mol%) were placed in an oven dried 100 mL round bottom flask. The flask was purged (argon) and sealed with a rubber septum prior to addition of benzene (65 mL)

and triethylamine (20 mL) by syringe. Stirring was effected overnight at which point the reaction was quenched with brine and extracted several times with ethyl acetate. The combined organic layers were washed with brine, dried (MgSO₄), evaporated in vacuo, and subjected to flash chromatography (elution with 50-100% ethyl acetate-hexanes) to give 606 mg (97%) of acetylene (+)-**107** as a solid foam: $[\alpha]_D = +25.2^\circ$ (c 0.82, CHCl₃). Spectroscopic data were identical to those of acetylene (-)-**107** and the mixture of two (+/-) pairs of the acetylene reported in the literature.⁸²

3.23 (+)-(6*R*,7*S*,6'*S*,7'*R*)-1-[1-(4,6,7-Trihydroxy-5,6,7,8-tetrahydronaphthyl)]-2-[1'-(6',7'-dihydroxy-5',6',7',8'-tetrahydronaphthyl)]ethyne [(+)-88**]**

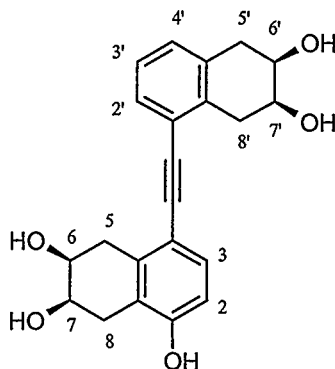


(+)-**88**

Acetylene (+)-**106** (430 mg, 0.826 mmol) was taken up in THF (20 mL) and treated with tetrabutylammonium fluoride (1.0 mL of a 1.0 M solution in THF, 1.0 mmol). Stirring was effected for 2 h at which time the reaction was quenched with NH₄Cl solution and extracted several time with ethyl acetate. The combined organic layers were

washed with brine, dried (MgSO_4), and evaporated in vacuo to leave a crude residue that was used immediately in the next step. Hence, TFA (5 mL) was added to a solution of the crude product in methanol (85 mL). The solution was refluxed for 2 h, after which the methanol and TFA were removed in vacuo leaving 238 mg (79%) of the desired mimetic (+)-**88** as a white solid which was purified by flash chromatography (10% methanol-ethyl acetate): $[\alpha]_D = +93.5^\circ$ (c 0.20, CH_3OH); mp 258-274 °C (lit⁸² mp for the mixture of two (+/-) pairs 278-281 °C); $^1\text{H NMR}$ δ 7.30 (m, 1 H, Ar), 7.21 (d, $J = 8.2$ Hz, 1 H, H-2 or H-3), 7.09 (m, 2 H, Ar), 6.62 (d, $J = 8.2$ Hz, 1 H, H-2 or H-3), 4.14-4.04 (m, 4 H, H-6, H-7, H-6', and H-7'), 3.17 (m, 4 H), 2.99 (m, 2 H), 2.87 (m, 2 H); $^{13}\text{C NMR}$ δ 154.9, 136.4, 134.4, 133.2, 130.0, 128.7, 128.0, 125.0, 123.1, 120.5, 113.2, 111.3, 92.7, 89.8, 68.3, 68.2, 68.1, 67.8, 33.7, 32.9, 32.8, 28.2. Spectroscopic data were in agreement with those of the mixture of two (+/-) pairs of mimetic **88** reported in the literature.⁸²

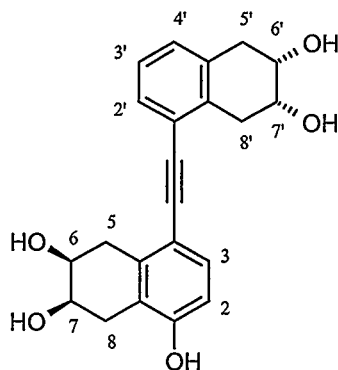
3.24 (-)-(6*S*,7*R*,6'*R*,7'*S*)-1-[1-(4,6,7-Trihydroxy-5,6,7,8-tetrahydronaphthyl)]-2-[1'-(6',7'-dihydroxy-5',6',7',8'-tetrahydronaphthyl)]ethyne [(-)-88]



(-)-88

Acetylene (-)-106 (573 mg, 1.10 mmol) was taken up in THF (30 mL) and treated with tetrabutylammonium fluoride (1.32 ml of a 1.0 M solution in THF, 1.32 mmol). Stirring was effected for 2 h at which time the reaction was quenched with NH_4Cl solution and extracted several time with ethyl acetate. The combined organic layers were washed with brine, dried (MgSO_4), and evaporated in vacuo to leave a crude residue that was used immediately in the next step. Hence, TFA (2 mL) was added to a solution of the crude product in methanol (30 mL). The solution was refluxed for 2 h, after which the methanol and TFA were removed in vacuo leaving 252 mg (63%) of the desired mimetic (-)-88 as a white solid which was purified by flash chromatography (10% methanol-ethyl acetate): $[\alpha]_D = -92.3^\circ$ (c 0.38, CH_3OH); mp 261-275 $^\circ\text{C}$ (lit⁸² mp for the mixture of two (+/-) pairs 278-281 $^\circ\text{C}$). Spectroscopic data were in agreement with those of mimetic (+)-88 and the mixture of two (+/-) pairs of the mimetic reported in the literature.⁸²

3.25 (-)-(6*S*,7*R*,6'*S*,7'*R*)-1-[1-(4,6,7-Trihydroxy-5,6,7,8-tetrahydronaphthyl)]-2-[1'-(6',7'-dihydroxy-5',6',7',8'-tetrahydronaphthyl)]ethyne [(-)-89]

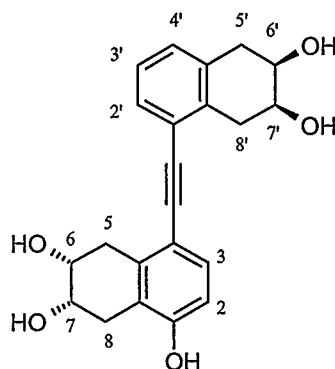


(-)-89

Acetylene (-)-107 (465 mg, 0.892 mmol) was taken up in THF (20 mL) and treated with tetrabutylammonium fluoride (1.07 mL of a 1.0 M solution in THF, 1.07 mmol). Stirring was effected for 2 h at which time the reaction was quenched with NH_4Cl solution and extracted several time with ethyl acetate. The combined organic layers were washed with brine, dried (MgSO_4), and evaporated in vacuo to leave a crude residue that was used immediately in the next step. Hence, TFA (2 mL) was added to a solution of the crude product in methanol (25 mL). The solution was refluxed for 2 h, after which the methanol and TFA were removed in vacuo leaving 258 mg (79%) of the desired mimetic (-)-89 as a white solid which was purified by flash chromatography (10% methanol-ethyl acetate): $[\alpha]_D = -4.3^\circ$ (c 0.30, CH_3OH); mp 258-271 °C (lit⁸² mp for the mixture of two (+/-) pairs 278-281 °C); $^1\text{H NMR}$ δ 7.30 (m, 1 H, Ar), 7.21 (d, $J = 8.2$ Hz, 1 H, H-2 or H-3), 7.09 (m, 2 H, Ar), 6.62 (d, $J = 8.2$ Hz, 1 H, H-2 or H-3), 4.14-4.04 (m, 4 H, H-6, H-7,

H-6', and H-7'), 3.17 (m, 4 H), 2.99 (m, 2 H), 2.87 (m, 2 H); ^{13}C NMR δ 154.9, 136.4, 134.4, 133.2, 130.0, 128.7, 128.0, 125.0, 123.1, 120.5, 113.2, 111.3, 92.7, 89.8, 68.3, 68.2, 68.1, 67.8, 33.7, 32.9, 32.8, 28.2. Spectroscopic data were in agreement with those of the mixture of two (+/-) pairs of mimetic **89** reported in the literature.⁸²

3.26 (+)-(6*R*,7*S*,6'*R*,7'*S*)-1-[1-(4,6,7-Trihydroxy-5,6,7,8-tetrahydronaphthyl)]-2-[1'-(6',7'-dihydroxy-5',6',7',8'-tetrahydronaphthyl)]ethyne [(+)-89**]**

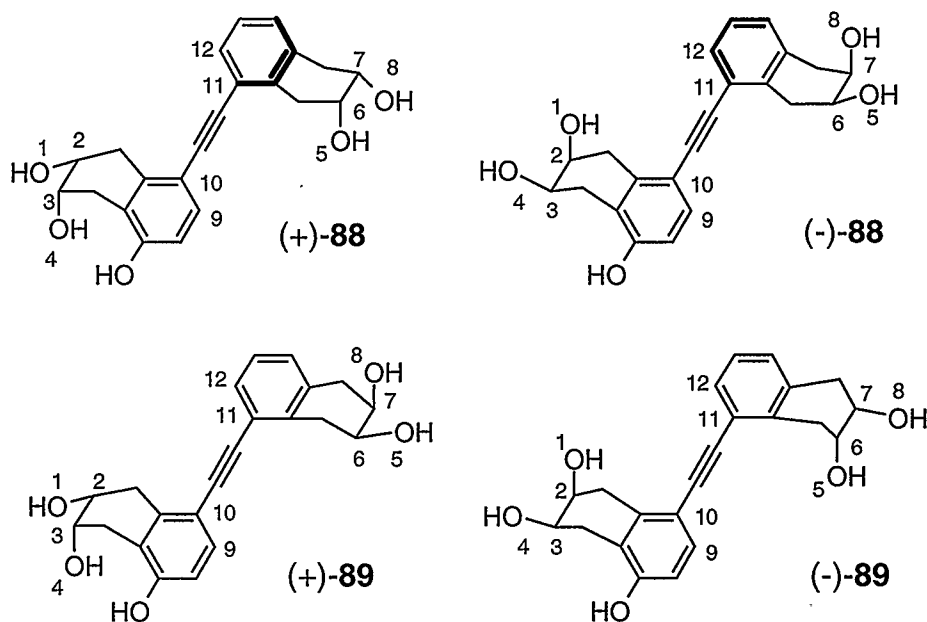


(+)-89

Acetylene (+)-**107** (606 mg, 1.16 mmol) was taken up in THF (30 mL) and treated with tetrabutylammonium fluoride (1.4 mL of a 1.0 M solution in THF, 1.4 mmol). Stirring was effected for 2 h at which time the reaction was quenched with NH_4Cl solution and extracted several time with ethyl acetate. The combined organic layers were washed with brine, dried (MgSO_4), and evaporated in vacuo to leave a crude residue that was used immediately in the next step. Hence, TFA (3 mL) was added to a solution of the crude product in methanol (30 mL). The solution was refluxed for 2 h, after which the methanol and TFA were removed in vacuo leaving 337 mg (79%) of the desired mimetic

(+)-**89** as a white solid which was purified by flash chromatography (10% methanol-ethyl acetate): $[\alpha]_D = +4.2^\circ$ (c 0.10, CH₃OH); mp 259-271 °C (lit⁸² mp for the mixture of two (+/-) pairs 278-281 °C). Spectroscopic data were in agreement with those of mimetic (-)-**89** and the mixture of two (+/-) pairs of the mimetic reported in the literature.⁸²

3.27 Molecular Modeling



Using Spartan® software, mimetics (+)-**88**, (-)-**88**, (+)-**89**, and (-)-**89** were constrained at 30° intervals around the C9-C10-C11-C12 dihedral angle. The constrained structures were minimized and then subjected to geometry optimization at the semi-empirical level with an AM1 force field.¹⁰¹ In order to determine which conformer had the greatest structural resemblance to brassinolide, the O1-O5 and O4-O8 interatomic distances of the constrained/minimized mimetics were found. These values were compared to the corresponding values of brassinolide (as established previously by

Andersen⁹⁹) to determine which conformer of each mimetic had the greatest structural resemblance to brassinolide. The selected conformers are shown in Table 2.2, Section 2.8. Also, the constrained structures which most closely matched brassinolide, were subjected to a standard minimization at the semi-empirical level with an AM1 force field to determine the minimum energy of the constrained conformer. These results are also given in Table 2.2, Section 2.8.

References

1. Friedrichsen, D.; Chory, J. *Bioessays* **2001**, *23*, 1028.
2. Campbell, N.A.; Reece, J.B. *Biology*, 6th Ed.; Benjamin Cummings: San Francisco, CA, 2002; pp. 802-833.
3. Arteca, R.N. *Plant Growth Substances: Principles and Applications*; Chapman & Hall: New York, NY, 1996; pp. 1-27.
4. Phillips, I.D.J. *Introduction to The Biochemistry and Physiology of Plant Growth Hormones*; McGraw-Hill: New York, NY, 1971; p. 2.
5. Davies, P.J. *Plant Hormones*; Kluwer Academic: Boston, MA, 1987; pp. 1-11.
6. Kende, H.; Zeevaart, J.A.D. *Plant Cell* **1997**, *9*, 1197.
7. Taiz, L.; Zeiger, E. *Plant Physiology* 3rd Ed.; Sinauer Associates, Inc.: Sunderland, MA, 2002; chapters 19-23.
8. Creelman, R.A.; Mullet, J.E. *Plant Cell* **1997**, *9*, 1211.
9. Kakkar, R.K.; Rai, V.K. *Phytochemistry* **1993**, *33*, 1281.
10. Raskin, I. *Ann. Rev. Plant Physiol. Plant. Mol. Biol.* **1992**, *43*, 439.
11. a) Sakurai, A.; Yokota, T.; Clouse, S.D. (Eds.) *Brassinosteroids: Steroidal Plant Hormones*; Springer Verlag: Tokyo, 1999. b) Khripach, V.A.; Zhabinskii, V.N.; de Groot, A.E. *Brassinosteroids: A New Class of Plant Hormones*; Academic Press: New York, NY, 1999. c) *Brassinosteroids: Chemistry, Bioactivity and Applications*; Cutler, H.G.; Yokota, T.; Adam, G., Eds.; ACS Symposium Series 474; American Chemical Society: Washington, DC, 1991.
12. Sasse, J. In reference 11c, Chapter 13.

13. Mandava, N.B. *Ann. Rev. Plant Physiol. Plant Mol. Biol.* **1988**, *39*, 23.
14. Khripach, V.A.; Zhabinskii, V.N.; Konstantinova, O.V.; Antonchick, A.P.; Schneider, B. *Steroids* **2002**, *67*, 587.
15. Yokota, T. In reference 11a, Chapter 1.
16. Mitchell, J.W.; Mandava, N.; Worley, J.F.; Plimmer, J.R.; Smith, M.V. *Nature* **1970**, *225*, 1065.
17. Grove, M.D.; Spencer, G.F.; Rohwedder, W.K.; Mandava, N.; Worley, J.F.; Warthen, J.D.; Steffens, G.L.; Flippen-Anderson, J.L.; Cook, J.C. *Nature* **1979**, *281*, 216.
18. Chen, S.C. *Chemistry in Canada* **1983**, *35*, 13.
19. a) Bajguz, A.; Tretyn, A. *Phytochemistry* **2003**, *62*, 1027. b) Yokota, T. *Trends Plant Sci.* **1997**, *2*, 137.
20. a) Park, K-H.; Saimoto, H.; Nakagawa, S.; Sakurai, A.; Yokota, T.; Takahashi, N.; Syono, K. *Agric. Biol. Chem.* **1989**, *53*, 805. b) Sakurai, A.; Fujioka, S. *Biosci. Biotech. Biochem.* **1997**, *61*, 757.
21. Fujioka, S.; Sakurai, A. *Nat. Prod. Rep.* **1997**, *14*, 1.
22. Choi, Y-H.; Fujioka, S.; Harada, A.; Yokota, T.; Takasuto, S.; Sakurai, A. *Phytochemistry*, **1996**, *43*, 593.
23. Fujioka, S.; Sakurai, A. *Physiol. Plant.* **1997**, *100*, 710.
24. Choi, Y-H.; Fujioka, S.; Nomura, T.; Harada, A.; Yokota, T.; Sakurai, A.; Takatsuto, S. *Phytochemistry* **1997**, *44*, 609.
25. a) Fujioka, S.; Yokota, T. *Annu. Rev. Plant Biol.* **2003**, *54*, 137. b) Sakurai, A. *Plant Physiol. Biochem.* **1999**, *37*, 351.

26. Clouse, S.D.; Sasse, J.M. *Ann. Rev. Plant Physiol. Plant. Mol. Biol.* **1998**, *49*, 427.
27. Dewick, P.M. *Medicinal Natural Products: A Biosynthetic Approach*; John Wiley & Sons: Chichester, England, 1997; Chapter 5.
28. Bishop, G.J.; Yokota, T. *Plant Cell Physiol.* **2001**, *42*, 114.
29. Suzuki, H.; Fujioka, S.; Takatsuto, S.; Yokota, T.; Murofushi, N.; Sakurai, A. *Biosci. Biotech. Biochem.* **1995**, *59*, 168.
30. Zullo, M.A.T.; Kohout, L.; de Azevedo, M.B.M. *Plant Growth Regul.* **2003**, *39*,1.
31. Shimada, Y.; Goda, H.; Nakamura, A.; Takatsuto, S.; Fujioka, S.; Yoshida, S. *Plant Physiol.* **2003**, *131*, 287.
32. Asami, T.; Yoshida, S. *Trends Plant Sci.* **1999**, *4*, 348.
33. Min, Y.K.; Asami, T.; Fujioka, S.; Murofushi, N.; Yamaguchi, I.; Yoshida, S. *Bioorg. Med. Chem. Lett.* **1999**, *9*, 425.
34. Kim, S-K.; Mizuno, K.; Hatori, M.; Marumo, S. *Tetrahedron Lett.* **1994**, *35*, 1731.
35. a) Li, J.; Nagpal, P.; Vitart, V.; McMorris, T.C.; Chory, J. *Science* **1996**, *272*, 398.
b) Clouse, S.D.; Langford, M.; McMorris, T.C. *Plant Physiol.* **1996**, *111*, 671.
36. Nomura, T.; Nakayama, M.; Reid, J.B.; Takeuchi, Y.; Yokota, T. *Plant Physiol.* **1997**, *113*, 31.
37. Schneider, B.; Kolbe, A.; Porzel, A.; Adam, G. *Phytochemistry*, **1994**, *36*, 319.
38. Hai, T.; Schneider, B.; Adam, G. *Phytochemistry* **1995**, *40*, 443.
39. Hai, T.; Schneider, B.; Porzel, A.; Adam, G. *Phytochemistry* **1996**, *41*, 197.
40. Kolbe, A.; Schneider, B.; Porzel, A.; Adam, G. *Phytochemistry*, **1996**, *41*, 163.

41. Adam, G.; Schneider, B. In reference 11a, Chapter 6.
42. Arteca, R.N. In reference 3, Chapter 2.
43. Wada, K.; Kondo, H.; Marumo, S. *Agric. Biol. Chem.* **1985**, *49*, 2249.
44. Takatsuto, S.; Yokota, T. In reference 11a, Chapter 3.
45. Maeda, E. *Physiol. Plant.* **1965**, *18*, 813.
46. Wada, K.; Marumo, S.; Ikekawa, N.; Morisaki, M.; Mori, K. *Plant & Cell Physiol.* **1981**, *22*, 323.
47. Takeno, K.; Pharis, R.P. *Plant & Cell Physiol.* **1982**, *23*, 1275.
48. Kamuro, Y.; Takatsuto, S. In reference 11a, Chapter 10.
49. Ikekawa, N.; Zhao, Y-J. In reference 11c, Chapter 24.
50. a) Back, T.G.; Pharis, R.P. *Plant Growth Regul.* **2003**, in press. b) Brosa, C. In reference 11a, Chapter 9.
51. Thompson, M.J.; Mandava, N.; Flippen-Anderson, J.L.; Worley, J.F.; Dutky, S.R.; Robbins, W.E.; Lusby, W. *J. Org. Chem.* **1979**, *44*, 5002.
52. a) Mori, K. *Agric. Biol. Chem.* **1980**, *44*, 1211. b) McMorris T.C.; Patil, P.A.; Chavez, R.G.; Baker, M.E.; Clouse, S.D. *Phytochemistry* **1994**, *36*, 585. b) Adam, G.; Marquardt, V.; Vorbrodt H.M.; Horhold, C.; Andreas, W.; Gartz, J. In reference 11c, Chapter 7.
53. Takatsuto, S.; Yazawa, N.; Ikekawa, N.; Morishita, T.; Abe, H. *Phytochemistry* **1983**, *22*, 1393.
54. Takatsuto, S.; Yazawa, N.; Ikekawa, N.; Takematsu, T.; Takeuchi, Y.; Koguchi, M. *Phytochemistry* **1983**, *22*, 2437.

55. Watanabe, T.; Noguchi, T.; Yokota, T.; Shibata, K.; Koshino, H.; Seto, H.; Kim, S.K.; Takatsuto, S. *Phytochemistry* **2001**, *58*, 343.
56. Takatsuto, S.; Yazawa, N.; Ikekawa, N. *Phytochemistry* **1984**, *23*, 525.
57. Takeuchi, T.; Mori, K. *Liebigs Ann. Chem.* **1988**, 815.
58. Back, T.G.; Janzen, L.; Nakajima, S.K.; Pharis, R.P. *J. Org. Chem.* **1999**, *64*, 5494.
59. Luo, W.; Janzen, L.; Pharis, R.P.; Back, T.G. *Phytochemistry* **1998**, *49*, 637.
60. Back, T.G.; Janzen, L.; Nakajima, S.K.; Pharis, R.P. *J. Org. Chem.* **2000**, *65*, 3047.
61. Pharis, R.P.; Janzen, L.; Nakajima, S.K.; Zhu, J.; Back, T.G. *Phytochemistry* **2001**, *58*, 1043.
62. a) Okada, K.; Mori, K. *Agric. Biol. Chem.* **1983**, *47*, 89. b) Takatsuto, S.; Ikekawa, N. *J. Chem. Soc., Perkin Trans. 1* **1984**, 439.
63. Anastasia, M.; Allevi, P.; Ciuffreda, P.; Fiecchi, A.; Scala, A. *J. Chem. Soc., Perkin Trans. 1* **1986**, 2117.
64. Kishi, T.; Wada, K.; Marumo, S.; Mori, K. *Agric. Biol. Chem.* **1986**, *50*, 1821.
65. Adam, G.; Marquardt, V. *Phytochemistry* **1986**, *25*, 1787.
66. Yokota, T.; Koba, S.; Kim, S.K.; Takatsuto, S.; Ikekawa, N.; Sakakibara, M.; Okada, K.; Mori, K.; Takahashi, N. *Agric. Biol. Chem.* **1987**, *51*, 1625.
67. Kim, S.K. In reference 11c, Chapter 3.
68. Brosa, C.; Capdevila, J.M.; Zamora, I. *Tetrahedron* **1996**, *52*, 2435.
69. Baron, D.L.; Luo, W.; Janzen, L.; Pharis, R.P.; Back, T.G. *Phytochemistry* **1998**, *49*, 1849.

70. Seto, H.; Fujioka, S.; Koshino, H.; Suenaga, T.; Yoshida, S.; Watanabe, T.; Takatsuto, S. *J. Chem. Soc., Perkin Trans. 1* **1998**, 3355.
71. Seto, H.; Fujioka, S.; Koshino, H.; Suenaga, T.; Yoshida, S.; Watanabe, T.; Takatsuto, S. *Phytochemistry* **1999**, *52*, 815.
72. Sung, C.C.Y.; Janzen, L.; Pharis, R.P.; Back, T.G. *Phytochemistry* **2000**, *55*, 121.
73. Back, T.G.; Janzen, L.; Pharis, R.P.; Yan, Z. *Phytochemistry* **2002**, *59*, 627.
74. a) McMorris, T.C. In reference 11a, Chapter 4. b) McMorris, T.C.; Donaubaueer, J.H.; Silveira, M.H.; Molinski, T.F. In reference 11c, Chapter 4.
75. Khripach, V.A.; Zhabinskii, V.N.; Litvinoskaya, R.P. In reference 11c, Chapter 5.
76. Back, T.G. In *Studies in Natural Products Chemistry*; Atta-ur-Rahman, Ed.; Elsevier: Amsterdam, 1995; Volume 16, pp. 321-364.
77. Kovganko, N.V.; Ananich, S.K. *Chem. Nat. Comp.* **2002**, *38*, 122.
78. Back, T.G.; Baron, D.L.; Luo, W.; Nakajima, S.K. *J. Org. Chem.* **1997**, *62*, 1179.
79. Back, T.G.; Blazecka, P.G.; Krishna, M.V. *Can. J. Chem.* **1993**, *71*, 156.
80. Sakakibara, M.; Okada, K.; Ichikawa, Y.; Mori, K. *Heterocycles* **1982**, *17*, 301.
81. Aburatani, M.; Takeuchi, T.; Mori, K. *Synthesis* **1987**, 181.
82. Andersen, D.L.; Back, T.G.; Janzen, L.; Michalak, K.; Pharis, R.P.; Sung, G.C.Y. *J. Org. Chem.* **2001**, *66*, 7129.
83. For a general review of catalytic asymmetric dihydroxylation see: Kolb, H.C.; VanNieuwenhze, M.S.; Sharpless, K.B. *Chem. Rev.* **1994**, *94*, 2483.
84. Gutsche, C.D.; Peter, H.H. *Org. Synthesis* **1958**, *37*, 80.
85. Hendrickson, J.B.; Bergeron, R. *Tetrahedron Lett.* **1973**, *14*, 4607.
86. Rowe, F.M.; Levin, E. *J. Chem. Soc.* **1920**, *117*, 1576.

87. Holzapfel, C.W.; Koekemoer, J.M.; van Dyk, M.S. *S. Afr. J. Chem.* **1986**, *39*, 158.
88. Wang, L.; Sharpless, K.B. *J. Am. Chem. Soc.* **1992**, *114*, 7568.
89. Smith, M.B.; March, J. *March's Advanced Organic Chemistry: Reactions, Mechanisms, and Structure*, 5th Edition; John Wiley & Sons: New York, NY, 2001; Chapter 4.
90. Klyashchitskii, B.A.; Shvets, V.I. *Russ. Chem. Rev.* **1972**, *41*, 592.
91. For a general procedure see: VanRheenen, V.; Kelly, R.C.; Cha, D.Y. *Tetrahedron Lett.* **1976**, *23*, 1973.
92. Whitesell, J.K.; Reynolds, D. *J. Org. Chem.* **1983**, *48*, 3548.
93. Corey, E.J.; Bakshi, R.K.; Shibata, S.; Chen, C.-P.; Singh, V.K. *J. Am. Chem. Soc.* **1987**, *109*, 7925.
94. For an easy preparation of *O*-acetylmandelic acid see: Barton, P.; Laws, A.P.; Page, M.I. *J. Chem. Soc., Perkin Trans. 2* **1994**, 2021.
95. a) Khorana, H.G. *Chem. Rev.* **1953**, *53*, 145. b) Williams, A.; Ibrahim, I.T. *Chem. Rev.* **1981**, *81*, 589.
96. Hassner, A.; Alexanian, V. *Tetrahedron Lett.* **1978**, *46*, 4475.
97. Mio, J.M.; Kopel, L.C.; Braun, J.B.; Gadzikwa, T.L.; Hull, K.L.; Brisbois, R.G.; Markworth, C.J.; Grieco, P.A. *Org. Lett.* **2002**, *4*, 3199.
98. Edgar, K.J.; Falling, S.N. *J. Org. Chem.* **1990**, *55*, 5287.
99. Andersen, D.L. Ph.D. Thesis, University of Calgary, 2000.
100. Spartan®, Wavefunction, California, 2002.
101. Dewar, M.J.S.; Zoebisch, E.G.; Healy, E.F.; Stewart, J.J.P. *J. Am. Chem. Soc.* **1985**, *107*, 3902.

Appendix I: X-Ray Crystal Report of (-)-101

Experimental:

A colorless needle crystal of $C_{30}H_{27}IO_8$ was coated with Paratone 8277 oil (Exxon) and mounted on a glass fiber. All measurements were made on a Nonius KappaCCD diffractometer with graphite monochromated Mo-K α radiation. Cell constants obtained from the refinement¹ of 16185 reflections in the range $6.0 < \theta < 27.5^\circ$ corresponded to a primitive monoclinic cell; details of crystal data and structure refinement have been provided in Table 1. The data were collected² at a temperature of 173(2) K using the ω and ϕ scans to a maximum θ value of 27.5° . The data were corrected for Lorentz and polarization effects and for absorption using multi-scan method¹. Since the crystal did not show any sign of decay during data collection a decay correction was deemed unnecessary.

The structure was solved by the direct methods³ and expanded using Fourier techniques.⁴ The non-hydrogen atoms were refined anisotropically. Hydrogen atoms were included at geometrically idealized positions and were not refined. The final cycle of full-matrix least-squares refinement using SHELXL97⁵ converged (largest parameter shift was 0.001 times its esd) with unweighted and weighted agreement factors, $R = 0.0529$ and $wR = 0.1169$ (all data), respectively, and goodness of fit, $S = 1.015$. The absolute structure was established by the Flack method⁶ with the absolute configuration at the chiral centers: C1 (R), C10 (S), C12 (R) and C22 (R). The Flack parameter for the inverted structure was 1.02(3). Therefore, the inverted structure was rejected as the one

present in the crystal. The weighting scheme was based on counting statistics and the final difference Fourier map was essentially featureless. The figures were plotted with the aid of ORTEPII.⁷

References:

1. Otwinowski, Z. & Minor, W. (1997). *Methods Enzymol.* **276**, 307.
2. Hooft, R. (1998). *COLLECT*. Nonius BV, Delft. The Netherlands.
3. Altomare, A., Cascarano, M., Giacovazzo, C. & Guagliardi, A. (1993). *SIR92*. *J. Appl. Cryst.*, **26**, 343
4. Beurskens, P.T., Admiraal, G., Beurskens, G., Bosman, W.P., de Gelder, R., Israel, R. & Smits, J.M.M. (1994). The *DIRDIF-94* program system, Technical Report of the Crystallography Laboratory, University of Nijmegen, The Netherlands.
5. Sheldrick, G.M. (1997). *SHELXL97*. University of Göttingen, Germany.
6. Flack, H. D. (1983). *Acta Cryst.* **A39**, 876.
7. Johnson, C.K. (1976). *ORTEPII*. Report ORNL-5138. Oak Ridge National Laboratory, Tennessee, USA.

Table 1. Crystal data and structure refinement for C₃₀H₂₇IO₈.

Identification code	T. Back – 7 (Mike – 2)
Empirical formula	C ₃₀ H ₂₇ IO ₈
Formula weight	642.42
Temperature	173(2) K
Wavelength	0.71073 Å
Crystal system	Monoclinic
Space group	P2 ₁
Unit cell dimensions	a = 12.765(2) Å b = 6.7187(11) Å c = 17.6937(17) Å
Volume	1450.0(4) Å ³
Z	2
Density (calculated)	1.471 Mg/m ³
Absorption coefficient	1.15 mm ⁻¹
F(000)	648
Crystal size	0.17 x 0.10 x 0.08 mm ³
Theta range for data collection	6.0 to 27.5°.
Index ranges	-16<=h<=16, -8<=k<=8, -22<=l<=22
Reflections collected	16185
Independent reflections	6174 [R(int) = 0.077]
Completeness to theta = 27.5°	98.5 %
Absorption correction	Multi-scan method
Max. and min. transmission	0.914 and 0.828
Refinement method	Full-matrix least-squares on F ²
Data / restraints / parameters	6174 / 1 / 354
Goodness-of-fit on F ²	1.015
Final R indices [I>2sigma(I)]	R1 = 0.0529, wR2 = 0.0976
R indices (all data)	R1 = 0.1214, wR2 = 0.1169
Absolute structure parameter	-0.04(2)
Largest diff. peak and hole	1.11 and -0.79 e.Å ⁻³

Table 2. Atomic coordinates ($\times 10^4$) and equivalent isotropic displacement parameters ($\text{\AA}^2 \times 10^3$) for $\text{C}_{30}\text{H}_{27}\text{IO}_8$. $U(\text{eq})$ is defined as one third of the trace of the orthogonalized U_{ij} tensor.

Atom	x	y	z	$U(\text{eq})$
I(1)	776(1)	95(1)	8027(1)	70(1)
O(1)	-3336(3)	6897(5)	8068(2)	28(1)
O(2)	-3706(3)	7227(5)	9229(2)	30(1)
O(3)	-5310(2)	10022(7)	8518(2)	30(1)
O(4)	-3745(3)	11688(6)	8691(3)	42(1)
O(5)	-1964(2)	5562(5)	7187(2)	27(1)
O(6)	-3654(3)	5708(5)	6298(2)	34(1)
O(7)	-2820(3)	8477(6)	5461(2)	34(1)
O(8)	-2895(3)	10207(9)	6531(2)	58(1)
C(1)	-2423(4)	5515(7)	8411(3)	27(1)
C(2)	-1391(4)	6679(9)	8801(3)	33(1)
C(3)	-377(4)	5403(11)	8954(3)	33(2)
C(4)	607(5)	6124(11)	9500(3)	48(2)
C(5)	1572(4)	5121(18)	9622(3)	58(2)
C(6)	1604(5)	3371(14)	9217(5)	64(2)
C(7)	647(5)	2672(10)	8679(4)	45(2)
C(8)	-365(4)	3636(9)	8557(3)	32(1)
C(9)	-1424(4)	2747(8)	8016(4)	36(1)
C(10)	-2314(4)	4287(7)	7734(3)	24(1)
C(11)	-3911(4)	7539(8)	8535(3)	25(1)
C(12)	-4926(4)	8640(8)	8048(3)	26(1)
C(13)	-4618(5)	11501(8)	8816(3)	35(1)
C(14)	-5060(5)	12849(9)	9317(4)	46(2)
C(15)	-5822(4)	7133(8)	7705(3)	32(1)
C(16)	-6739(4)	6931(9)	7968(3)	33(1)
C(17)	-7518(4)	5501(11)	7659(3)	44(2)
C(18)	-7410(5)	4260(11)	7078(5)	65(2)
C(19)	-6493(6)	4416(12)	6812(5)	81(3)
C(20)	-5716(5)	5867(12)	7112(4)	63(2)
C(21)	-2695(4)	6093(8)	6502(3)	31(1)

C(22)	-2095(4)	7129(8)	5992(3)	30(1)
C(23)	-3195(4)	9982(12)	5826(4)	42(1)
C(24)	-3981(6)	11287(10)	5235(4)	53(2)
C(25)	-1725(4)	5569(8)	5504(3)	36(2)
C(26)	-2226(5)	5296(13)	4702(3)	49(2)
C(27)	-1897(7)	3861(12)	4284(4)	67(2)
C(28)	-1066(6)	2520(12)	4695(6)	71(2)
C(29)	-582(6)	2743(12)	5464(5)	66(2)
C(30)	-892(5)	4276(10)	5885(4)	48(2)

Table 3. Bond lengths [\AA] and angles [$^\circ$] for $\text{C}_{30}\text{H}_{27}\text{IO}_8$.

I(1)-C(7)	2.113(7)
O(1)-C(11)	1.328(6)
O(1)-C(1)	1.474(6)
O(2)-C(11)	1.197(6)
O(3)-C(13)	1.331(7)
O(3)-C(12)	1.427(6)
O(4)-C(13)	1.205(6)
O(5)-C(21)	1.342(6)
O(5)-C(10)	1.457(6)
O(6)-C(21)	1.198(6)
O(7)-C(23)	1.360(8)
O(7)-C(22)	1.431(6)
O(8)-C(23)	1.202(6)
C(1)-C(10)	1.495(7)
C(1)-C(2)	1.513(7)
C(2)-C(3)	1.509(8)
C(3)-C(8)	1.381(9)
C(3)-C(4)	1.425(8)
C(4)-C(5)	1.364(10)
C(5)-C(6)	1.384(12)
C(6)-C(7)	1.390(10)
C(7)-C(8)	1.405(8)
C(8)-C(9)	1.528(8)
C(9)-C(10)	1.509(7)

C(11)-C(12)	1.520(7)
C(12)-C(15)	1.514(7)
C(13)-C(14)	1.490(8)
C(15)-C(16)	1.388(7)
C(15)-C(20)	1.388(8)
C(16)-C(17)	1.375(8)
C(17)-C(18)	1.362(9)
C(18)-C(19)	1.387(10)
C(19)-C(20)	1.381(9)
C(21)-C(22)	1.515(7)
C(22)-C(25)	1.520(7)
C(23)-C(24)	1.500(9)
C(25)-C(30)	1.384(8)
C(25)-C(26)	1.386(8)
C(26)-C(27)	1.355(10)
C(27)-C(28)	1.418(11)
C(28)-C(29)	1.327(10)
C(29)-C(30)	1.395(9)

C(11)-O(1)-C(1)	117.6(4)
C(13)-O(3)-C(12)	114.5(3)
C(21)-O(5)-C(10)	119.2(4)
C(23)-O(7)-C(22)	114.1(4)
O(1)-C(1)-C(10)	105.5(4)
O(1)-C(1)-C(2)	109.8(4)
C(10)-C(1)-C(2)	112.1(4)
C(3)-C(2)-C(1)	111.9(5)
C(8)-C(3)-C(4)	119.8(6)
C(8)-C(3)-C(2)	122.3(5)
C(4)-C(3)-C(2)	117.8(6)
C(5)-C(4)-C(3)	120.9(7)
C(4)-C(5)-C(6)	120.0(6)
C(5)-C(6)-C(7)	119.2(6)
C(6)-C(7)-C(8)	122.1(7)
C(6)-C(7)-I(1)	117.2(5)
C(8)-C(7)-I(1)	120.7(5)

C(3)-C(8)-C(7)	117.7(6)
C(3)-C(8)-C(9)	120.9(5)
C(7)-C(8)-C(9)	121.3(6)
C(10)-C(9)-C(8)	112.3(5)
O(5)-C(10)-C(1)	109.1(4)
O(5)-C(10)-C(9)	105.9(4)
C(1)-C(10)-C(9)	110.6(4)
O(2)-C(11)-O(1)	126.0(5)
O(2)-C(11)-C(12)	124.0(5)
O(1)-C(11)-C(12)	109.9(4)
O(3)-C(12)-C(15)	108.7(4)
O(3)-C(12)-C(11)	111.6(4)
C(15)-C(12)-C(11)	108.6(4)
O(4)-C(13)-O(3)	123.1(5)
O(4)-C(13)-C(14)	125.4(5)
O(3)-C(13)-C(14)	111.4(5)
C(16)-C(15)-C(20)	118.3(5)
C(16)-C(15)-C(12)	122.9(5)
C(20)-C(15)-C(12)	118.8(5)
C(17)-C(16)-C(15)	121.1(5)
C(18)-C(17)-C(16)	120.4(5)
C(17)-C(18)-C(19)	119.6(6)
C(20)-C(19)-C(18)	120.3(6)
C(19)-C(20)-C(15)	120.3(5)
O(6)-C(21)-O(5)	126.3(5)
O(6)-C(21)-C(22)	124.8(5)
O(5)-C(21)-C(22)	108.7(4)
O(7)-C(22)-C(21)	109.8(4)
O(7)-C(22)-C(25)	108.2(4)
C(21)-C(22)-C(25)	108.6(4)
O(8)-C(23)-O(7)	122.5(6)
O(8)-C(23)-C(24)	126.3(7)
O(7)-C(23)-C(24)	111.2(5)
C(30)-C(25)-C(26)	118.2(6)
C(30)-C(25)-C(22)	118.6(5)
C(26)-C(25)-C(22)	123.1(5)

C(27)-C(26)-C(25)	121.9(7)
C(26)-C(27)-C(28)	118.5(7)
C(29)-C(28)-C(27)	120.4(7)
C(28)-C(29)-C(30)	120.7(7)
C(25)-C(30)-C(29)	120.1(6)

Table 4. Anisotropic displacement parameters ($\text{\AA}^2 \times 10^3$) for $\text{C}_{30}\text{H}_{27}\text{IO}_8$.

The anisotropic displacement factor exponent takes the form:

$$-2p^2[h^2 a^* 2U^{11} + \dots + 2 h k a^* b^* U^{12}]$$

Atom	U ¹¹	U ²²	U ³³	U ²³	U ¹³	U ¹²
I(1)	60(1)	49(1)	118(1)	24(1)	52(1)	27(1)
O(1)	31(2)	26(2)	29(2)	3(2)	13(2)	8(2)
O(2)	31(2)	32(2)	29(2)	-4(2)	11(2)	0(2)
O(3)	26(2)	26(2)	41(2)	-4(2)	12(1)	0(2)
O(4)	40(2)	35(3)	62(3)	-6(2)	30(2)	-9(2)
O(5)	28(2)	29(3)	24(2)	3(2)	8(2)	3(2)
O(6)	22(2)	47(3)	31(2)	-1(2)	6(2)	1(2)
O(7)	52(2)	26(2)	22(2)	1(2)	7(2)	3(2)
O(8)	77(3)	44(3)	40(2)	-15(3)	-2(2)	10(3)
C(1)	26(2)	25(4)	30(3)	7(2)	8(2)	7(2)
C(2)	35(3)	37(3)	27(3)	-12(3)	8(3)	-5(3)
C(3)	27(3)	46(5)	20(3)	9(3)	0(2)	-5(3)
C(4)	51(4)	63(4)	27(3)	10(3)	7(3)	-11(3)
C(5)	27(3)	100(6)	40(4)	20(5)	1(3)	2(5)
C(6)	25(4)	101(7)	66(5)	55(5)	15(4)	18(4)
C(7)	39(4)	51(4)	53(4)	29(3)	25(3)	14(3)
C(8)	25(3)	37(4)	35(3)	16(3)	10(3)	3(2)
C(9)	30(3)	30(3)	49(4)	6(3)	14(3)	5(2)
C(10)	29(3)	21(3)	24(3)	-2(2)	11(2)	-2(2)
C(11)	25(3)	22(3)	26(3)	-8(3)	3(3)	-7(2)
C(12)	28(3)	28(3)	27(3)	2(2)	13(2)	2(2)
C(13)	48(4)	24(3)	38(3)	8(3)	19(3)	6(3)
C(14)	60(4)	25(3)	66(4)	1(3)	39(3)	5(3)
C(15)	33(3)	33(3)	29(3)	-1(3)	8(3)	2(2)

C(16)	29(3)	43(4)	25(3)	4(3)	6(2)	-5(3)
C(17)	31(3)	60(6)	40(3)	18(4)	8(3)	-6(3)
C(18)	45(4)	70(5)	78(5)	-22(4)	16(4)	-30(3)
C(19)	73(5)	99(8)	80(5)	-66(5)	34(4)	-38(5)
C(20)	38(4)	97(7)	57(4)	-43(4)	19(3)	-28(4)
C(21)	34(3)	26(3)	34(3)	-5(2)	11(3)	3(2)
C(22)	28(3)	29(3)	31(3)	4(3)	6(2)	-2(2)
C(23)	51(3)	27(3)	43(4)	-4(4)	7(3)	-5(4)
C(24)	65(4)	32(4)	53(4)	6(3)	3(3)	13(3)
C(25)	37(3)	38(4)	41(3)	-1(3)	23(3)	-4(3)
C(26)	57(3)	53(5)	39(4)	-9(4)	17(3)	8(4)
C(27)	88(6)	73(5)	50(4)	-14(4)	37(4)	-1(5)
C(28)	64(5)	67(6)	96(7)	-26(5)	46(5)	6(4)
C(29)	47(4)	73(6)	77(6)	-6(5)	19(4)	11(4)
C(30)	40(3)	53(4)	56(4)	0(3)	19(3)	7(3)

Table 5. Hydrogen coordinates ($\times 10^4$) and isotropic displacement parameters ($\text{\AA}^2 \times 10^3$) for $\text{C}_{30}\text{H}_{27}\text{IO}_8$.

Atom	x	y	z	U(eq)
H(1)	-2608	4638	8810	32
H(2A)	-1332	7809	8456	40
H(2B)	-1438	7231	9308	40
H(4)	591	7320	9783	58
H(5)	2223	5623	9985	69
H(6)	2271	2655	9306	76
H(9A)	-1270	2128	7552	43
H(9B)	-1686	1689	8305	43
H(10)	-3028	3632	7457	29
H(12)	-4751	9367	7607	32
H(14A)	-5202	12083	9748	69
H(14B)	-5744	13453	8994	69
H(14C)	-4524	13897	9539	69
H(16)	-6830	7796	8369	39
H(17)	-8136	5377	7852	53

H(18)	-7958	3295	6856	78
H(19)	-6400	3519	6422	98
H(20)	-5107	6000	6912	76
H(22)	-1446	7866	6333	36
H(24A)	-4120	12500	5498	80
H(24B)	-4671	10572	5010	80
H(24C)	-3664	11644	4812	80
H(26)	-2818	6140	4438	58
H(27)	-2216	3756	3728	80
H(28)	-855	1455	4418	85
H(29)	-18	1848	5732	79
H(30)	-532	4434	6434	58

Table 6. Torsion angles [$^{\circ}$] for $C_{30}H_{27}IO_8$.

C(11)-O(1)-C(1)-C(10)	151.9(4)
C(11)-O(1)-C(1)-C(2)	-87.1(5)
O(1)-C(1)-C(2)-C(3)	-163.7(4)
C(10)-C(1)-C(2)-C(3)	-46.8(6)
C(1)-C(2)-C(3)-C(8)	19.8(7)
C(1)-C(2)-C(3)-C(4)	-163.3(5)
C(8)-C(3)-C(4)-C(5)	1.9(8)
C(2)-C(3)-C(4)-C(5)	-175.1(6)
C(3)-C(4)-C(5)-C(6)	-0.4(10)
C(4)-C(5)-C(6)-C(7)	1.0(10)
C(5)-C(6)-C(7)-C(8)	-3.0(9)
C(5)-C(6)-C(7)-I(1)	176.1(5)
C(4)-C(3)-C(8)-C(7)	-3.7(8)
C(2)-C(3)-C(8)-C(7)	173.1(5)
C(4)-C(3)-C(8)-C(9)	175.3(5)
C(2)-C(3)-C(8)-C(9)	-7.9(8)
C(6)-C(7)-C(8)-C(3)	4.3(8)
I(1)-C(7)-C(8)-C(3)	-174.7(4)
C(6)-C(7)-C(8)-C(9)	-174.6(5)
I(1)-C(7)-C(8)-C(9)	6.3(7)
C(3)-C(8)-C(9)-C(10)	21.9(7)

C(7)-C(8)-C(9)-C(10)	-159.2(5)
C(21)-O(5)-C(10)-C(1)	-105.1(4)
C(21)-O(5)-C(10)-C(9)	135.9(4)
O(1)-C(1)-C(10)-O(5)	66.0(4)
C(2)-C(1)-C(10)-O(5)	-53.4(5)
O(1)-C(1)-C(10)-C(9)	-177.9(4)
C(2)-C(1)-C(10)-C(9)	62.6(5)
C(8)-C(9)-C(10)-O(5)	69.9(5)
C(8)-C(9)-C(10)-C(1)	-48.2(6)
C(1)-O(1)-C(11)-O(2)	6.3(7)
C(1)-O(1)-C(11)-C(12)	-170.1(4)
C(13)-O(3)-C(12)-C(15)	-176.2(4)
C(13)-O(3)-C(12)-C(11)	64.1(6)
O(2)-C(11)-C(12)-O(3)	27.9(7)
O(1)-C(11)-C(12)-O(3)	-155.6(4)
O(2)-C(11)-C(12)-C(15)	-91.9(6)
O(1)-C(11)-C(12)-C(15)	84.6(5)
C(12)-O(3)-C(13)-O(4)	1.2(8)
C(12)-O(3)-C(13)-C(14)	-178.5(4)
O(3)-C(12)-C(15)-C(16)	-13.1(7)
C(11)-C(12)-C(15)-C(16)	108.4(6)
O(3)-C(12)-C(15)-C(20)	168.1(5)
C(11)-C(12)-C(15)-C(20)	-70.3(7)
C(20)-C(15)-C(16)-C(17)	0.8(9)
C(12)-C(15)-C(16)-C(17)	-177.9(5)
C(15)-C(16)-C(17)-C(18)	-0.7(9)
C(16)-C(17)-C(18)-C(19)	1.5(11)
C(17)-C(18)-C(19)-C(20)	-2.5(12)
C(18)-C(19)-C(20)-C(15)	2.6(12)
C(16)-C(15)-C(20)-C(19)	-1.7(10)
C(12)-C(15)-C(20)-C(19)	177.0(7)
C(10)-O(5)-C(21)-O(6)	4.3(7)
C(10)-O(5)-C(21)-C(22)	-171.2(4)
C(23)-O(7)-C(22)-C(21)	62.9(6)
C(23)-O(7)-C(22)-C(25)	-178.7(4)
O(6)-C(21)-C(22)-O(7)	31.2(7)

O(5)-C(21)-C(22)-O(7)	-153.2(4)
O(6)-C(21)-C(22)-C(25)	-87.0(6)
O(5)-C(21)-C(22)-C(25)	88.6(5)
C(22)-O(7)-C(23)-O(8)	3.7(8)
C(22)-O(7)-C(23)-C(24)	-177.9(5)
O(7)-C(22)-C(25)-C(30)	170.5(5)
C(21)-C(22)-C(25)-C(30)	-70.3(6)
O(7)-C(22)-C(25)-C(26)	-13.6(7)
C(21)-C(22)-C(25)-C(26)	105.6(6)
C(30)-C(25)-C(26)-C(27)	-2.5(10)
C(22)-C(25)-C(26)-C(27)	-178.4(6)
C(25)-C(26)-C(27)-C(28)	4.5(11)
C(26)-C(27)-C(28)-C(29)	-3.7(11)
C(27)-C(28)-C(29)-C(30)	1.0(12)
C(26)-C(25)-C(30)-C(29)	-0.3(9)
C(22)-C(25)-C(30)-C(29)	175.7(6)
C(28)-C(29)-C(30)-C(25)	1.0(10)

Appendix II: X-Ray Crystal Report of (-)-102

Experimental:

A colorless needle crystal of $C_{32}H_{30}O_{10}$ was coated with Paratone 8277 oil (Exxon) and mounted on a glass fiber. All measurements were made on a Nonius KappaCCD diffractometer with graphite monochromated Mo- $K\alpha$ radiation. Cell constants obtained from the refinement¹ of 4051 reflections in the range $1.0 < \theta < 30.0^\circ$ corresponded to a primitive monoclinic cell; details of crystal data and structure refinement have been provided in Table 1. The data were collected² at a temperature of 173(2) K using the ω and φ scans to a maximum θ value of 30.0° . The data were corrected for Lorentz and polarization effects and for absorption using multi-scan method¹. Since the crystal did not show any sign of decay during data collection a decay correction was deemed unnecessary.

The structure was solved by the direct methods³ and expanded using Fourier techniques.⁴ The non-hydrogen atoms were refined anisotropically. Hydrogen atoms were located from a difference map, were included at geometrically idealized positions and were not refined. The final cycle of full-matrix least-squares refinement using SHELXL97⁵ converged (largest parameter shift was 0.00 times its esd) with unweighted and weighted agreement factors, $R = 0.040$ and $wR = 0.100$ (all data), respectively, and goodness of fit, $S = 1.00$. The weighting scheme was based on counting statistics and the final difference map was essentially featureless. The figures were plotted with the aid of ORTEPII.⁶

References:

8. Otwinowski, Z. & Minor, W. (1997). *Methods Enzymol.* **276**, 307.
9. Hooft, R. (1998). *COLLECT*. Nonius BV, Delft. The Netherlands.
10. Altomare, A., Cascarano, M., Giacovazzo, C. & Guagliardi, A. (1993). *SIR92*. *J. Appl. Cryst.*, **26**, 343
11. Beurskens, P.T., Admiraal, G., Beurskens, G., Bosman, W.P., de Gelder, R., Israel, R. & Smits, J.M.M. (1994). The *DIRDIF-94* program system, Technical Report of the Crystallography Laboratory, University of Nijmegen, The Netherlands.
12. Sheldrick, G.M. (1997). *SHELXL97*. University of Göttingen, Germany.
13. Johnson, C.K. (1976). *ORTEPII*. Report ORNL-5138. Oak Ridge National Laboratory, Tennessee, USA.

Table 1. Crystal data and structure refinement for C₃₂H₃₀O₁₀.

Identification code	T. Back – 2 (Mike – 1)
Empirical formula	C ₃₂ H ₃₀ O ₁₀
Formula weight	574.56
Temperature	173(2) K
Wavelength	0.71073 Å
Crystal system	Monoclinic
Space group	P2 ₁
Unit cell dimensions	a = 13.4032(3) Å b = 6.5158(2) Å β = 106.6346(13)° c = 17.5055(5) Å
Volume	1464.82(7) Å ³
Z	2
Density (calculated)	1.303 Mg/m ³
Absorption coefficient	0.097 mm ⁻¹
F(000)	604
Crystal size	0.25 x 0.15 x 0.10 mm ³
Theta range for data collection	3.8 to 30.0°.
Index ranges	-18 ≤ h ≤ 18, -9 ≤ k ≤ 8, -24 ≤ l ≤ 24
Reflections collected	8061
Independent reflections	4573 [R(int) = 0.024]
Observed data [I > 2σ(I)]	3857
Completeness to theta = 30.0°	98.8 %
Absorption correction	Multi-scan method
Max. and min. transmission	0.990 and 0.976
Refinement method	Full-matrix least-squares on F ²
Data / restraints / parameters	4573 / 1 / 379
Goodness-of-fit on F ²	1.000
Final R indices [I > 2σ(I)]	R1 = 0.040, wR2 = 0.093
R indices (all data)	R1 = 0.052, wR2 = 0.100
Weighting scheme	w = 1/[σ ² (F _o ²) + (0.0458P) ² + 0.279P] where P = (F _o ² + 2F _c ²)/3
Absolute structure parameter	-0.6(8)
Largest diff. peak and hole	0.19 and -0.20 e.Å ⁻³

Table 2. Atomic coordinates ($\times 10^4$) and equivalent isotropic displacement parameters ($\text{\AA}^2 \times 10^3$) for $\text{C}_{32}\text{H}_{30}\text{O}_{10}$. $U(\text{eq})$ is defined as one third of the trace of the orthogonalized U_{ij} tensor.

Atom	x	y	z	$U(\text{eq})$
O(1)	4435(1)	-2700(3)	1548(1)	35(1)
O(2)	4196(1)	-1395(3)	2674(1)	45(1)
O(3)	6916(1)	2116(2)	2849(1)	26(1)
O(4)	8549(1)	2120(3)	3694(1)	33(1)
O(5)	7892(1)	4906(2)	4629(1)	34(1)
O(6)	7801(2)	6827(3)	3549(1)	54(1)
O(7)	8202(1)	3681(2)	1923(1)	27(1)
O(8)	8538(1)	3952(2)	733(1)	32(1)
O(9)	10129(1)	6658(2)	1419(1)	31(1)
O(10)	8679(1)	8518(3)	1281(1)	43(1)
C(1)	7227(2)	916(3)	2247(1)	25(1)
C(2)	6363(2)	-624(3)	1920(1)	27(1)
C(3)	5371(2)	365(3)	1408(1)	25(1)
C(4)	4430(2)	-702(3)	1240(1)	30(1)
C(5)	3511(2)	78(4)	750(1)	35(1)
C(6)	3517(2)	1987(4)	405(1)	37(1)
C(7)	4438(2)	3097(3)	562(1)	32(1)
C(8)	5366(1)	2307(3)	1067(1)	26(1)
C(9)	6339(2)	3613(3)	1266(1)	27(1)
C(10)	7314(1)	2338(3)	1585(1)	25(1)
C(11)	4319(2)	-2859(4)	2295(1)	35(1)
C(12)	4386(2)	-5045(5)	2551(2)	49(1)
C(13)	7644(2)	2548(3)	3533(1)	27(1)
C(14)	7139(2)	3573(4)	4116(1)	30(1)
C(15)	6825(2)	1927(4)	4611(1)	31(1)
C(16)	7384(2)	1551(4)	5397(1)	41(1)
C(17)	7107(2)	-51(5)	5818(1)	49(1)
C(18)	6268(2)	-1294(5)	5456(1)	46(1)
C(19)	5704(2)	-918(4)	4677(1)	44(1)
C(20)	5975(2)	670(4)	4255(1)	38(1)

C(21)	8186(2)	6504(4)	4245(1)	38(1)
C(22)	9031(2)	7726(4)	4793(2)	46(1)
C(23)	8757(2)	4270(3)	1437(1)	25(1)
C(24)	9758(2)	5319(3)	1927(1)	27(1)
C(25)	10566(2)	3668(4)	2251(1)	29(1)
C(26)	11396(2)	3303(4)	1938(1)	34(1)
C(27)	12071(2)	1673(4)	2227(1)	39(1)
C(28)	11930(2)	423(4)	2821(2)	46(1)
C(29)	11111(2)	786(5)	3134(2)	53(1)
C(30)	10433(2)	2400(5)	2853(1)	44(1)
C(31)	9480(2)	8244(3)	1111(1)	32(1)
C(32)	9882(2)	9498(4)	558(1)	41(1)

Table 3. Bond lengths [\AA] and angles [$^\circ$] for $\text{C}_{32}\text{H}_{30}\text{O}_{10}$.

O(1)-C(11)	1.364(2)
O(1)-C(4)	1.409(3)
O(2)-C(11)	1.200(3)
O(3)-C(13)	1.340(2)
O(3)-C(1)	1.466(2)
O(4)-C(13)	1.197(2)
O(5)-C(21)	1.358(3)
O(5)-C(14)	1.435(2)
O(6)-C(21)	1.197(3)
O(7)-C(23)	1.336(2)
O(7)-C(10)	1.458(2)
O(8)-C(23)	1.201(2)
O(9)-C(31)	1.359(3)
O(9)-C(24)	1.433(2)
O(10)-C(31)	1.207(3)
C(1)-C(10)	1.513(3)
C(1)-C(2)	1.515(3)
C(2)-C(3)	1.517(3)
C(3)-C(4)	1.396(3)
C(3)-C(8)	1.398(3)
C(4)-C(5)	1.381(3)

C(5)-C(6)	1.384(4)
C(6)-C(7)	1.388(3)
C(7)-C(8)	1.402(3)
C(8)-C(9)	1.512(3)
C(9)-C(10)	1.514(3)
C(11)-C(12)	1.488(4)
C(13)-C(14)	1.531(3)
C(14)-C(15)	1.511(3)
C(15)-C(16)	1.388(3)
C(15)-C(20)	1.397(3)
C(16)-C(17)	1.388(3)
C(17)-C(18)	1.383(4)
C(18)-C(19)	1.379(3)
C(19)-C(20)	1.379(3)
C(21)-C(22)	1.488(3)
C(23)-C(24)	1.531(3)
C(24)-C(25)	1.517(3)
C(25)-C(30)	1.390(3)
C(25)-C(26)	1.394(3)
C(26)-C(27)	1.393(3)
C(27)-C(28)	1.375(3)
C(28)-C(29)	1.380(3)
C(29)-C(30)	1.384(4)
C(31)-C(32)	1.481(3)

C(11)-O(1)-C(4)	116.61(17)
C(13)-O(3)-C(1)	118.04(15)
C(21)-O(5)-C(14)	113.99(15)
C(23)-O(7)-C(10)	116.96(14)
C(31)-O(9)-C(24)	114.37(15)
O(3)-C(1)-C(10)	108.92(16)
O(3)-C(1)-C(2)	106.32(14)
C(10)-C(1)-C(2)	109.55(15)
C(1)-C(2)-C(3)	112.79(16)
C(4)-C(3)-C(8)	117.85(18)
C(4)-C(3)-C(2)	119.94(17)

C(8)-C(3)-C(2)	122.17(17)
C(5)-C(4)-C(3)	122.6(2)
C(5)-C(4)-O(1)	118.90(19)
C(3)-C(4)-O(1)	118.35(18)
C(4)-C(5)-C(6)	119.1(2)
C(5)-C(6)-C(7)	119.9(2)
C(6)-C(7)-C(8)	120.8(2)
C(3)-C(8)-C(7)	119.76(18)
C(3)-C(8)-C(9)	120.85(17)
C(7)-C(8)-C(9)	119.33(18)
C(8)-C(9)-C(10)	111.87(16)
O(7)-C(10)-C(1)	106.92(14)
O(7)-C(10)-C(9)	109.73(16)
C(1)-C(10)-C(9)	111.73(15)
O(2)-C(11)-O(1)	122.7(2)
O(2)-C(11)-C(12)	126.9(2)
O(1)-C(11)-C(12)	110.4(2)
O(4)-C(13)-O(3)	126.23(18)
O(4)-C(13)-C(14)	123.86(17)
O(3)-C(13)-C(14)	109.81(16)
O(5)-C(14)-C(15)	109.42(15)
O(5)-C(14)-C(13)	108.32(16)
C(15)-C(14)-C(13)	108.71(18)
C(16)-C(15)-C(20)	118.6(2)
C(16)-C(15)-C(14)	122.25(19)
C(20)-C(15)-C(14)	119.08(17)
C(15)-C(16)-C(17)	120.6(2)
C(18)-C(17)-C(16)	120.2(2)
C(17)-C(18)-C(19)	119.5(2)
C(20)-C(19)-C(18)	120.6(2)
C(19)-C(20)-C(15)	120.5(2)
O(6)-C(21)-O(5)	122.5(2)
O(6)-C(21)-C(22)	126.1(2)
O(5)-C(21)-C(22)	111.47(19)
O(8)-C(23)-O(7)	125.89(18)
O(8)-C(23)-C(24)	124.71(17)

O(7)-C(23)-C(24)	109.32(15)
O(9)-C(24)-C(25)	109.05(15)
O(9)-C(24)-C(23)	109.19(15)
C(25)-C(24)-C(23)	108.04(17)
C(30)-C(25)-C(26)	119.1(2)
C(30)-C(25)-C(24)	118.18(17)
C(26)-C(25)-C(24)	122.61(18)
C(25)-C(26)-C(27)	119.7(2)
C(28)-C(27)-C(26)	120.7(2)
C(27)-C(28)-C(29)	119.6(2)
C(28)-C(29)-C(30)	120.3(2)
C(29)-C(30)-C(25)	120.5(2)
O(10)-C(31)-O(9)	121.87(19)
O(10)-C(31)-C(32)	126.6(2)
O(9)-C(31)-C(32)	111.55(18)

Table 4. Anisotropic displacement parameters ($\text{\AA}^2 \times 10^3$) for $\text{C}_{32}\text{H}_{30}\text{O}_{10}$.

The anisotropic displacement factor exponent takes the form:

$$-2\pi^2 [h^2 a^* 2U_{11} + \dots + 2 h k a^* b^* U_{12}]$$

Atom	U ₁₁	U ₂₂	U ₃₃	U ₂₃	U ₁₃	U ₁₂
O(1)	44(1)	32(1)	33(1)	-6(1)	15(1)	-11(1)
O(2)	49(1)	52(1)	36(1)	-1(1)	18(1)	6(1)
O(3)	28(1)	30(1)	22(1)	-1(1)	6(1)	2(1)
O(4)	27(1)	44(1)	28(1)	0(1)	6(1)	-1(1)
O(5)	44(1)	29(1)	27(1)	-2(1)	5(1)	-5(1)
O(6)	70(1)	42(1)	39(1)	11(1)	-2(1)	-11(1)
O(7)	29(1)	30(1)	26(1)	-3(1)	11(1)	-5(1)
O(8)	32(1)	39(1)	24(1)	1(1)	9(1)	-3(1)
O(9)	28(1)	30(1)	38(1)	4(1)	12(1)	-1(1)
O(10)	43(1)	37(1)	54(1)	7(1)	23(1)	9(1)
C(1)	26(1)	25(1)	24(1)	-1(1)	7(1)	1(1)
C(2)	27(1)	24(1)	28(1)	2(1)	6(1)	-1(1)
C(3)	28(1)	27(1)	20(1)	-3(1)	7(1)	0(1)
C(4)	33(1)	33(1)	25(1)	-6(1)	9(1)	-5(1)

C(5)	27(1)	48(1)	28(1)	-9(1)	4(1)	-5(1)
C(6)	29(1)	50(1)	27(1)	-5(1)	1(1)	4(1)
C(7)	33(1)	35(1)	24(1)	0(1)	3(1)	5(1)
C(8)	28(1)	28(1)	21(1)	-2(1)	7(1)	1(1)
C(9)	32(1)	24(1)	26(1)	3(1)	9(1)	1(1)
C(10)	26(1)	25(1)	24(1)	-2(1)	7(1)	-4(1)
C(11)	25(1)	45(1)	34(1)	-1(1)	10(1)	-3(1)
C(12)	50(2)	49(2)	53(1)	10(1)	20(1)	-6(1)
C(13)	31(1)	27(1)	22(1)	2(1)	6(1)	-3(1)
C(14)	31(1)	31(1)	26(1)	-1(1)	5(1)	1(1)
C(15)	32(1)	36(1)	27(1)	-5(1)	13(1)	-1(1)
C(16)	42(1)	51(1)	29(1)	-1(1)	9(1)	-12(1)
C(17)	55(2)	62(2)	30(1)	7(1)	11(1)	-12(1)
C(18)	51(1)	52(2)	42(1)	4(1)	22(1)	-9(1)
C(19)	41(1)	51(2)	44(1)	-4(1)	16(1)	-13(1)
C(20)	33(1)	47(1)	32(1)	-3(1)	9(1)	-5(1)
C(21)	47(1)	28(1)	36(1)	2(1)	8(1)	0(1)
C(22)	55(2)	33(1)	45(1)	-1(1)	6(1)	-7(1)
C(23)	24(1)	25(1)	28(1)	4(1)	9(1)	3(1)
C(24)	26(1)	30(1)	27(1)	2(1)	9(1)	-1(1)
C(25)	24(1)	35(1)	28(1)	-1(1)	5(1)	1(1)
C(26)	32(1)	38(1)	33(1)	1(1)	11(1)	2(1)
C(27)	31(1)	45(1)	41(1)	-4(1)	12(1)	8(1)
C(28)	40(1)	47(1)	49(1)	9(1)	10(1)	14(1)
C(29)	45(1)	64(2)	54(1)	28(1)	19(1)	18(1)
C(30)	34(1)	60(2)	42(1)	18(1)	16(1)	14(1)
C(31)	35(1)	24(1)	35(1)	-2(1)	9(1)	-1(1)
C(32)	54(1)	30(1)	45(1)	4(1)	22(1)	0(1)

Table 5. Hydrogen coordinates ($\times 10^4$) and isotropic displacement parameters ($\text{\AA}^2 \times 10^3$) for $\text{C}_{32}\text{H}_{30}\text{O}_{10}$.

Atom	x	y	z	U(eq)
H(1)	7903	199	2490	30
H(2A)	6209	-1350	2370	32
H(2B)	6604	-1656	1597	32
H(5)	2883	-686	651	42
H(6)	2892	2537	61	44
H(7)	4439	4407	324	38
H(9A)	6299	4651	1669	33
H(9B)	6379	4348	781	33
H(10)	7445	1512	1142	30
H(12A)	4307	-5135	3089	59
H(12B)	5064	-5606	2551	59
H(12C)	3831	-5833	2181	59
H(14)	6513	4378	3817	36
H(16)	7961	2398	5650	49
H(17)	7495	-295	6356	59
H(18)	6082	-2398	5743	55
H(19)	5124	-1762	4428	53
H(20)	5580	911	3719	45
H(22A)	9226	8863	4499	55
H(22B)	9638	6846	5014	55
H(22C)	8785	8275	5228	55
H(24)	9623	6116	2376	33
H(26)	11501	4162	1530	41
H(27)	12634	1422	2012	46
H(28)	12395	-684	3016	55
H(29)	11011	-76	3544	63
H(30)	9873	2642	3073	53
H(32A)	9398	10625	348	49
H(32B)	9951	8638	117	49
H(32C)	10565	10061	845	49

Table 6. Torsion angles [°] for b2.

C(13)-O(3)-C(1)-C(10)	-104.30(18)
C(13)-O(3)-C(1)-C(2)	137.74(16)
O(3)-C(1)-C(2)-C(3)	70.70(18)
C(10)-C(1)-C(2)-C(3)	-46.9(2)
C(1)-C(2)-C(3)-C(4)	-162.75(16)
C(1)-C(2)-C(3)-C(8)	19.7(2)
C(8)-C(3)-C(4)-C(5)	0.6(3)
C(2)-C(3)-C(4)-C(5)	-177.05(18)
C(8)-C(3)-C(4)-O(1)	176.92(15)
C(2)-C(3)-C(4)-O(1)	-0.7(2)
C(11)-O(1)-C(4)-C(5)	-95.9(2)
C(11)-O(1)-C(4)-C(3)	87.6(2)
C(3)-C(4)-C(5)-C(6)	0.4(3)
O(1)-C(4)-C(5)-C(6)	-175.89(17)
C(4)-C(5)-C(6)-C(7)	-0.7(3)
C(5)-C(6)-C(7)-C(8)	0.0(3)
C(4)-C(3)-C(8)-C(7)	-1.3(2)
C(2)-C(3)-C(8)-C(7)	176.29(17)
C(4)-C(3)-C(8)-C(9)	175.85(16)
C(2)-C(3)-C(8)-C(9)	-6.6(3)
C(6)-C(7)-C(8)-C(3)	1.0(3)
C(6)-C(7)-C(8)-C(9)	-176.16(17)
C(3)-C(8)-C(9)-C(10)	21.1(2)
C(7)-C(8)-C(9)-C(10)	-161.73(16)
C(23)-O(7)-C(10)-C(1)	146.33(16)
C(23)-O(7)-C(10)-C(9)	-92.33(18)
O(3)-C(1)-C(10)-O(7)	68.02(18)
C(2)-C(1)-C(10)-O(7)	-176.06(15)
O(3)-C(1)-C(10)-C(9)	-52.0(2)
C(2)-C(1)-C(10)-C(9)	63.9(2)
C(8)-C(9)-C(10)-O(7)	-168.15(13)
C(8)-C(9)-C(10)-C(1)	-49.7(2)
C(4)-O(1)-C(11)-O(2)	1.5(3)
C(4)-O(1)-C(11)-C(12)	-177.5(2)

C(1)-O(3)-C(13)-O(4)	3.3(3)
C(1)-O(3)-C(13)-C(14)	-173.14(16)
C(21)-O(5)-C(14)-C(15)	-176.90(17)
C(21)-O(5)-C(14)-C(13)	64.7(2)
O(4)-C(13)-C(14)-O(5)	32.4(3)
O(3)-C(13)-C(14)-O(5)	-150.99(16)
O(4)-C(13)-C(14)-C(15)	-86.4(2)
O(3)-C(13)-C(14)-C(15)	90.21(19)
O(5)-C(14)-C(15)-C(16)	-13.9(3)
C(13)-C(14)-C(15)-C(16)	104.2(2)
O(5)-C(14)-C(15)-C(20)	169.34(18)
C(13)-C(14)-C(15)-C(20)	-72.5(2)
C(20)-C(15)-C(16)-C(17)	0.5(4)
C(14)-C(15)-C(16)-C(17)	-176.3(2)
C(15)-C(16)-C(17)-C(18)	0.0(4)
C(16)-C(17)-C(18)-C(19)	-0.5(4)
C(17)-C(18)-C(19)-C(20)	0.5(4)
C(18)-C(19)-C(20)-C(15)	0.0(4)
C(16)-C(15)-C(20)-C(19)	-0.5(3)
C(14)-C(15)-C(20)-C(19)	176.4(2)
C(14)-O(5)-C(21)-O(6)	4.2(3)
C(14)-O(5)-C(21)-C(22)	-175.20(19)
C(10)-O(7)-C(23)-O(8)	7.4(3)
C(10)-O(7)-C(23)-C(24)	-169.48(16)
C(31)-O(9)-C(24)-C(25)	-178.16(16)
C(31)-O(9)-C(24)-C(23)	64.0(2)
O(8)-C(23)-C(24)-O(9)	26.7(3)
O(7)-C(23)-C(24)-O(9)	-156.35(15)
O(8)-C(23)-C(24)-C(25)	-91.7(2)
O(7)-C(23)-C(24)-C(25)	85.17(18)
O(9)-C(24)-C(25)-C(30)	170.2(2)
C(23)-C(24)-C(25)-C(30)	-71.2(2)
O(9)-C(24)-C(25)-C(26)	-13.6(3)
C(23)-C(24)-C(25)-C(26)	105.0(2)
C(30)-C(25)-C(26)-C(27)	0.5(3)
C(24)-C(25)-C(26)-C(27)	-175.7(2)

C(25)-C(26)-C(27)-C(28)	-0.3(3)
C(26)-C(27)-C(28)-C(29)	0.1(4)
C(27)-C(28)-C(29)-C(30)	-0.1(5)
C(28)-C(29)-C(30)-C(25)	0.3(4)
C(26)-C(25)-C(30)-C(29)	-0.5(4)
C(24)-C(25)-C(30)-C(29)	175.9(2)
C(24)-O(9)-C(31)-O(10)	2.6(3)
C(24)-O(9)-C(31)-C(32)	-176.93(17)